
Doctoral Dissertations

Student Theses and Dissertations

1973

A study of the dynamic loading of hydrodynamically lubricated journal bearings

Nader Khorzad

Follow this and additional works at: https://scholarsmine.mst.edu/doctoral_dissertations



Part of the [Mechanical Engineering Commons](#)

Department: Mechanical and Aerospace Engineering

Recommended Citation

Khorzad, Nader, "A study of the dynamic loading of hydrodynamically lubricated journal bearings" (1973). *Doctoral Dissertations*. 249.

https://scholarsmine.mst.edu/doctoral_dissertations/249

This thesis is brought to you by Scholars' Mine, a service of the Missouri S&T Library and Learning Resources. This work is protected by U. S. Copyright Law. Unauthorized use including reproduction for redistribution requires the permission of the copyright holder. For more information, please contact scholarsmine@mst.edu.

A STUDY OF THE DYNAMIC LOADING OF HYDRODYNAMICALLY
LUBRICATED JOURNAL BEARINGS

by

NADER KHORZAD, 1939-

A DISSERTATION

Presented to the Faculty of the Graduate School of the
UNIVERSITY OF MISSOURI - ROLLA

In Partial Fulfillment of the Requirements for the Degree

DOCTOR OF PHILOSOPHY

in

MECHANICAL ENGINEERING

1973

T2992
111 pages
c.1

Charles L. Edwards
Advisor

Robert A. Medrow

J. R. Faucett

R. T. Johnson

Ralph Eschmaltz

R. J. Penico

243108

PUBLICATION THESIS OPTION

The paper presented within the body of this thesis has been prepared in the style utilized by the American Society of Mechanical Engineers. Pages 1 - 53 will be submitted to the A.S.M.E. Journal of Lubrication Technology for publication.

Appendices have been added for purposes normal to thesis writing.

PREFACE

Lubrication in one sense is as old in civilization as the wheel and axle. When a tomb was opened in Egypt some years ago, one of the chariots still had some of the original lubricant on the axle. This was analyzed and found to be "sticky and slightly greasy"¹.

The new science of lubrication, however, was not recognized as such until 1883 when hydrodynamic theory was originated by Reynolds. But, it was 1920 before dynamically loaded bearings were first studied. Still, the problem is not completely solved.

The large volume of literature devoted to predicting the motion of dynamically loaded journal bearings contain surprisingly little information of direct use to the designer. This thesis responds to that need by finding the response of a journal bearing to unidirectional dynamic loading; both analytically and experimentally. This type of load exists in many industrial problems, for example, railroad car bearings where there is a large static load with a superimposed dynamic load in the same direction. Also it is shown here that a journal bearing at different eccentricity ratios has different dynamic response, effecting the degree of importance of dynamic analysis. It is believed that this dynamic analysis will be useful to the designer.

Appendices of this thesis were prepared to give detailed information and derivations.

1. Parish, W.F., "Lubricants", Encyclopedia Britannica, 14th ed., vol. 14, 1929, pp. 451-453

The Author is indebted to the University of Missouri-Rolla and the Department of Mechanical and Aerospace Engineering for supporting this research and for provision of the Author's graduate assistantship during its conduct.

I am especially grateful to Dr. C.L. Edwards for his guidance, encouragement, and technical assistance in the preparation of this work and to Dr. T.R. Faucett for suggesting the problem. My sincere thanks goes to Prof. R.E. Schowalter for his assistance and encouragement throughout the Ph.D. program.

My sincere thanks goes to Dr. C.R. Barker for his computer programming assistance and Dr. R.K. Riley for guidance in choosing control equipment.

Drs. R.A. Medrow, R.T. Johnson, A.J. Penico and H. Sauer have also contributed significantly to this thesis and have my sincere thanks.

I am especially thankful to Tehran Polytechnic for allowing this study and their support.

Thanks are also due to Mr. Lee Clover for his assistance in machining and alignment of the journal.

My sincere thanks goes to Mrs. Beverly Braun for her work in typing this thesis.

Last, but not least, I thank my wife, Mrs. Katalin Khorzad for her help and patience.

TABLE OF CONTENTS

	Page
PUBLICATION THESIS OPTION.....	ii
PREFACE.....	iii
LIST OF ILLUSTRATIONS.....	iv
LIST OF TABLES.....	viii
NOMENCLATURE.....	ix
INTRODUCTION.....	2
I. ANALYTICAL WORK.....	4
Pressure Forces.....	7
Dynamic Forces.....	8
(i) Forces due to displacement of journal center.....	8
(ii) Forces due to velocity of journal center.....	11
(iii) Forces due to acceleration of journal center.....	11
II. EXPERIMENTAL WORK.....	19
Description of Apparatus.....	19
Instrumentation.....	20
RESULTS.....	23
CONCLUSIONS AND RECOMMENDATIONS.....	27
APPENDICES	
A. Literature Review.....	54
B. Derivation of General Reynolds' Equation.....	59
C. An Approximate Solution to Reynolds' Equation....	66
D. Determination of Eigenvalues.....	70
E. Integration Constants for Pressure and Load Equations.....	73
F. Elastic Coefficients.....	75
G. Inertia Coefficients.....	77

	Page
H. Numerical Solutions of the General and Eigenvalue Equations.....	79
I. A Method for Identifying Journal Center Loci.....	84
J. Effect of Journal Mass.....	88
K. Integrals and Differentiation.....	90
L. Dynamic Response of Bearing.....	91
VITA.....	99

LIST OF ILLUSTRATIONS

Figures

1. Full journal bearing coordinate systems.
2. Pressure Forces.
3. Displacement due to dynamic forces.
4. Film element.
5. General view of apparatus.
6. Schematic of apparatus.
7. Control diagram.
8. Experimental and analytical pressure distribution for various static load.
9. Experimental and analytical pressure distribution.
10. Comparison of $P(\phi, z)$ and $P_a(\phi, z)$.
11. Dynamic displacement of journal center
12. Corrected dynamic displacements.
13. Variation of maximum pressure.
14. Corrected maximum pressure.
15. Journal center loci.
16. Ψ vs. time
17. ϵ vs. time
18. $\dot{\Psi}$ vs. time
19. $\dot{\epsilon}$ vs. time
20. Eccentricity ratio vs. Sommerfeld no.
21. Non-dimensional inertia coefficients.
22. Non-dimensional damping coefficients.
23. Non-dimensional elastic coefficient K_{xx} .
24. Non-dimensional cross elastic coefficients.

Figure

25. Non-dimensional elastic coefficient K_{yy}
26. Side leakage factor - η .

LIST OF TABLES

Table		Page
1	$F(\phi)$ Functions.....	29
2	$F'(\phi)$ Functions.....	30

NOMENCLATURE

a_c	= circumferential acceleration of lubricant in the film
a_j	= radial acceleration of journal center
a_z	= axial acceleration of lubricant in the film
B_{xx}, B_{yy}	= damping coefficients in x and y direction respectively
B_{xy}, B_{yx}	= cross damping coefficients
c	= radial clearance
e	= journal eccentricity (Figure 1)
D	= journal diameter
$F(\phi)$	= function of ϕ only (Table 1)
$F'(\phi)$	= definite function of ϕ (Table 2)
F_x, F_y	= film forces in x and y direction
g	= orthogonal function from Equation (7)
h	= film thickness
K_{xx}, K_{yy}	= spring coefficient in x and y direction respectively
K_{xy}, K_{yx}	= cross spring coefficient
L	= bearing width
M_{xx}, M_{yy}	= inertia coefficient in x and y direction respectively
M_{xy}, M_{yx}	= cross inertia coefficients
N	= speed of journal in revolutions per minute
N'	= speed of journal in revolutions per second
O_b	= bearing center
O_j	= journal center

- $P(\phi, z)$ = hydrodynamic film pressure
 $P_a(\phi, z)$ = pressure in the film due to acceleration
 P_i = inlet pressure
 P_o = film pressure at $\phi = 0$
 q = function of z only
 r = journal radius
 S = Sommerfeld number for finite bearings $S = \frac{S_\infty}{\eta}$
 S_∞ = Sommerfeld number for infinitely long bearing
 $S_\infty = \frac{\mu NDL}{W} \left(\frac{r}{c}\right)^2$
 t = time (second)
 U_o, V_o = velocities of a point on the surface of the bearing in x and y direction respectively
 U_1, V_1 = velocities of a point on the journal surface in x and y direction respectively
 u_j, v_j = coordinate system fixed on bearing center (Figure 3)
 W = bearing load
 W_o = bearing static load
 W_1 = amplitude of dynamic load
 W_p = force due to film pressure
 x, y, z = coordinate system fixed on center of journal at steady state
 $X, Y, Z,$ = coordinate system, (see Figure 1)
 β = bearing arc length
 ϵ = eccentricity ratio, $= \frac{e}{c}$
 ϵ_o = eccentricity ratio at $t = 0$
 $\dot{\epsilon}$ = $\frac{d\epsilon}{dt}$

ζ	= damping ratio of system
η	= side leakage factor for dynamic load
η_a	= side leakage factor due to acceleration
η_s	= side leakage factor for static load
Θ_T	= $\Psi + \phi$
λ_r	= characteristic value from Equation (7)
λ_a^r	= characteristic value of Equation (D-8)
μ	= viscosity of lubricant
ρ	= lubricant mass density
τ	= time constant of system
ϕ	= coordinate measured from line of centers
Ψ	= attitude angle (Figure 1)
Ψ_0	= attitude angle at $t = 0$
$\dot{\Psi}$	= $\frac{d\Psi}{dt}$
Ω	= non-dimensional form of inertia coefficients $\Omega = \frac{M}{r^3 L \rho \eta_a / c}$
ω	= journal angular velocity
ω_d	= dynamic load frequency
ω_n	= natural frequency

A STUDY OF THE DYNAMIC LOADING OF HYDRODYNAMICALLY
LUBRICATED JOURNAL BEARINGS

by

Nader Khorzad

and

Dr. C.L. Edwards

and

Dr. T.R. Faucett

ABSTRACT

The analytical and experimental investigation presented here examined the response of a full journal bearing to a unidirectional dynamic load. Frequency response of the bearing at different eccentricity ratios was investigated. It was concluded that the response of the bearing varies with eccentricity.

The experimental data obtained was compared to an analytical model which considered inertial, damping, and elastic characteristics of the lubricant film.

An investigation of film pressure revealed that the pressure due to journal center acceleration is smaller than the hydrodynamic and squeeze-film pressures.

INTRODUCTION

Most previous work involving the dynamic analysis of journal bearings predicts the motion of the journal center, due to a constant magnitude rotating-load vector, (1), (2), (3). Transverse flow, or side-leakage is generally ignored. Shawki (4), for example, presents a basic theoretical investigation into the performance of a complete journal bearing of infinite length under variable load, excluding negative pressures. However, Burwell [5] applied a side-leakage factor, obtained by Waters [6], to Swift's [2] equations. Booker [7] has introduced the Mobility method which predicts the motion of a journal bearing center under arbitrary loading.

Hahn [8] used a finite difference method to calculate the pressure distribution of a finite 360° journal bearing with dynamic loading. Hays [9,10] solved Reynolds' equation by variational methods and applied this general solution to a finite 360° non-rotating journal bearing under dynamic loading.

An important paper by Warner [11] has a solution of Reynolds' equation using separation of variables; reducing Reynolds' equation to two ordinary differential equations. The solutions of the two equations are combined into one series solution. He, then, approximated the pressure series to the first term of the series and used it as a side-leakage factor.

Smith [12] introduced a technique for calculating the

inertia effect of a hydrodynamic film in journal bearings. Huggins [13], by experimenting with a 24 inch diameter journal, indicated that even at low speeds journal bearing variables have a pronounced dependence on the mass density of lubricant.

Buske and Rolli [14] in 1937 carried out pressure measurements in the oil film of a full journal bearing under alternating loads applied at the same frequency as that of the rotation of the journal. Recorded diagrams give evidence that film pressures at any cross-section vanish along a portion of the journal periphery, thus confirming that negative pressures (below vapor pressure of lubricant) do not exist in a bearing.

Dayton and Simons [15], by an experimental investigation of shaft center location and displacement for various ratios of rotating load to journal speed, showed that the shaft reaches an equilibrium point despite Swift's theoretical work which indicates that the shaft will not be static under no load or a constant load.

The investigation presented here examined response of a full journal bearing subjected to a unidirectional load whose magnitude was time dependent. This type of dynamic loading was chosen, because it exists in many industrial problems. For example, railroad car bearings, where there is a large static load with a superimposed dynamic load in the same direction. Also, frequency response of the bearing at different eccentricity ratios was investigated.

The experimental data obtained was compared to an analytical model which considered inertial, damping, and elastic characteristics of the lubricant film. It was assumed that the principle of superposition applies to this case. Thus, the separate effects of the above characteristics were determined to obtain the general differential equation.

I. ANALYTICAL WORK

It is assumed that the film thickness everywhere around the bearing is small compared to the journal dimensions, and that the journal axis is parallel to the bearing axis. Oil viscosity and density are uniform throughout the film.

It can be shown that a general form of Reynolds' differential equation for journal bearings is:

$$\frac{\partial}{\partial X} \left[\frac{h^3}{6\mu} \frac{\partial P}{\partial X} \right] + \frac{\partial}{\partial Z} \left[\frac{h^3}{6\mu} \frac{\partial P}{\partial Z} \right] = (U_1 - U_0) \frac{\partial h}{\partial X} + h \frac{\partial}{\partial X} (U_1 + U_0) + 2V_0 - 2V_1 \quad (1)$$

By assuming that the bearing is stationary i.e., $U_0 = V_0 = 0$, and also transforming Equation (1) to cylindrical coordinates:

$$\frac{1}{r^2} \frac{\partial}{\partial \phi} \left[\frac{h^3}{\mu} \frac{\partial P}{\partial \phi} \right] + \frac{\partial}{\partial Z} \left[\frac{h^3}{\mu} \frac{\partial P}{\partial Z} \right] = \frac{6}{r} \frac{\partial}{\partial \phi} (U_1 h) - 12V_1 \quad (2)$$

The right-hand side of Equation (2) is a function of ϕ alone, and Equation (2) can be written as (see Figure 1):

$$\frac{1}{r^2} \frac{\partial}{\partial \phi} \left[\frac{h^3}{\mu} \frac{\partial P}{\partial \phi} \right] + \frac{\partial}{\partial Z} \left[\frac{h^3}{\mu} \frac{\partial P}{\partial Z} \right] = 12C \frac{d\epsilon}{dt} \cos \phi - 6(\omega - 2\frac{d\psi}{dt}) c\epsilon \sin \phi \quad (3)$$

As can be seen, Equation (3) is a nonhomogeneous second order partial differential equation, and the exact solution for it is quite complicated, if not impossible, in explicit form. Warner [11] presented an approximate analytical solution using separation of variables to reduce Equation (3) to two ordinary differential equations:

$$\frac{d}{d\phi} \left(\frac{h^3}{\mu} \frac{dF}{d\phi} \right) = r^2 [12C\dot{\epsilon} \cos \phi - 6(\omega - 2\dot{\psi}) C\epsilon \sin \phi] \quad (4)$$

and

$$\frac{\mu}{h^3 r^2} \frac{d}{d\phi} \left(\frac{h^3}{\mu} \frac{dg}{d\phi} \right) + \frac{d^2 q}{dZ^2} = 0 \quad (5)$$

Where F and g are functions of ϕ and q is a function of Z only. Equation (5) could be written as:

$$\frac{d^2 q}{dZ^2} - \lambda^2 q = 0 \quad (6)$$

and

$$\frac{d}{d\phi} \left(\frac{h^3}{\mu} \frac{dg}{d\phi} \right) + (\lambda r)^2 \frac{h^3}{\mu} g = 0 \quad (7)$$

Where λ is an eigenvalue, which can be determined from Equation (7). Therefore, the solution to Equation (3) is:

$$P(\phi, Z) = \left[1 - \frac{q_1(Z)}{q_1(L/2)} \right] F(\phi) \quad (8)$$

Equation (8) is an approximate solution because the coefficient of $F(\phi)$ is the leading term of an infinite

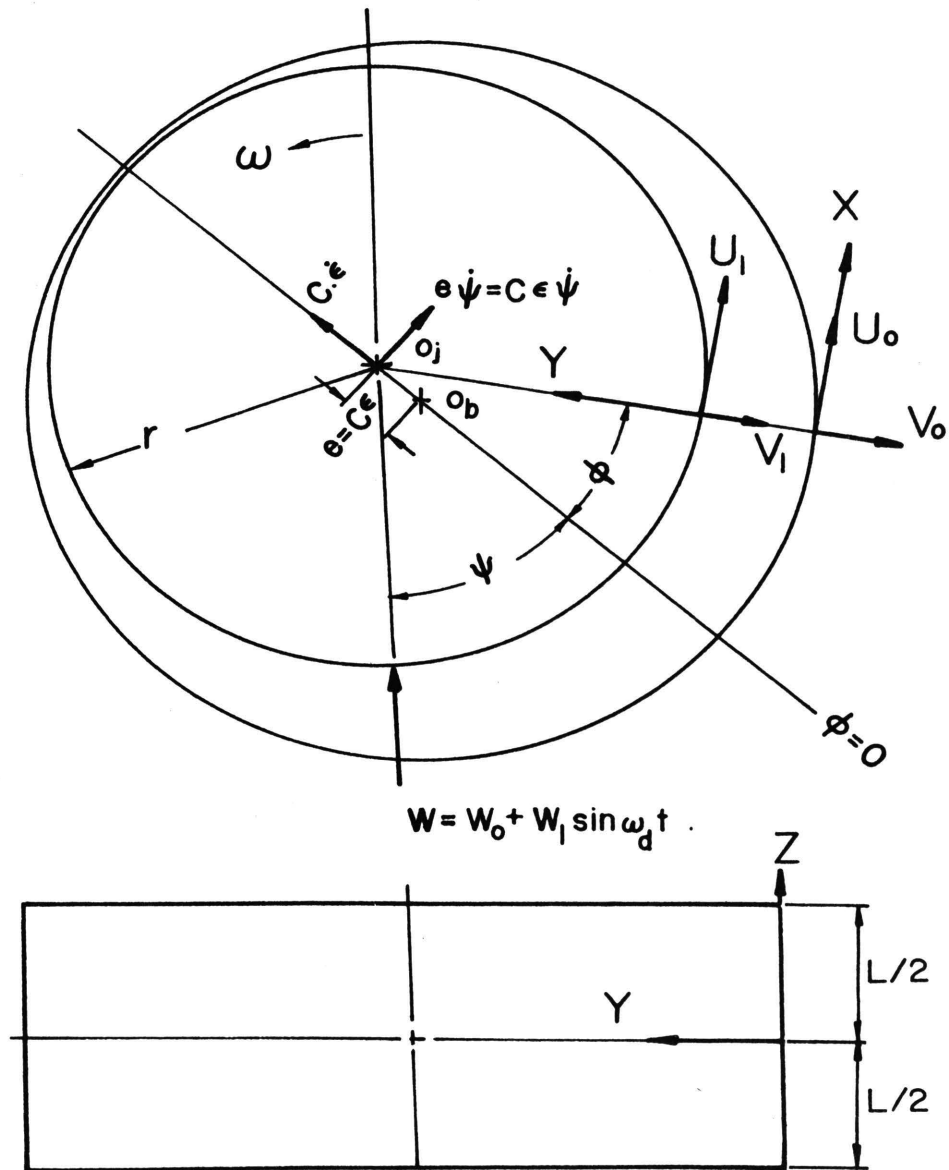


Fig. 1. Full Journal Bearing Coordinate Systems.

series. Therefore, assuming the journal and bearing to be circular and streamlined flow to exist, from Figure (1):

$$h = c(1 + \epsilon \cos \phi) \quad (9)$$

Considering the boundary conditions due to film continuity i.e., $P(0, Z) = P(2\pi, Z) = 0$, the pressure equation becomes:

$$P(\phi, Z) = \left[1 - \frac{\text{Cosh}(\lambda Z)}{\text{Cosh}(\lambda L/2)} \right] [F_a(\phi) + F_b(\phi)] \quad (10)$$

where

$$F_a(\phi) = 12 \left(\frac{r}{c}\right)^2 \mu \dot{\epsilon} [F_1(\phi) + C_1 F_2(\phi) + C_2] \quad (11)$$

and

$$F_b(\phi) = 6\mu \left(\frac{r}{c}\right)^2 (\omega - 2\dot{\Psi}) [F_3(\phi) + C_3 F_2(\phi) + C_4] \quad (12)$$

The C's are integral constants, and F_1, F_2, \dots etc. are given in Table 1.

By evaluating the above functions for a full journal bearing, the pressure equations becomes:

$$P(\phi, Z) = \left[1 - \frac{\text{Cosh}(\lambda Z)}{\text{Cosh}(\lambda L/2)} \right] \left[6 \left(\frac{r}{c}\right)^2 \mu \right] \left\{ \dot{\epsilon} \left[\frac{1}{\epsilon(1+\epsilon \cos \phi)^2} - \frac{1}{\epsilon(1+\epsilon^2)^2} \right] \right. \\ \left. + (\omega - 2\dot{\Psi}) \left[\frac{\epsilon \sin \phi (2 + \epsilon \cos \phi)}{(2 + \epsilon^2)(1 + \epsilon \cos \phi)^2} \right] \right\} + P_0 \quad (13)$$

P_0 is the pressure at $\phi = 0$, which during the derivation of Equation (13) was assumed to be zero gauge for simplicity. The pressure as given by Equation (13) attains positive as well as negative values, and will give the pressure of the lubricating film at any point along the width of the bearing (Z directions).

Pressure Forces:

For now it is assumed that all the load carried by the bearing, identified as W_p , may be determined from the

pressure distribution $P(\phi, Z)$. Later, other load terms will be added due to dynamic effects.

From Figure (2):

$$W_{px} = - \int_{-L/2}^{L/2} \int_0^{2\pi} P(\phi, Z) r \cos\phi \, d\phi dZ, \quad (14)$$

$$W_{py} = - \int_{-L/2}^{L/2} \int_0^{2\pi} P(\phi, Z) r \sin\phi \, d\phi dZ \quad (15)$$

Thus, substituting the value of $P(\phi, Z)$ and integrating:

$$W_{px} = - 6rL \left(\frac{r}{c}\right)^2 \mu \eta \{ 2\dot{\epsilon} [F_4(\phi) + C_1 F_5(\phi) + C_2 \sin\phi] + (\omega - 2\dot{\psi}) [F_6(\phi) + C_3 F_5(\phi) + C_4 \sin\phi] \} \quad (16)$$

and

$$W_{py} = 6rL \left(\frac{r}{c}\right)^2 \mu \eta \{ 2\dot{\epsilon} [F_7(\phi) + C_1 F_8(\phi) - C_2 \cos\phi] + (\omega - 2\dot{\psi}) [F_9(\phi) + C_3 F_8(\phi) - C_4 \cos\phi] \} \quad (17)$$

where η , is an oil side-leakage factor for load,

$$\eta = \left[1 - \frac{\tanh\left(\frac{\lambda L}{Z}\right)}{\lambda L/2} \right] \quad (18)$$

Dynamic Forces:

(i) Forces due to displacement of journal center.

In Figure (3), point A represents the location of the journal center at steady-state with ϵ_0, ψ_0 as eccentricity ratio and attitude angle respectively. The coordinate system (x, y) , where the x axis is along the line of centers, has its origin on point A. Point B is the new position of the journal center slightly displaced from point A. Coordinate system (u_i, v_j) has its origin fixed on the bearing center.

Considering forces due to small motion from equilibrium position A to B with respect to coordinate system (x, y) :

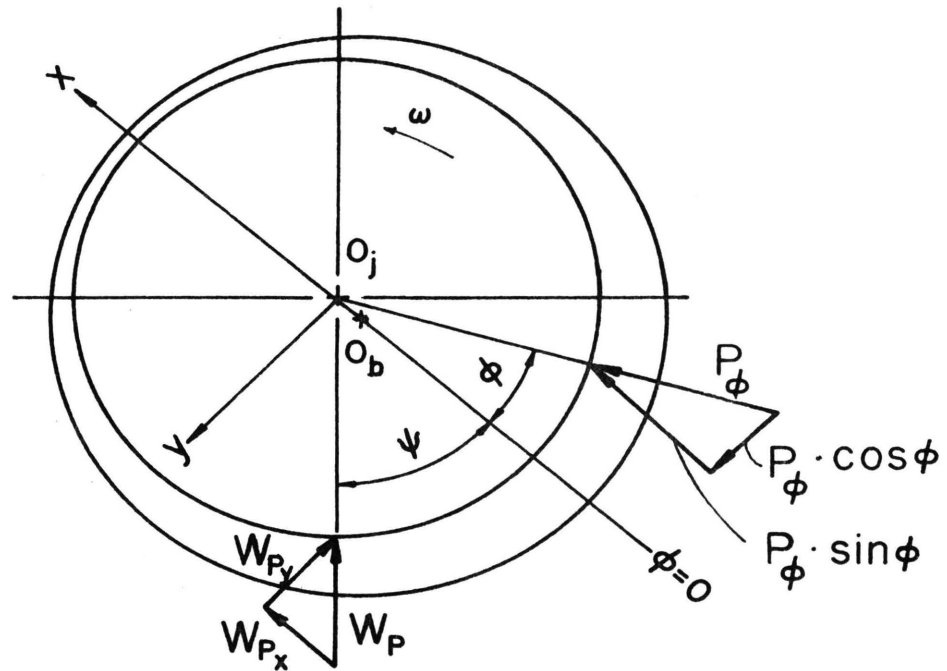


Fig. 2. Pressure Forces.

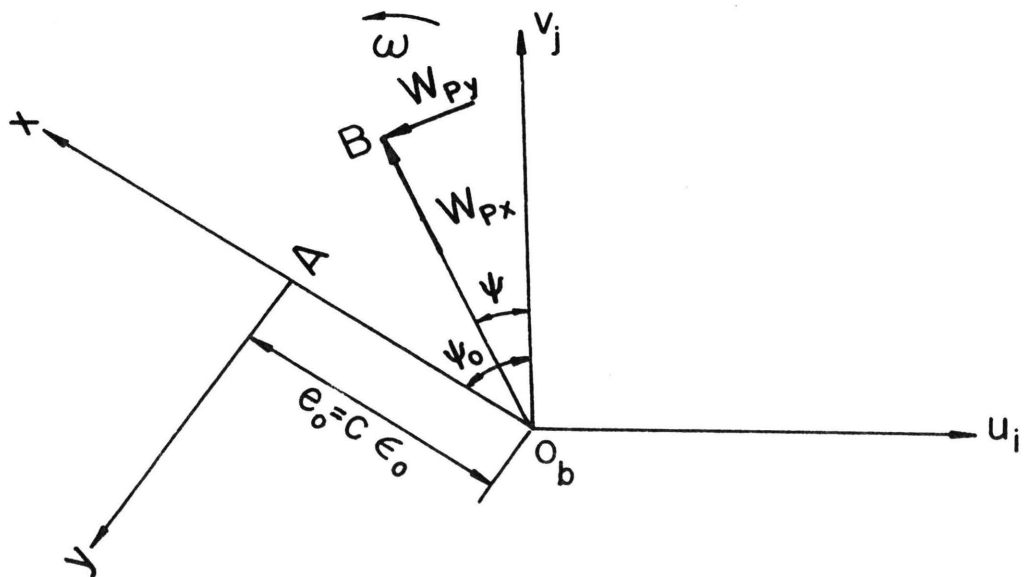


Fig. 3. Displacement Due to Dynamic Forces.

$$F_x = W_{px} \cos(\Psi_0 - \Psi) + W_{py} \sin(\Psi_0 - \Psi) \quad (19)$$

$$F_y = W_{px} \sin(\Psi_0 - \Psi) + W_{py} \cos(\Psi_0 - \Psi) \quad (20)$$

Note from Figure (3) that,

$$\Psi = \Psi_0 + \frac{Y}{e} \quad \text{and} \quad \varepsilon = \varepsilon_0 + \frac{X}{c} \quad (21)$$

Also, assuming a small displacement from point A to B, it may be assumed that:

$$\sin(\Psi_0 - \Psi) = 0, \quad \cos(\Psi_0 - \Psi) = 1 \quad (22)$$

Expanding Equation (19) and Equation (20) by Taylor's series about (ε_0, Ψ_0) :

$$F_x(\varepsilon, \Psi) = F_x(\varepsilon_0, \Psi_0) + K_{xx} X + K_{xy} Y \quad (23)$$

and

$$F_y(\varepsilon, \Psi) = F_y(\varepsilon_0, \Psi_0) + K_{xy} X - K_{yy} Y \quad (24)$$

where:

$$K_{xx} = \frac{1}{c} \frac{\partial W_{px}}{\partial \varepsilon} - \left[\frac{\partial W_{px}}{\partial \Psi} - W_{py} \right] \frac{Y}{e^2} \quad (25)$$

$$K_{xy} = \frac{1}{ce} \left[\frac{\partial W_{px}}{\partial \Psi} - W_{py} \right] \quad (26)$$

$$K_{yx} = \frac{1}{c} \frac{\partial W_{py}}{\partial \varepsilon} - \left[\frac{\partial W_{py}}{\partial \Psi} + W_{px} \right] \frac{Y}{e^2} \quad (27)$$

$$K_{yy} = \frac{1}{ce} \left[W_{px} + \frac{\partial W_{py}}{\partial \Psi} \right] \quad (28)$$

By neglecting higher-order terms, the elastic coefficients will be:

$$K_{xx} = -6L \eta \mu \left(\frac{r}{c}\right)^3 \omega \left[\frac{\partial F_6}{\partial \varepsilon} + C_3 \frac{\partial F_5}{\partial \varepsilon} + F_5 \frac{\partial C_3}{\partial \varepsilon} + \frac{\partial C_4}{\partial \varepsilon} \sin \phi \right]_0^{2\pi} \quad (29)$$

$$K_{xy} = -6L \eta \mu \left(\frac{r}{c}\right)^3 \frac{\omega}{\varepsilon} \left[F_5 \frac{\partial C_3}{\partial \Psi} + \frac{\partial C_4}{\partial \Psi} \sin \phi - F_9 - C_3 F_8 + C_4 \cos \phi \right]_0^{2\pi} \quad (30)$$

$$K_{yx} = 6L \eta \mu \left(\frac{r}{c}\right)^3 \left[\frac{\partial F_9}{\partial \varepsilon} + \frac{\partial C_3}{\partial \varepsilon} F_8 + C_3 \frac{\partial F_8}{\partial \varepsilon} - \frac{\partial C_4}{\partial \varepsilon} \cos \phi \right]_0^{2\pi} \quad (31)$$

$$K_{YY} = -6L \eta \mu \left(\frac{r}{C}\right)^3 \frac{\omega}{\epsilon} [F_6 + C_3 F_5 + C_4 \sin\phi + \frac{\partial C}{\partial \Psi}^3 F_8 - \frac{\partial C}{\partial \Psi}^4 \text{Cos}\phi]_0^{2\pi} (32)$$

(ii) Forces due to velocity of the journal center.

By taking the time derivative of equations (21) and assuming small motions:

$$\dot{\epsilon} = \frac{\dot{X}}{C}, \quad \dot{\Psi} = \frac{\dot{Y}}{e} \quad (33)$$

The velocity vector of the journal center, caused by moving the journal center from A to B in Figure (3), generates forces in the oil film. These forces are thus proportional to the components of velocity \dot{x} and \dot{y} and not the shaft angular velocity ω . Equation (33) is substituted into equations (19) and (20) using the approximation of Equation (22):

$$F_x = B_{xx} \dot{X} + B_{xy} \dot{Y} \quad (34)$$

$$F_y = B_{yx} \dot{X} + B_{yy} \dot{Y} \quad (35)$$

where the damping coefficients are:

$$B_{xx} = -12L \eta \mu \left(\frac{r}{C}\right)^3 [F_4 + C_1 F_5 + C_2 \sin\phi]_0^{2\pi} \quad (36)$$

$$B_{xy} = 12L \eta \mu \left(\frac{r}{C}\right)^3 \frac{1}{\epsilon} [F_6 + C_3 F_5 + C_4 \sin\phi]_0^{2\pi} \quad (37)$$

$$B_{yx} = -12L \eta \mu \left(\frac{r}{C}\right)^3 [F_7 + C_1 F_8 - C_2 \text{Cos}\phi]_0^{2\pi} \quad (38)$$

$$B_{yy} = 12L \eta \mu \left(\frac{r}{C}\right)^3 [F_9 + C_3 F_8 - C_4 \text{Cos}\phi]_0^{2\pi} \quad (39)$$

(iii) Forces due to acceleration of journal center.

Evaluation of the acceleration terms will necessitate taking the inertia of the lubricant into account. The inertia of the journal was considered and found to be small relative to the effect of the lubricant inertia.

Acceleration applied on the running journal will produce

a sudden change in the pressure of the film. The lubricant in the film is accelerated circumferentially and axially in making way for the journal. There is also radial acceleration of the film, but since it is of smaller order compared to the axial and circumferential components, it is neglected.

Figure (4) illustrates a film element of angle $d\phi$ and axial length dz .

In Figure (4b), a_j is the radial acceleration of the journal, a_c the circumferential acceleration, and a_z the axial acceleration of lubricant at angle ϕ . Considering the flow across faces of this element, it is obvious that by virtue of the continuity equation, the summation of volumetric flow for the element must be zero. Thus, differentiating the continuity equation with respect to time, and dividing by $rd\phi dz$ gives:

$$a_j = \frac{1}{r} \frac{\partial}{\partial \phi} (a_c h) + h \frac{\partial a_z}{\partial z} \quad (40)$$

The general form of Navier-Stokes equation (16) consists of an inertia term, pressure gradient terms, and shear terms. In the derivation of Reynolds' equation inertia is neglected. Therefore, neglecting the shear term and considering the inertia terms, the Navier-Stokes equations reduce to:

$$\rho a_c = - \frac{1}{r} \frac{\partial P_a}{\partial \phi} \quad (41)$$

$$\rho a_z = - \frac{\partial P_a}{\partial z} \quad (42)$$

where P_a is the pressure in the film due to acceleration only.

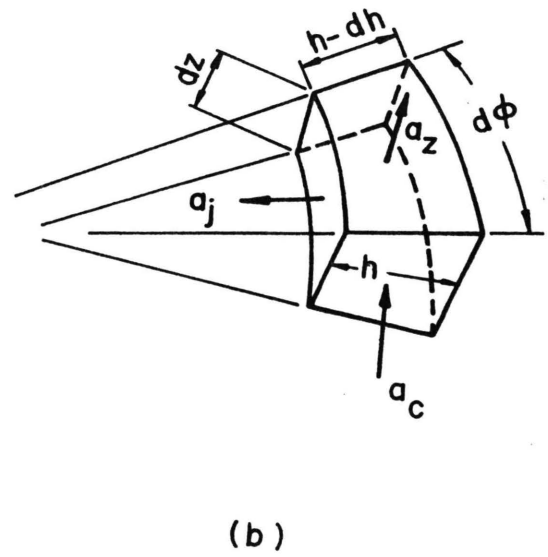
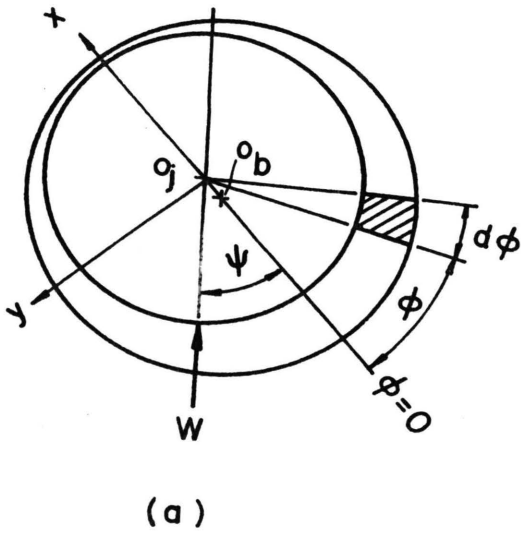


Fig. 4. Film Element.

Substituting Equations (41), (42) and (9) into Equation (40), and writing a_j in terms of its components of the (x,y) coordinate system:

$$\frac{1}{r} \frac{\partial}{\partial \phi} [1 + \epsilon \cos \phi] \frac{\partial P_a}{\partial \phi} + (1 + \cos \phi) \frac{\partial^2 P_a}{\partial z^2} = \frac{\rho}{c} [a_x \cos \phi + a_y \sin \phi] \quad (43)$$

where a_x and a_y are components of a_j in the x and y directions respectively.

Due to the similarity of form between Equation (43) and Equation (3), the same procedure for solution will be employed here. Thus, the pressure distribution due to acceleration will be:

$$P_a(\phi, z) = \left[\frac{\cosh(\lambda_a z)}{\cosh(\lambda_a L/2)} \right] \frac{\rho r^2}{c \epsilon} \left\{ a_x \log_e \left(\frac{1 + \epsilon}{1 + \cos \phi} \right) + a_y [(2\pi - \phi) + \cos^{-1} \left(\frac{\epsilon + \cos \phi}{1 + \epsilon \cos \phi} \right)] \right\} \quad (44)$$

Where λ_a is the eigenvalue calculated from the solution of Equation (43)

Forces due to $P_a(\phi, z)$ can be given as:

$$W_{ax} = M_{xx} \ddot{X} + M_{xy} \ddot{Y} \quad (45)$$

$$W_{ay} = M_{yx} \ddot{X} + M_{yy} \ddot{Y} \quad (46)$$

where in general form:

$$M_{xx} = \frac{r^3 L \rho \eta_a}{c} \left\{ [F'(\phi)]_{\phi_1}^{\phi_1 + \beta} - \frac{[F_2'(\phi)]_{\phi_1}^{\phi_1 + \beta}}{[F_1'(\phi)]_{\phi_1}^{\phi_1 + \beta}} [F_5(\phi)]_{\phi_1}^{\phi_1 + \beta} + [-F_2'(\phi_1 + \beta)] + \frac{[F_2'(\phi)]_{\phi_1}^{\phi_1 + \beta}}{[F_2'(\phi)]_{\phi_1}^{\phi_1 + \beta}} F_1'(\phi_1 + \beta) \right\} [\sin \phi]_{\phi_1}^{\phi_1 + \beta} \quad (47)$$

$$M_{xy} = -\frac{r^3 L \rho \eta_a}{C} \left\{ [F_5(\phi)]_{\phi_1}^{\phi_1+\beta} + \frac{[F_3(\phi)]_{\phi_1}^{\phi_1+\beta}}{[F_1(\phi)]_{\phi_1}^{\phi_1+\beta}} [F_5(\phi)]_{\phi_1}^{\phi_1+\beta} + \right. \\ \left. [F_3(\phi_1+\beta) - \frac{[F_3(\phi)]_{\phi_1}^{\phi_1+\beta}}{[F_1(\phi)]_{\phi_1}^{\phi_1+\beta}} F_1(\phi_1+\beta)] [\sin\phi]_{\phi_1}^{\phi_1+\beta} \right\} \quad (48)$$

$$M_{yx} = \frac{r^3 L \rho \eta_a}{C} \left\{ [F_6(\phi)]_{\phi_1}^{\phi_1+\beta} - \frac{[F_2(\phi)]_{\phi_1}^{\phi_1+\beta}}{[F_1(\phi)]_{\phi_1}^{\phi_1+\beta}} [F_4(\phi)]_{\phi_1}^{\phi_1+\beta} + \right. \\ \left. [F_2(\phi_1+\beta) - \frac{[F_2(\phi)]_{\phi_1}^{\phi_1+\beta}}{[F_1(\phi)]_{\phi_1}^{\phi_1+\beta}} F_1(\phi_1+\beta)] [\cos\phi]_{\phi_1}^{\phi_1+\beta} \right\} \quad (49)$$

$$M_{yy} = \frac{r^3 L \rho \eta_a}{C} \left\{ -[F_8(\phi)]_{\phi_1}^{\phi_1+\beta} + \frac{[F_3(\phi)]_{\phi_1}^{\phi_1+\beta}}{[F_1(\phi)]_{\phi_1}^{\phi_1+\beta}} [F_4(\phi)]_{\phi_1}^{\phi_1+\beta} - \right. \\ \left. [F_3(\phi_1+\beta) - \frac{[F_3(\phi)]_{\phi_1}^{\phi_1+\beta}}{[F_1(\phi)]_{\phi_1}^{\phi_1+\beta}} F_1(\phi_1+\beta)] [\cos\phi]_{\phi_1}^{\phi_1+\beta} \right\} \quad (50)$$

For a full journal bearing, $\phi_1=0$, $\beta=2\pi$ and,

$$\eta_a = \left[1 - \frac{\tanh\left(\frac{\lambda a L}{2}\right)}{\lambda_a L/2} \right] \quad (51)$$

F's are given in Table (2).

General Equation:

Assuming that the principle of superposition applies to a full journal bearing subjected to a unidirectional load with time-varying magnitude, the equation of motion can be written by adding equations (23), (24), (34), (35), (45) and (46):

$$\begin{array}{l}
 \text{External} \\
 \text{Load}
 \end{array}
 \begin{array}{l}
 \left\{ \begin{array}{l} W_x \\ W_y \end{array} \right\} \\
 = \\
 \begin{array}{l}
 \text{Steady State} \\
 \text{Force} \\
 \left\{ \begin{array}{l} F_x(\epsilon_0, \psi_0) \\ F_y(\epsilon_0, \psi_0) \end{array} \right\} \\
 + \\
 \underbrace{\hspace{10em}}_{\text{Dynamic - Forces}} \\
 \left[\begin{array}{cc} K_{xx} & K_{xy} \\ K_{yx} & -K_{yy} \end{array} \right] \begin{Bmatrix} X \\ Y \end{Bmatrix} + \left[\begin{array}{cc} B_{xx} & B_{xy} \\ -B_{yx} & -B_{yy} \end{array} \right] \begin{Bmatrix} \dot{X} \\ \dot{Y} \end{Bmatrix} + \left[\begin{array}{cc} M_{xx} & M_{xy} \\ -M_{yx} & -M_{yy} \end{array} \right] \begin{Bmatrix} \ddot{X} \\ \ddot{Y} \end{Bmatrix}
 \end{array}
 \end{array}
 \quad (52)$$

For an external load shown in Figure (1):

$$W = W_0 + W_1 \sin \omega_d t$$

$$W_x = W \cos \psi_0 \quad W_y = W \sin \psi_0$$

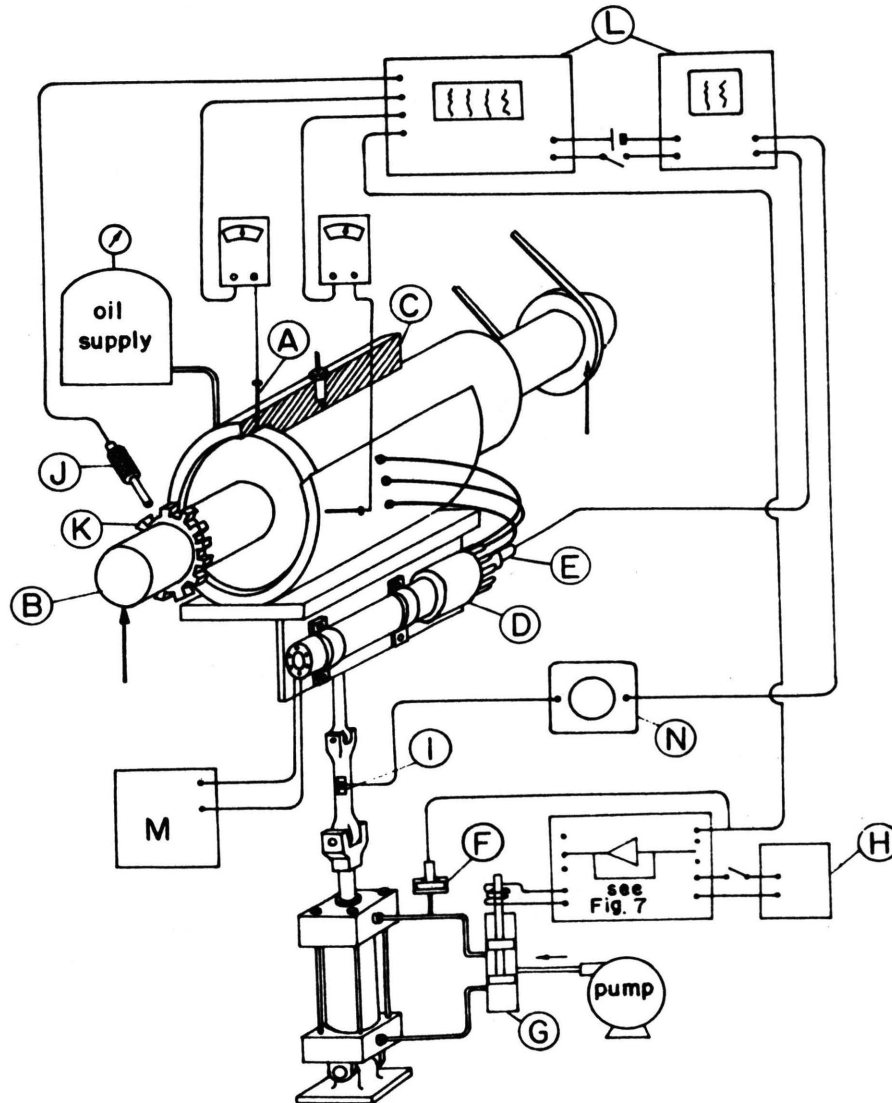
Also

$$F_x(\epsilon_0, \psi_0) = W_0 \cos \psi_0, \quad F_y(\epsilon_0, \psi_0) = W_0 \sin \psi_0$$

Equation (52) can be solved by the Runge-Kutta fourth-order numerical method employing a digital computer.



Fig. 5 General view of apparatus



- | | |
|-----------------------------------|----------------------------------|
| A - Proximity sensors | H - Oscillator |
| B - Journal | I - Strain gage |
| C - Bearing | J - Magnetic sensor |
| D - Scanning valve | K - Timing gear |
| E - Pressure transducer | L - Recorders |
| F - Feed-back pressure transducer | M - Scanning valve control panel |
| G - Servo-valve | N - Amplifier |

Fig. 6. Schematic of Apparatus.

II. EXPERIMENTAL WORK

Experimentation was necessary in order to assess the validity of simplifications in the analytical model. Specifically, the experiment examined the soundness of the assumptions governing the form and extent of the pressure distribution in the oil film.

A test rig was designed to investigate the performance of a full journal bearing under a unidirectional cyclic load, $W = W_0 + W_1 \cdot \sin(\omega_d t)$.

Description of the Apparatus:

The complete test rig is shown in Figure (5), and the schematic arrangement of the apparatus is shown in Figure (6). The method of loading and the apparatus for measuring the bearing displacement and pressure in the clearance space are shown in Figure (6).

The 127.0mm. (5.0in) diameter steel shaft was carried in two tapered roller bearings, which were pre-loaded to absorb any play of the journal. The journal was driven by a $\frac{1}{2}$ hp. D.C. motor, thru a V belt variable-speed drive.

The recess shoulder of the bearing, Figure (6), was aligned with the step on the journal. Proximity devices mounted in the bearing shoulder were employed to measure the relative displacement of the bearing and journal.

Twenty-three equally-spaced holes one millimeter in diameter were drilled radially into the bearing to measure the pressure distribution. The effect of the one millimeter

diameter holes on the film pressure was considered negligible. Oil was supplied to the bearing thru one of the holes which was enlarged and connected to a pressurized oil tank.

The load was applied to the loading block beneath the journal bearing through a hydraulic cylinder and tie rod. The tie rod was connected at both ends to spherical bearings in order to eliminate force components along the journal-bearing length.

Instrumentation:

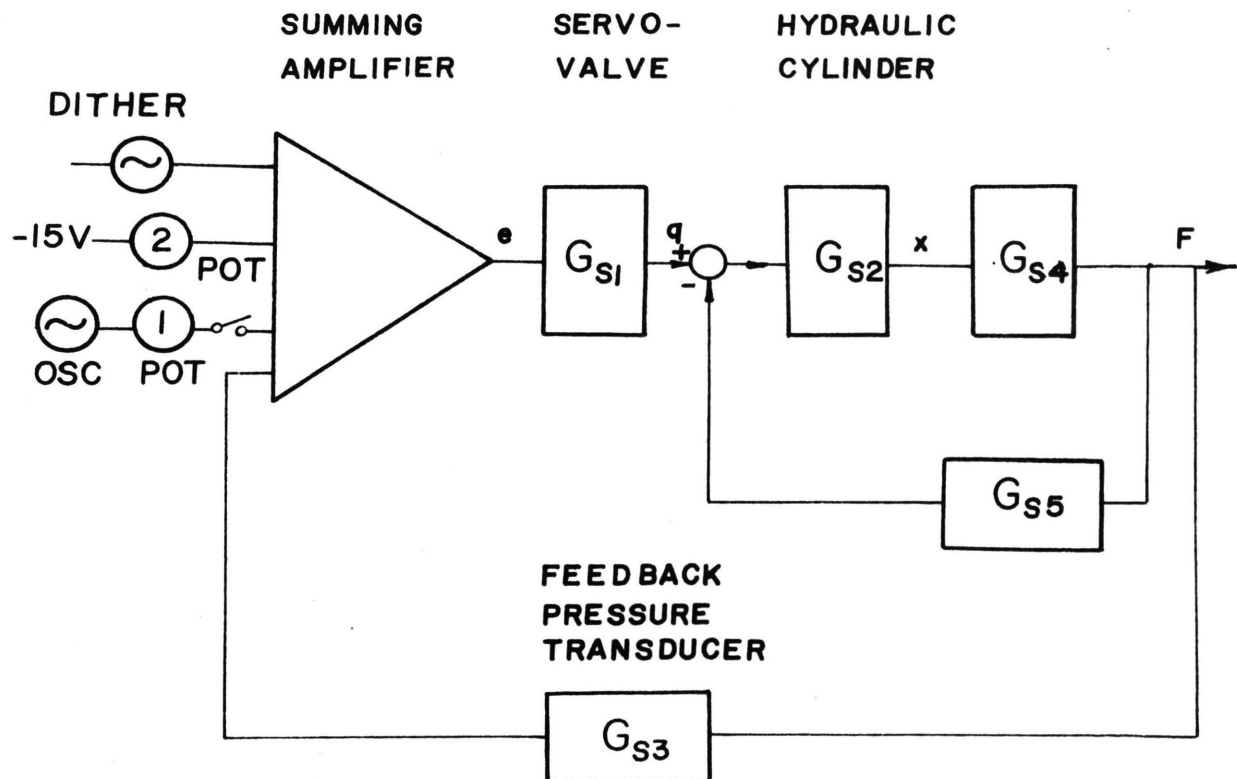
The relative displacement between journal and bearing in both the horizontal and vertical directions was measured with photonic proximity sensors (A), (Figure 6), whose outputs were recorded. These sensors were calibrated to compensate for the finish of the journal step surface.

A magnetic sensor was installed on the frame in proximity to an irregular spline on the journal to serve as an accurate means of measuring journal rotational speed, and as a reference for the rotational position of various data.

Pressure measurements in the oil film were taken with a scanning valve allowing the measurement of pressure from twelve ports with a single pressure transducer.

A servo-valve feedback control system, Figure (7) enabled dynamic loading of the hydraulic cylinder. A potentiometer type pressure transducer was used to feed back cylinder pressure to the summing amplifier Figure (6). This prevented drifting of the load.

For load measurement, a strain gage was mounted on the



G_{S1} = Servo-valve constant

POT - Potentiometer

G_{S2} = Hydraulic cylinder constant

OSC = Oscillator

G_{S3} = Feedback pressure transducer

e = Voltage

G_{S4} = Elastic constant of the system

q = Flow

x = Displacement

G_{S5} = Resistance of the system to hydraulic cylinder

F = Force to bearing

Fig. 7. Control Diagram.

tie rod. Temperature of the outlet oil was measured by a thermocouple.

The output of the two-channel and four-channel recorders was time synchronized by the use of an external circuit.

Test procedure:

The bearing was pressure-fed with oil, and an oil film was allowed to surround the journal before the motor was started under zero external load. Next, some small amount of load was placed on the bearing, and allowed to run until the outlet oil temperature and all apparatus reached steady state.

The desired static load was reached by adjusting potentiometer 2. Then, a complete set of data was taken, which included, journal center loci, film pressure, journal speed, outlet oil temperature, and the feedback pressure transducer output.

Since steady-state and transient data were to be taken for the case of dynamic loading, potentiometer 1 [Figure (7)] was adjusted to a pre-determined position before the oscillator was actuated. Hence, transient data was obtained instantly after the oscillator was switched into the system.

A complete set of observations was taken under this dynamic load. This included, recording of journal center loci, film pressure, load, rotational speed of journal, output of feed back pressure transducer, and oil temperature. Also recorded were frequency of the oscillator, recorder speeds, density and viscosity of oil for proper temperatures.

Results:

Experimental and analytical bearing film pressure distribution for various loads is shown in Figure (8). In all tests the same oil inlet position was used. Oil entered the bearing through a partial circumferential groove. It is apparent from Figure (8) that a shift exists between the experimental and analytical curves. Carl [17] has shown that if viscosity is assumed to be a function of both temperature and pressure, the shift can be minimized. Although the pressure equation used by Carl is not exactly the same as the one used here, it is assumed that his procedure could be used to correct for the shift.

Figure (9) is a polar plot of typical experimental and analytical pressure distribution. The analytical curve demonstrates that pressure increases gradually from the inlet pressure of 29 psi at $\phi = 337.5^\circ$, to a maximum value. The peak pressure is followed by a sharp decline which falls rapidly to a negative pressure over a certain arc of the bearing. The length of the arc of negative pressure depends on the lubricant inlet location. Radzimovsky [18] points out that, oil cannot withstand tension or negative pressure, therefore, the oil film breaks soon after the pressure becomes less than atmospheric. Hence, the actual pressure in the region becomes atmospheric. This is confirmed by the experimental curve. Note that the same shift exists here as in Figure (8).

Figure (10) shows the hydrodynamic pressure $P(\phi, z)$, of

Equation (13), around the dynamically loaded bearing, and $P_a(\phi, a)$ of Equation (44), the pressure due to journal center acceleration. The plots show the value of $P_a(\phi, z)$ to be much smaller than the hydrodynamic pressure $P(\phi, a)$. The maximum, intermediate, and minimum pressures for $P(\phi, z)$ and $P_a(\phi, z)$ have been plotted for a given dynamic load. The time variation of $P_a(\phi, z)$ is more pronounced than the variation of $P(\phi, z)$. As far as pressure magnitude is concerned, the effect of lubricant inertial is small.

Figure (11) illustrates the experimental and analytical time variation of journal center displacement under a dynamic load. The amplitudes of the two curves correspond closely, but there is a phase lag between the experimental and analytical results. In an attempt to correlate the phase lag to physical phenomena a load was placed on the bearing in the form of a step function. The experimental response was assumed to be that of a first order system. This approach gives the bearing load as $W_0 + \frac{W_0}{\sqrt{1+(\tau\omega_d)^2}} \sin[\omega_d t - \tan^{-1}(\tau\omega_d)]$,

where, τ , is the time constant of the system. Calculation of u_i and v_j for this load gives much closer correlation between experimental and analytical results as shown in Figure (12).

Figure (13) shows the pressure fluctuation for the point of maximum pressure under dynamic load at $\phi = 11.0^\circ$. The same phase lag is present. Thus, by using the same time constant Figure (14) is obtained. Note that the amplitude of the analytical results is smaller than the

experimental.

Further investigation indicated that the system response depends on eccentricity ratio.

The experimental and analytical loci of the journal center is shown in Figure (15). It can be seen that the experimental data follows approximately a semi-circular path. Due to the limitation of the D.C. Motor, which drove the journal, higher eccentricities could not be obtained.

Figures (16) and (17) show the analytical results of the time variation of the attitude angle, ψ , and eccentricity ratio, ϵ , respectively. There is a small transient time before reaching steady-state sinusoidal values for both, ψ , and ϵ .

Figure (18), the plot of $\dot{\psi}$, is also the angular velocity of the line of centers versus time. It shows how the line of centers oscillates for the dynamic loading. The same is true for $\dot{\epsilon}$, [Figure (19)] which is proportional to the velocity of the journal center along the x axis.

The curve in Figure (20) represents the relationship between the eccentricity ratio, ϵ , and the Sommerfeld number S .

Figure (21) shows the inertia terms of Equation (52) in non-dimensional form vs. the Sommerfeld number. The values of terms M_{xy} and M_{yx} are zero. M_{yy} is larger than M_{xx} for all the Sommerfeld numbers larger than $S = .125$. This complies with the fact that there is more mass of oil located along an arc normal to the y axis because of larger clearance.

The curves in Figure (22) represent the variation of damping coefficients with respect to Sommerfeld number ($B_{xy} = B_{yx} = 0$). Damping coefficients increase very rapidly for high eccentricity ratios (low S).

The non-dimensional K terms in Figures (23), (24) and (25) approach large values for high eccentricity ratios.

In Figure (26), the calculated side leakage factor for the load is compared to two previous works. The value of η , agrees rather closely to the analytical results of Pinkus [19], but the factor that is given by Fuller [20] is somewhat larger. However, the trend of all three curves are similar. Fuller obtained these values for full journal bearing by interpolating and extrapolating from the original work done by Kingsbury and Needs [21], which was for the 120-degree centrally loaded partial journal bearings. It is necessary to point out that for calculating, η , the function $g(\phi) = F_a(\phi) + F_b(\phi)$ in Equation (7) was used.

Conclusions and Recommendations:

Examination of results obtained show that there is a reasonable correlation between the experimental and analytical results.

As was mentioned in the previous section in studying the dynamic response of the bearing, an experimental frequency response was performed. Concurrent to this, the characteristic equations were determined for x , and y . They are fourth-order polynomials, having negative, real and/or imaginary roots. The analytical values of natural frequencies, ω_n , and damping ratios, ζ , for the various eccentricity ratios were examined. Because $B_{xy} = B_{yx} = 0$, the analysis became easier.

After studying these values and also examining the result of the experimental frequency response, it was concluded that the response of the bearing is different at different eccentricity ratios. In other words, at low eccentricity ratios, the bearing acts as a second order lightly damped system, and at high eccentricity ratios, it would act as a second order heavily-damped system. This, of course, is quite important for the designer to know, since it enables him, for a given operating load, to choose the kind of system he desires. Hence, if he obtains a system which has its natural frequencies much lower than the dynamic load frequency, ω_d , the effect of dynamic load would be quite small. He then could design the bearing considering only static load and obtain a very good approximate solution.

However, if the break-points are relatively close to ω_d , he should then proceed to choose an operating range of eccentricity ratio ε_0 . Knowing journal diameter, static load, dynamic load and frequency, angular speed of the journal, and parameters like clearance ratio, viscosity of lubricant and others, he could determine dynamic displacements (u_i, v_j) . Minimum film thickness can be found, which should be within the recommended range for a particular bearing surface finish.

The relative error for the analytical results was found to be less than 7.0 percent. But, in calculating the loci of journal center, it was noticed that the results are sensitive to the variation of radial clearance. Therefore, care should be exercised in obtaining the value of radial clearance.

TABLE 1

$A = 1 + \epsilon \cos \phi$	$= \frac{\epsilon + \cos \phi}{1 + \epsilon \cos \phi}$	$B = 1 - \epsilon^2$ $\delta = \begin{cases} \text{lsin} \phi > 0 \\ -\text{lsin} \phi < 0 \end{cases}$
$F_1(\phi) = \int \frac{\sin \phi d\phi}{A^3} = \frac{1}{2A}$		
$F_2(\phi) = \int \frac{d}{A^3} \frac{1}{2B} \left[\frac{-\epsilon \sin \phi}{A^2} - \frac{3\epsilon \sin \phi}{A \cdot B} + \frac{\delta(2+\epsilon^2)}{B^{3/2}} \cos^{-1} \gamma \right]$		
$F_3(\phi) = \int \frac{d\phi}{A^2} = \frac{1}{B} \left[\frac{-\epsilon \sin \phi}{A} + \frac{\delta}{B^{1/2}} \cos^{-1} \gamma \right]$		
$F_4(\phi) = \int F_1 \cos \phi d\phi = \frac{1}{2B} \left[\frac{\sin \phi}{\epsilon A} - \frac{\delta}{B^{1/2}} \cos^{-1} \gamma \right]$		
$F_5(\phi) = \int F_2(\phi) \cos \phi d\phi = \frac{1}{2B} \left[\frac{B+3\epsilon A \cos \phi}{\epsilon \cdot A \cdot B} + (\delta-1) \frac{2+\epsilon^2}{\epsilon B} \log_e A + \frac{\delta(2+\epsilon^2)}{B^{3/2}} \cos^{-1} \gamma \right]$		
$F_6(\phi) = \int F_3(\phi) \cos \phi d\phi = \frac{1}{B} \left[\cos \phi + \frac{(\delta-1)}{\epsilon} \log_e A + \frac{\delta \sin \phi}{B^{1/2}} \cos^{-1} \gamma \right]$		
$F_7(\phi) = \int F_1(\phi) \sin \phi d\phi = \frac{1}{2\epsilon^2 A}$		
$F_8(\phi) = \int F_1(\phi) \sin \phi d\phi = \frac{1}{2B} \left[\frac{2+\epsilon^2+3\epsilon \cos \phi}{A \cdot B} \sin \phi + \frac{\delta[2B-A(2+\epsilon^2)]}{\epsilon B^{3/2}} \cos^{-1} \gamma \right]$		
$F_9(\phi) = \int F_3(\phi) \sin \phi d\phi = \frac{1}{B} \left[\sin \phi + \frac{\delta(B-A)}{\epsilon \cdot B^{1/2}} \cos^{-1} \gamma \right]$		
$F_{10}(\phi) = \int \frac{d\phi}{A} = \frac{\delta}{B^{1/2}} \cos^{-1} \gamma$		
$F_{11}(\phi) = \int \frac{\sin^2 \phi}{A^3} d\phi = \frac{1}{\epsilon^2} [-BF_2(\phi) + 2F_3(\phi) - F_{10}(\phi)]$		
$F_{12}(\phi) = \int \frac{\sin}{A^2} = \frac{1}{\epsilon A}$		

TABLE 2

$A = 1 + \cos\phi$	$\gamma = \frac{\epsilon + \cos\phi}{1 + \epsilon\cos\phi}$	$B = 1 - \epsilon^2$
		$\delta = 1$ if $\sin\phi > 0$
		$= -1$ if $\sin\phi < 0$
$F_1'(\phi) = \int \frac{d\phi}{A} = \frac{\delta}{B^{1/2}} \cos^{-1} \gamma$		
$F_2'(\phi) = \int \frac{\sin\phi d\phi}{A} = -\frac{1}{\epsilon} \log_e A$		
$F_3'(\phi) = \int \frac{\cos\phi d\phi}{A} = \frac{1}{\epsilon} [-F_1'(\phi) + \phi]$		
$F_4'(\phi) = \int F_1'(\phi) \sin\phi d\phi = \frac{\delta}{B^{1/2}} [\cos\phi \cos^{-1} \gamma - \frac{\delta}{\epsilon} \cos\gamma^{-1} + \frac{\phi}{\epsilon B^{1/2}}]$		
$F_5'(\phi) = \int F_1'(\phi) \cos\phi d\phi = \frac{\delta}{B^{1/2}} [\sin\phi \cos^{-1} \gamma + \frac{B^{1/2}}{\epsilon} \log_e A]$		
$F_6'(\phi) = \int F_2'(\phi) \sin\phi d\phi = \frac{1}{\epsilon} [(\cos\phi + \frac{1}{\epsilon}) \log_e A - \cos\phi]$		
$F_7'(\phi) = \int F_2'(\phi) \cos\phi d\phi = \frac{-\sin\phi}{\epsilon} \log_e A + \frac{B^{1/2}}{\epsilon^2} \cos^{-1} \gamma$		
$F_8'(\phi) = \int F_3'(\phi) \sin\phi d\phi = \frac{1}{\epsilon} [-F_4'(\phi) + \sin\phi - \phi \cdot \cos\phi]$		
$F_9'(\phi) = \int F_3'(\phi) \cos\phi d\phi = \frac{1}{\epsilon} [-F_5'(\phi) + \phi \sin\phi + \cos\phi]$		

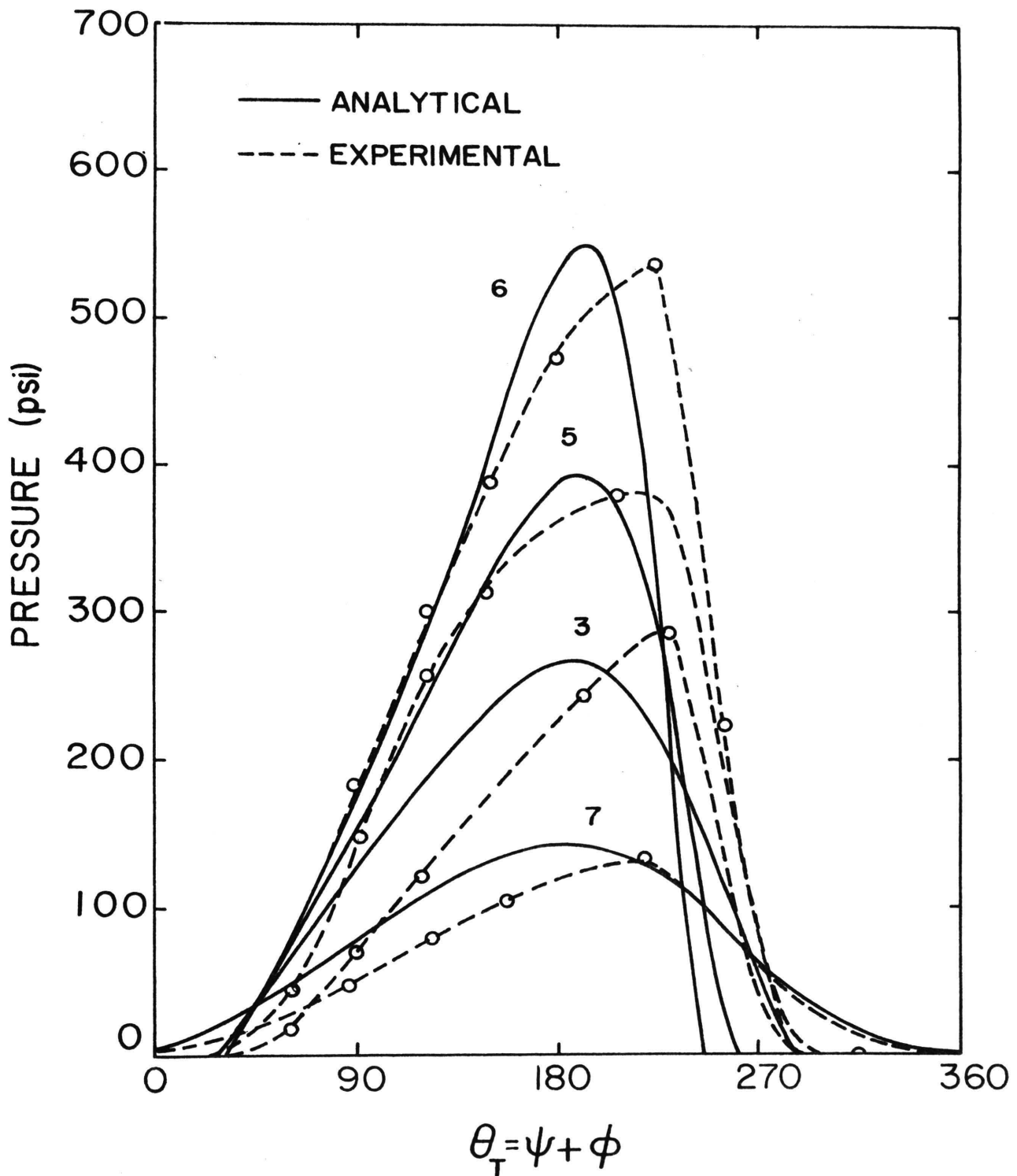
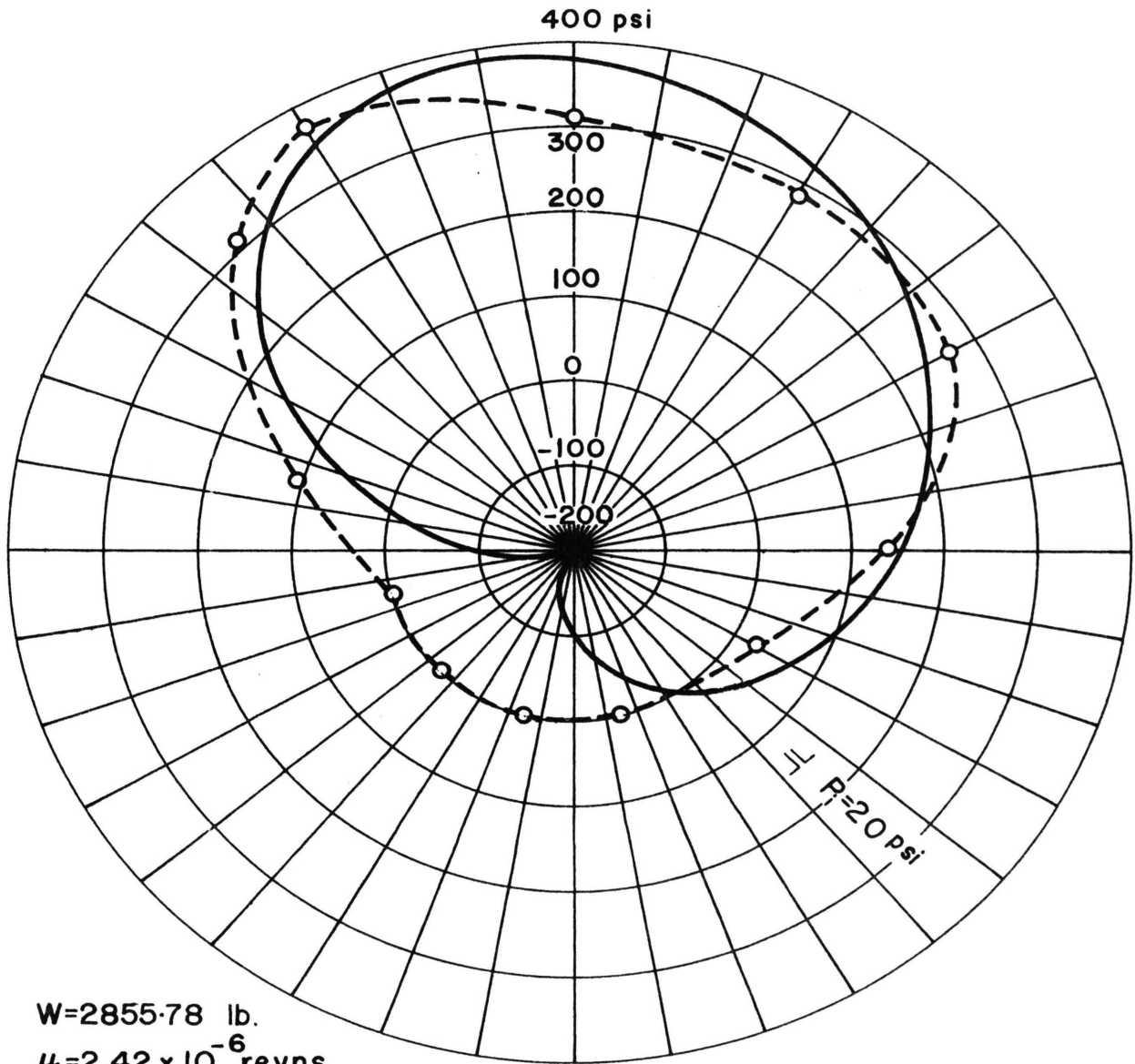


Fig. 8. Experimental and Analytical Pressure Distribution For Various Static Load.

Data For Fig. 8

Curve No.	W (lb.)	(reyns) μ	(R.P.M.) N	(PSI) P_o	(in.) C
3	1550	2.42×10^{-6}	533	29	0.00255
5	2750	2.44×10^{-6}	490	28	"
6	4250	2.43×10^{-6}	474	26	"
7	650	2.46×10^{-6}	510	27	"



$W=2855.78$ lb.
 $\mu=2.42 \times 10^{-6}$ reyns.

$N=495$ RPM.

——— ANALYTICAL
 - - - - EXPERIMENTAL

Fig. 9. Experimental and Analytical Pressure Distribution

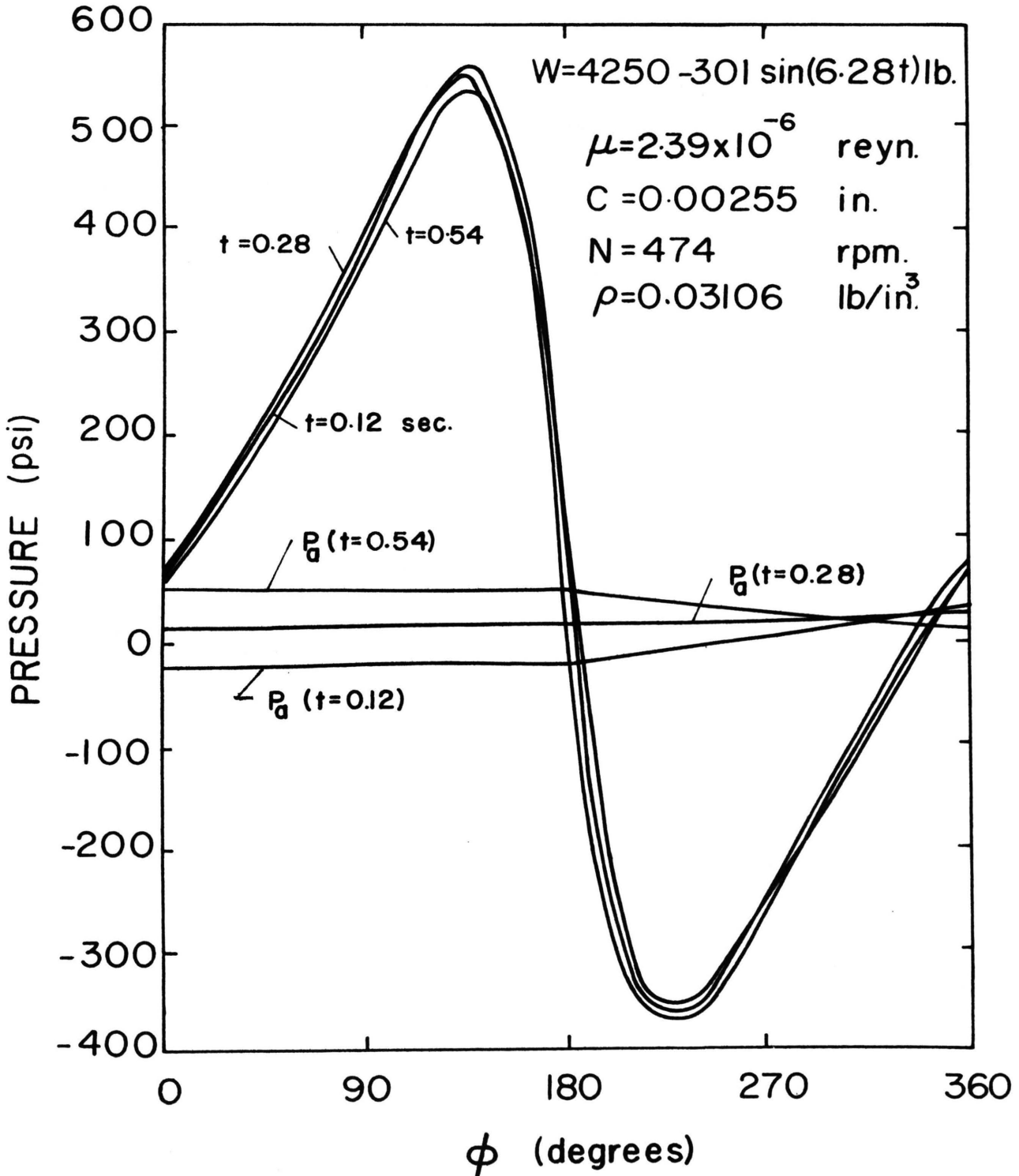


Fig. 10. Comparison of $P(\phi, Z)$ and $P_a(\phi, Z)$.

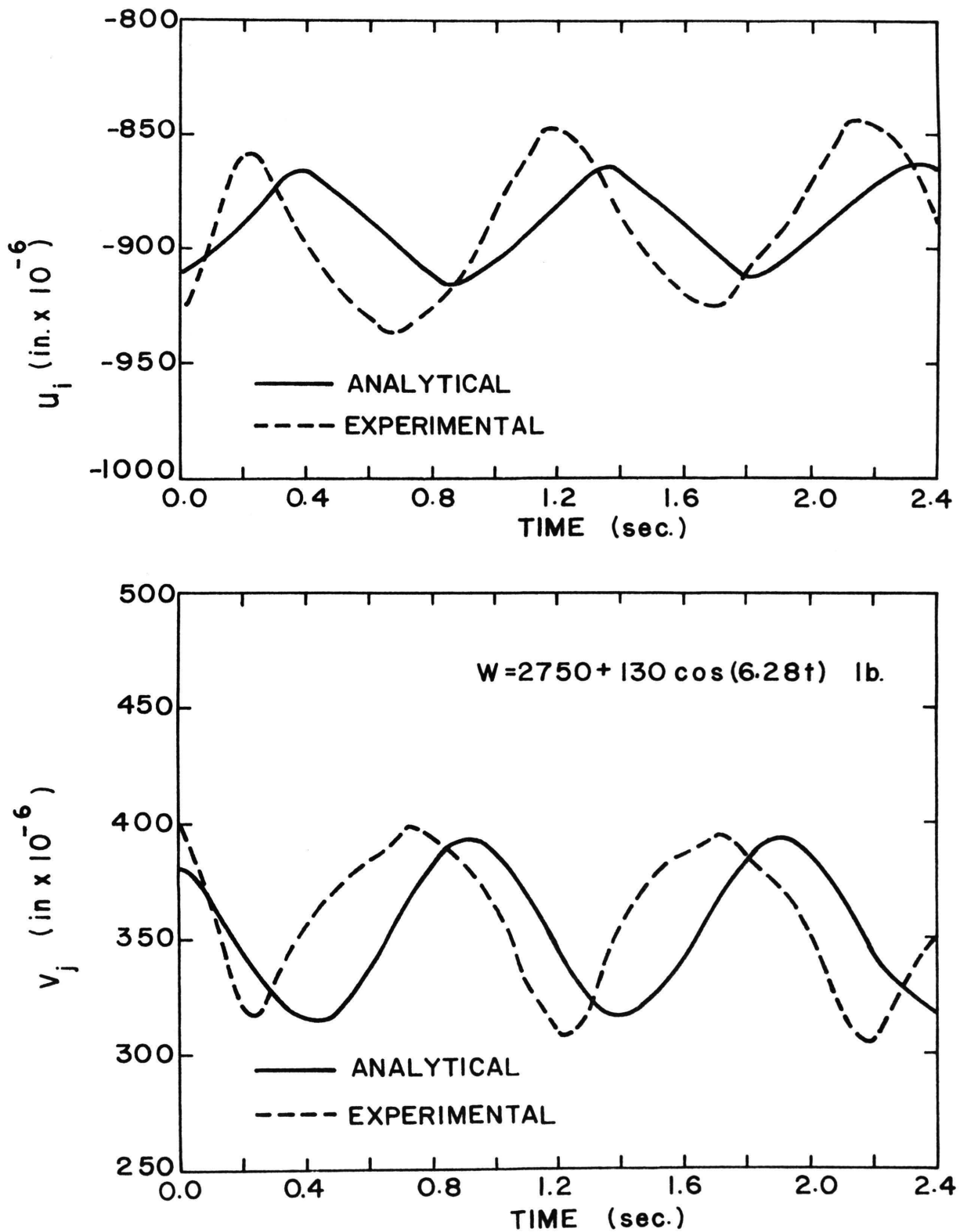


Fig. 11. Dynamic Displacement of Journal Center.

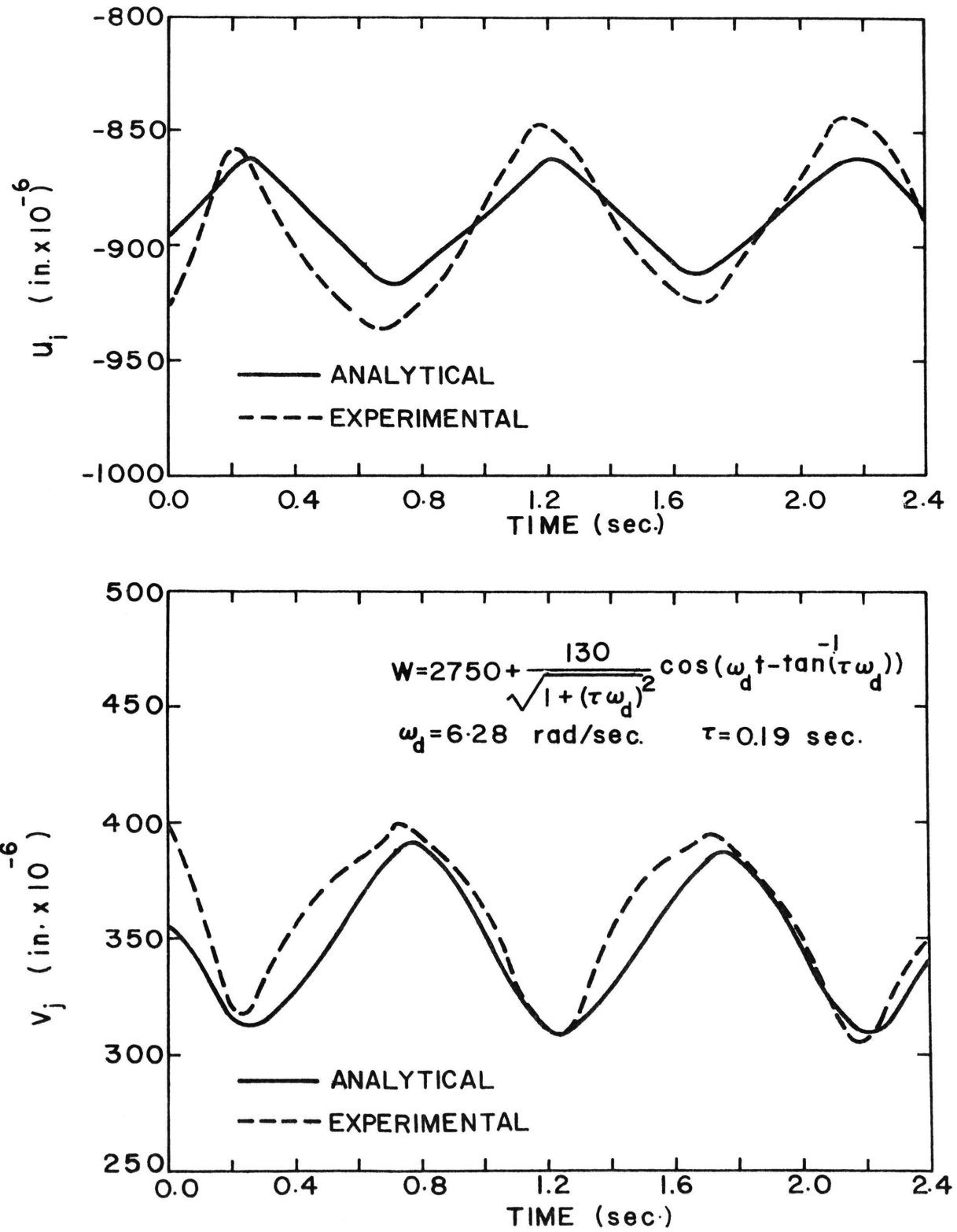


Fig. 12. Corrected Dynamic Displacements.

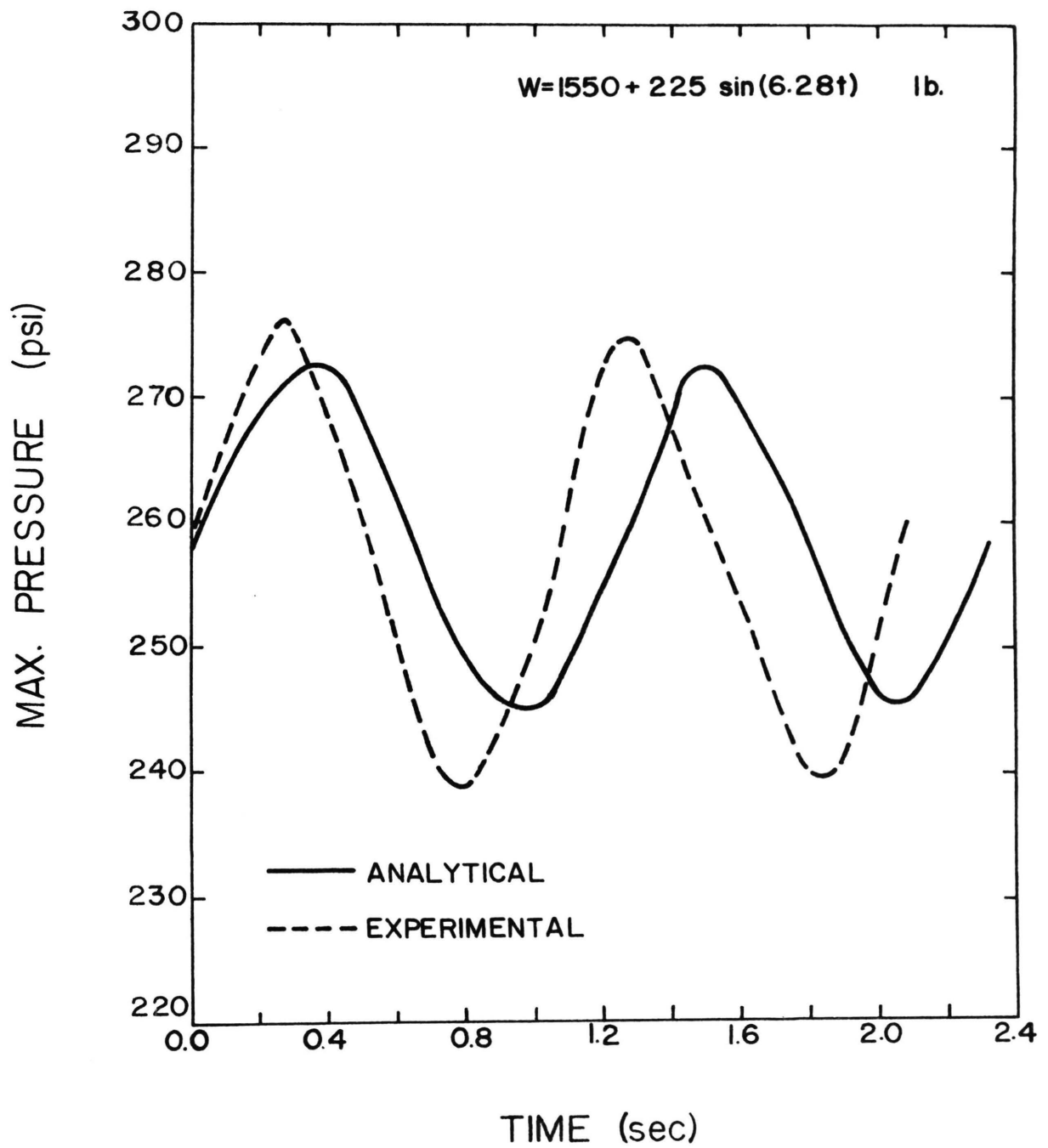


Fig. 13. Variation of Maximum Pressure.

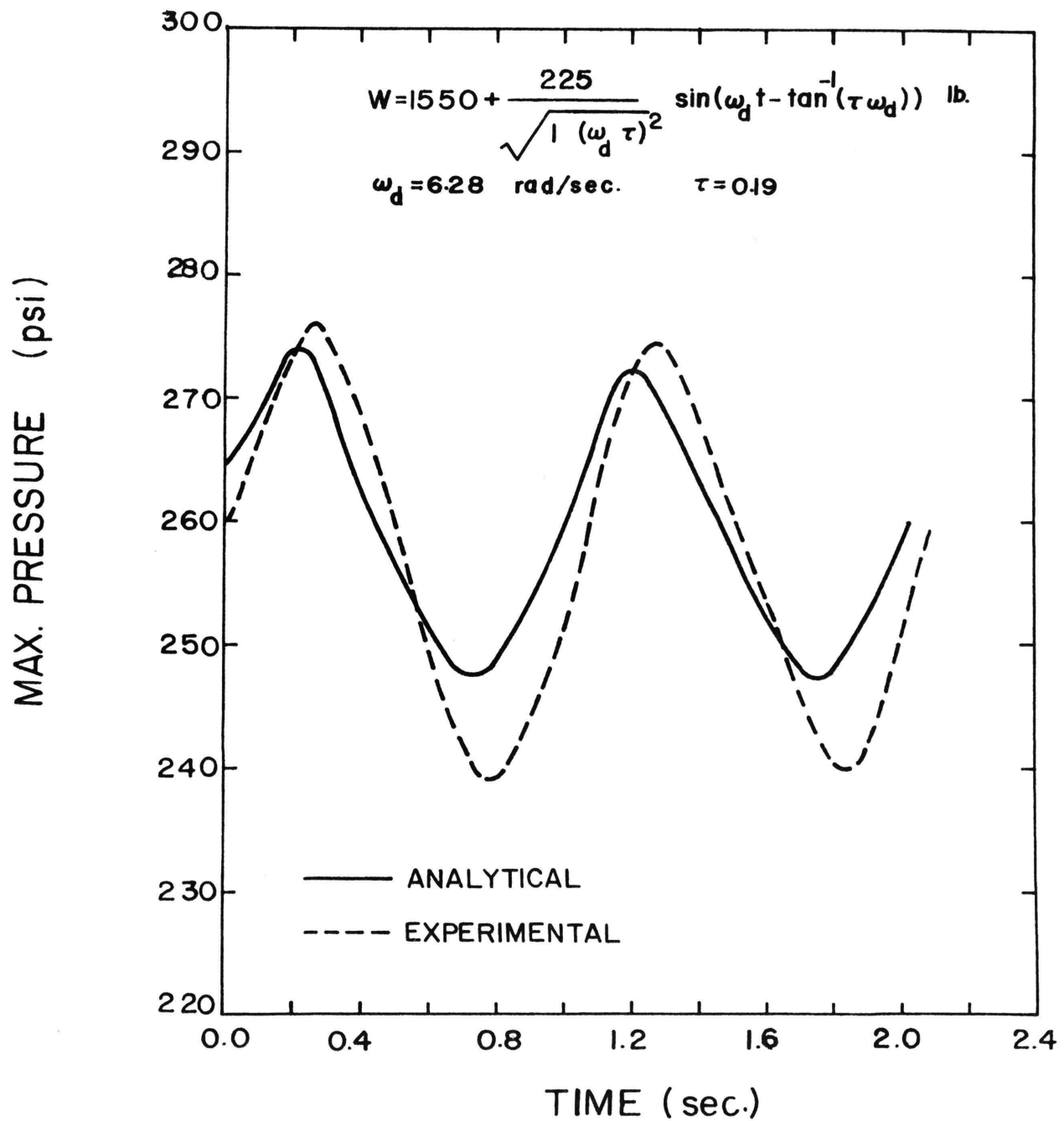


Fig. 14. Corrected Maximum Pressure.

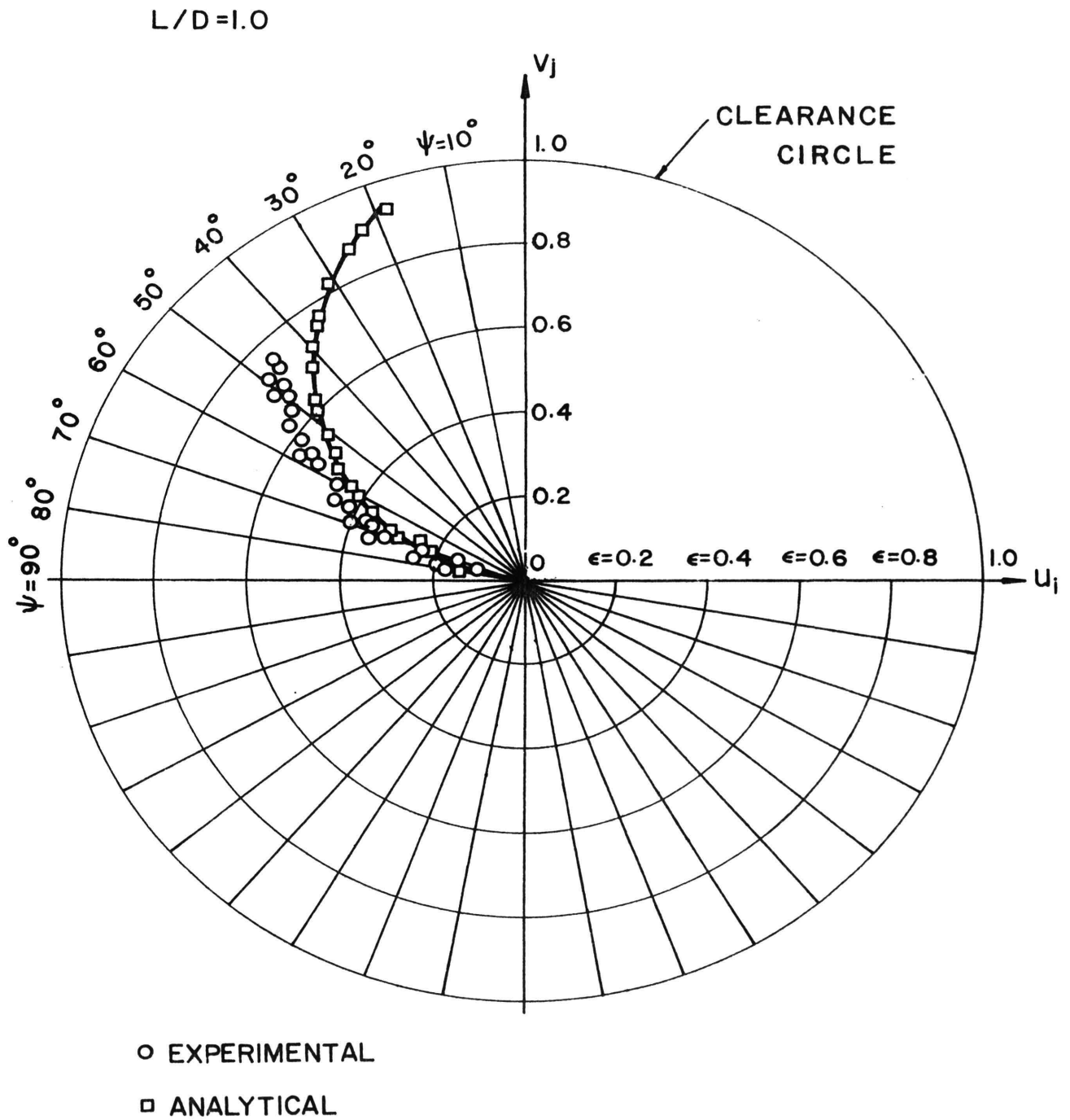


Fig. 15. Journal Center Loci.

$$W = 4250 + 30 \sin(6.28t) \text{ lb.}$$

$$\mu = 2.39 \times 10^{-6} \text{ reyns.}$$

$$C = 0.00255 \text{ in.}$$

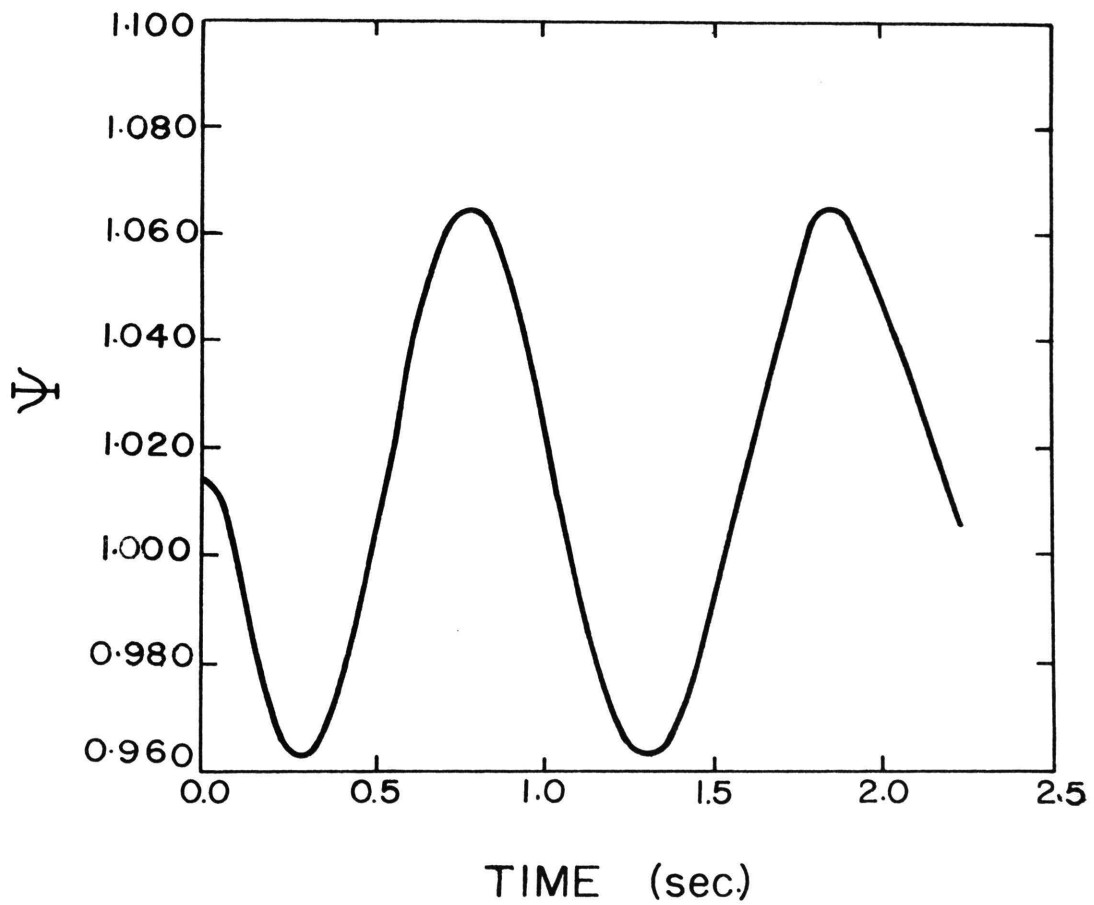


Fig. 16. Ψ vs. time.

$$w = 4250 + 301 \sin(6.28t) \text{ lb.}$$

$$\mu = 2.39 \times 10^{-6} \text{ reyns.}$$

$$C = 0.00255 \text{ in.}$$

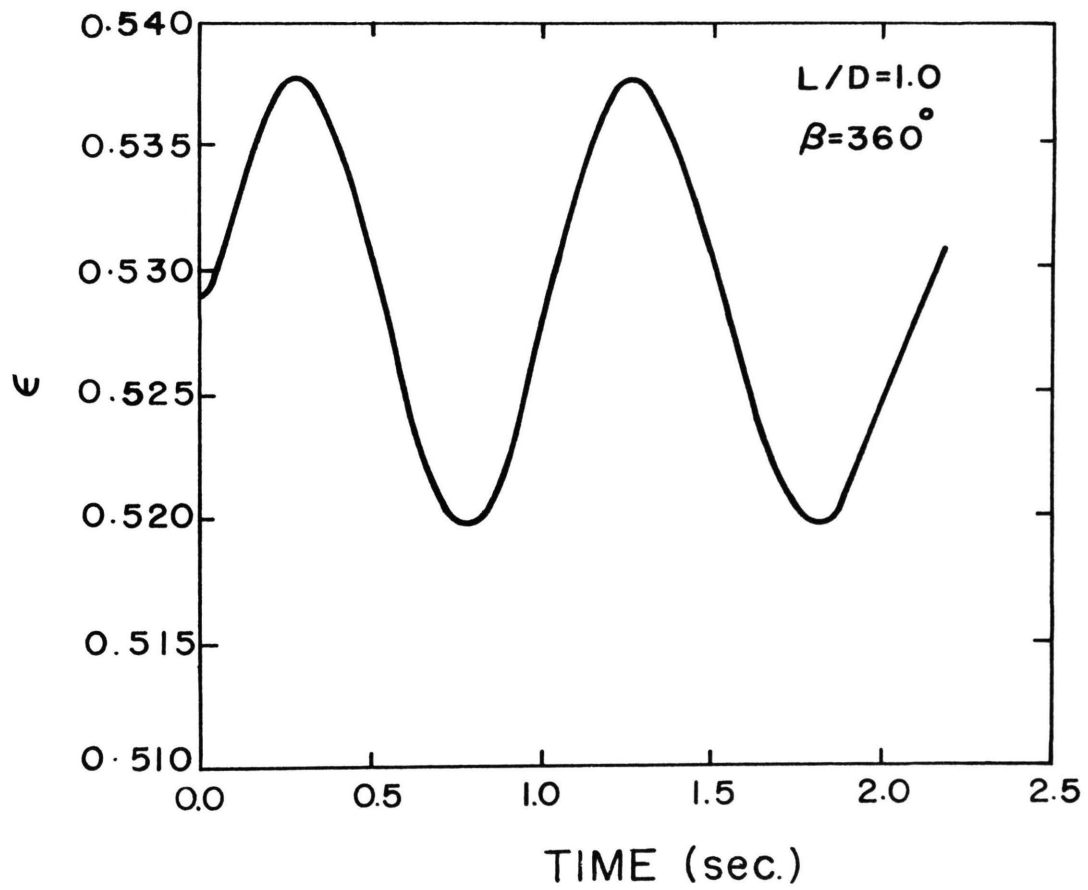


Fig. 17. ϵ vs. time.

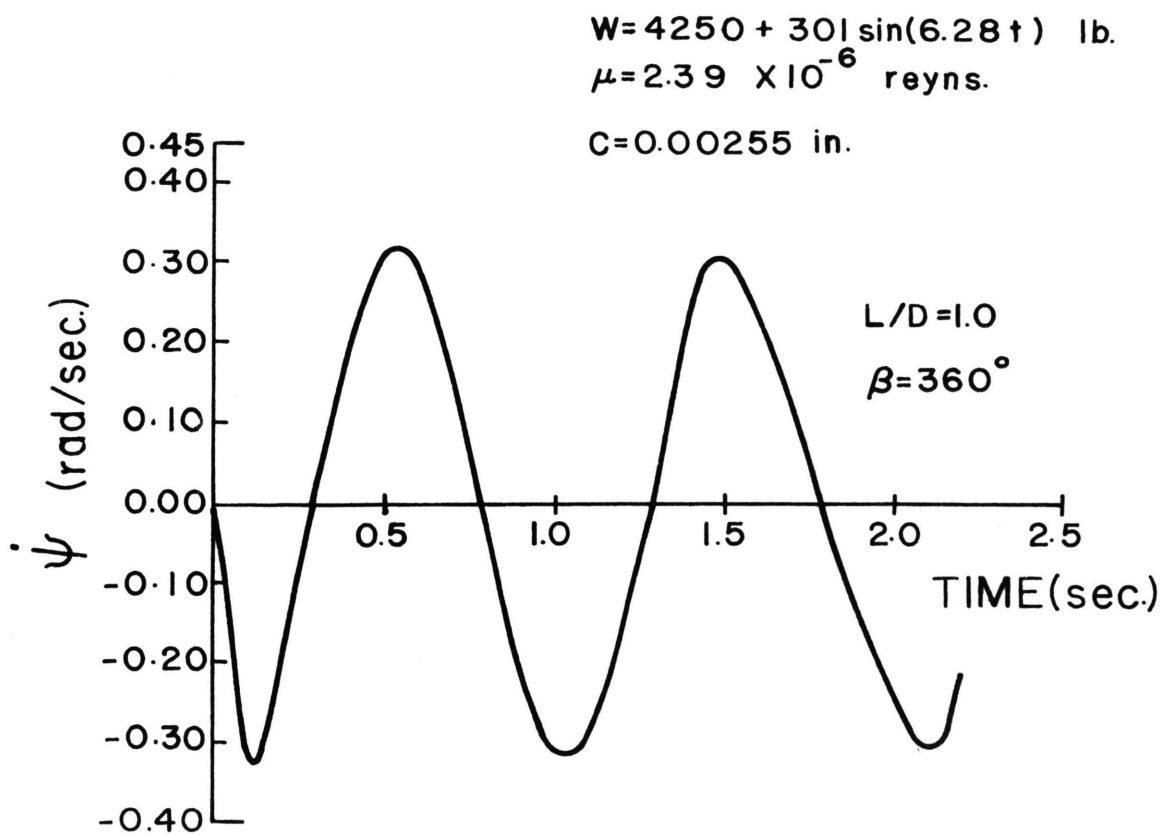


Fig. 18. $\dot{\psi}$ vs. time.

$$W = 4250 + 30 \sin(6.28 t) \text{ lb.}$$
$$\mu = 2.39 \times 10^{-6} \text{ reyns.}$$
$$C = 0.00255 \text{ in.}$$

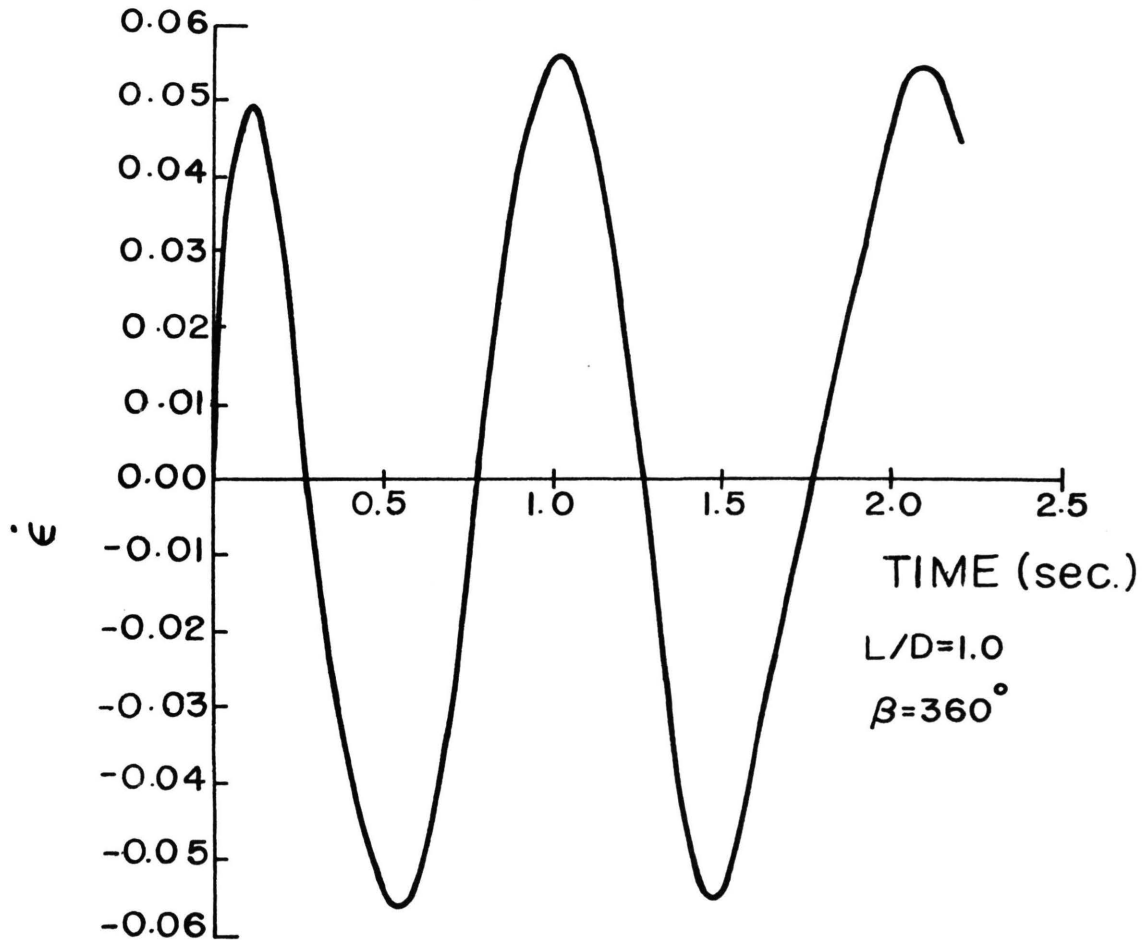


Fig. 19. $\dot{\epsilon}$ vs. time.

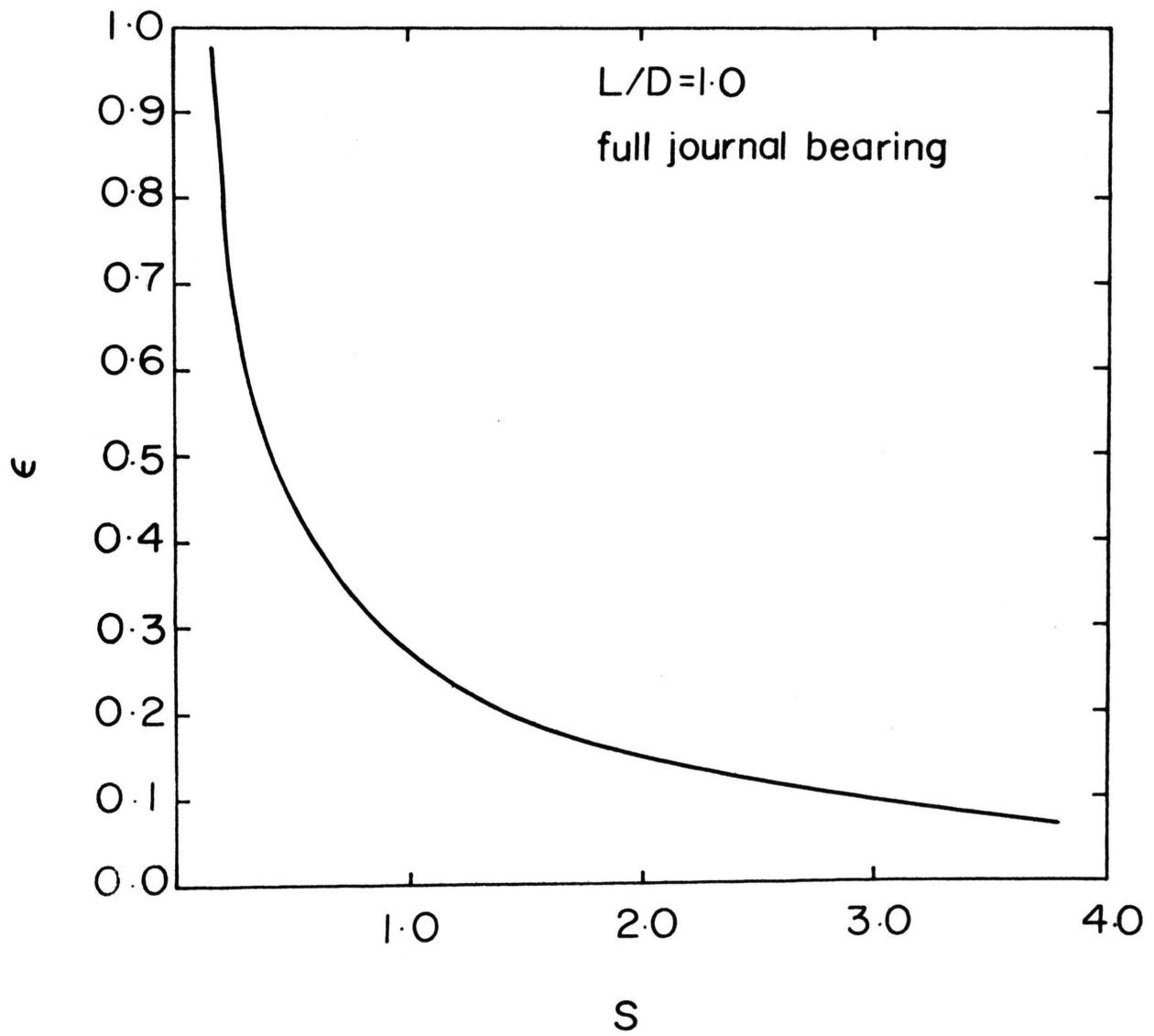


Fig. 20. Eccentricity Ratio vs. Sommerfeld Number.

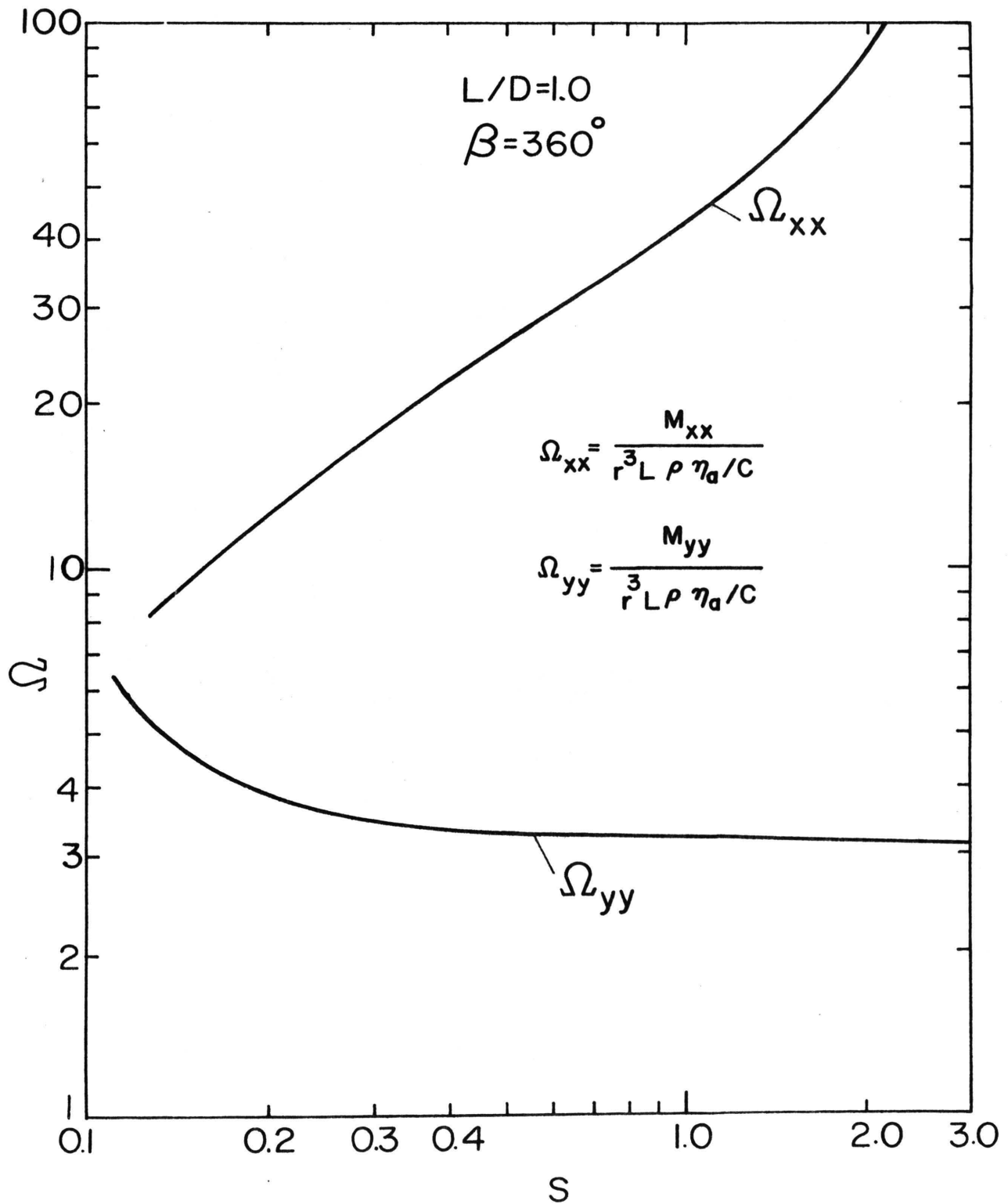


Fig. 21. Non-dimensional Inertia Coefficients.

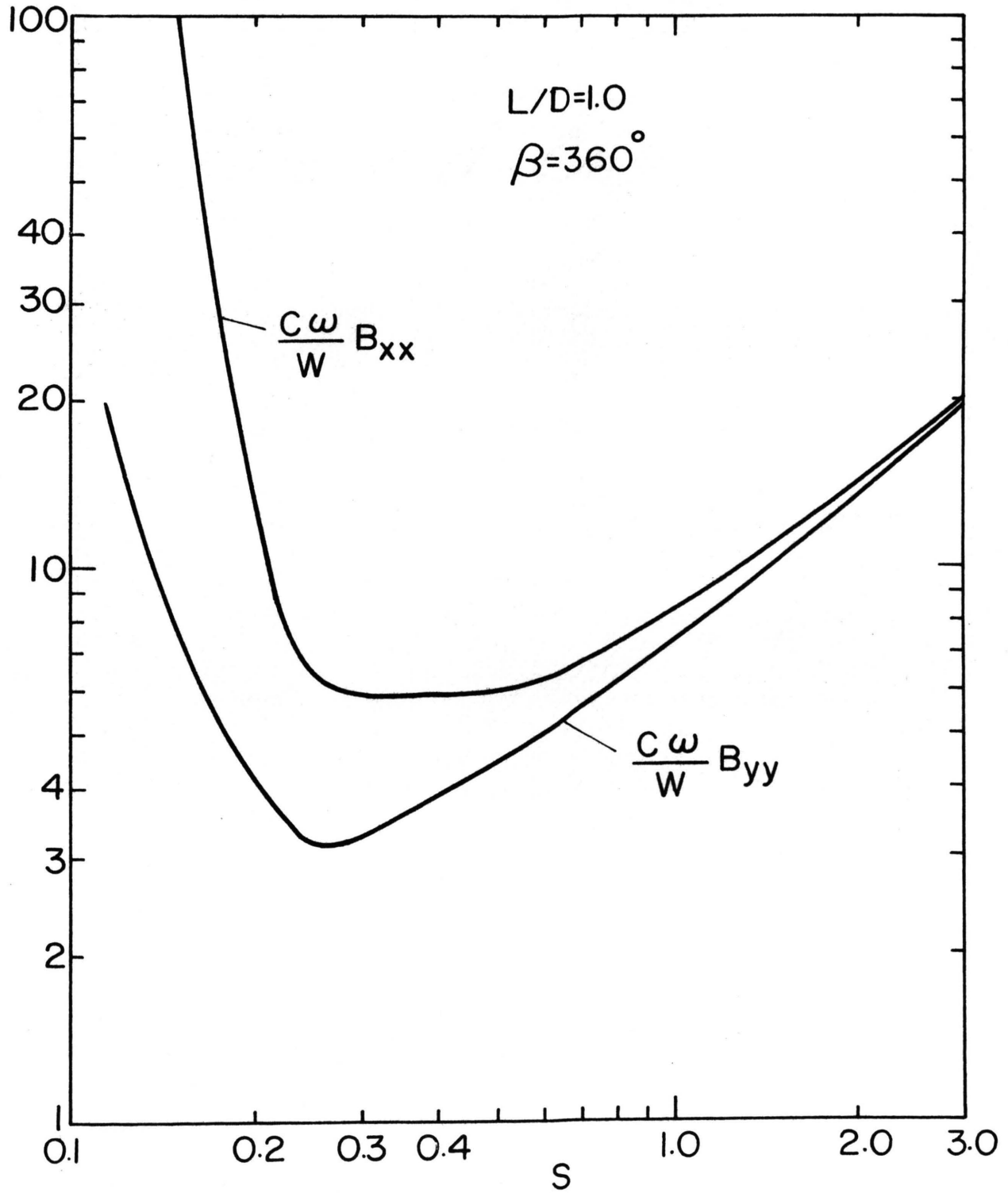


Fig. 22. Non-dimensional Damping Coefficients.

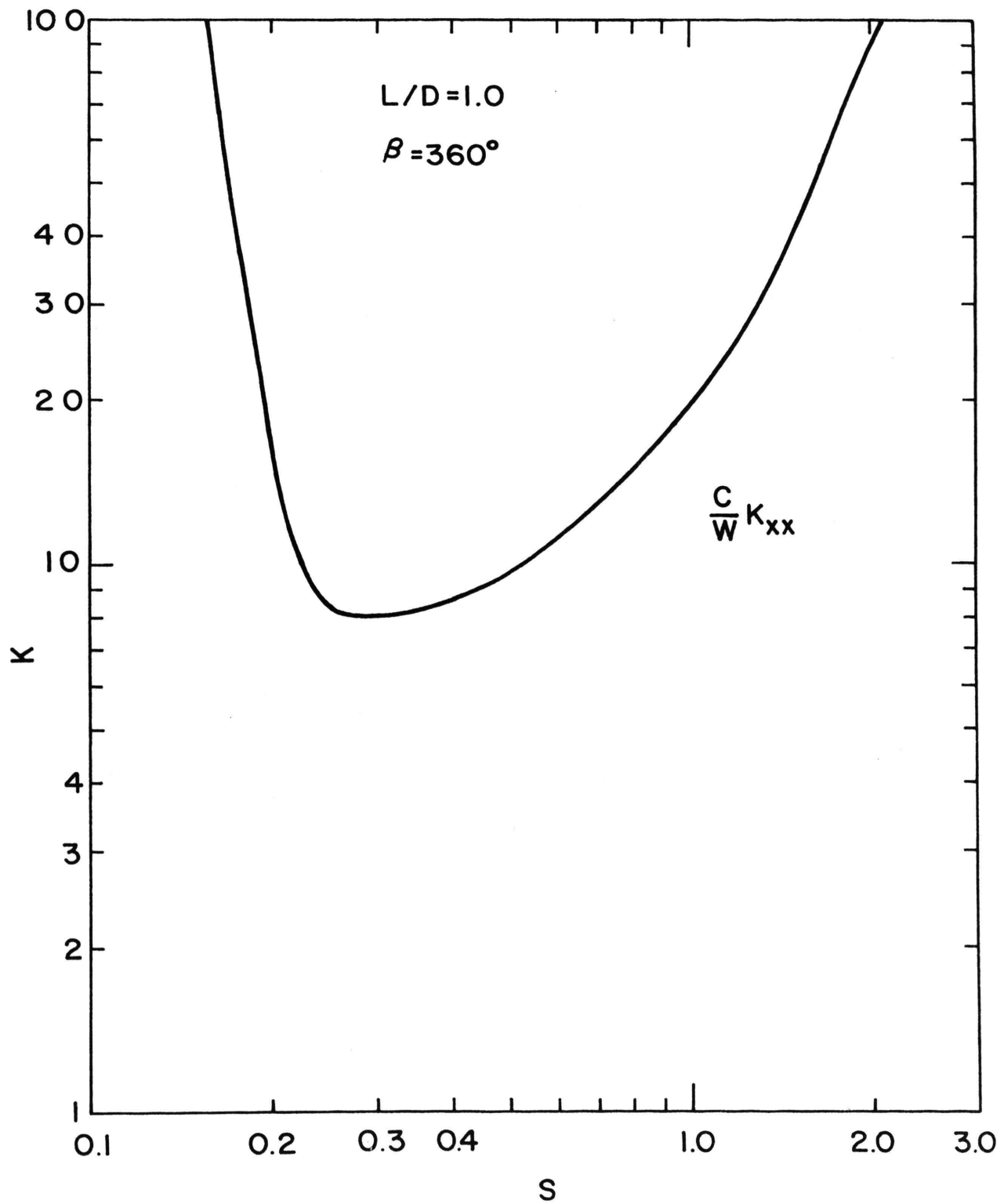


Fig. 23. Non-dimensional Elastic Coefficient K_{xx} .

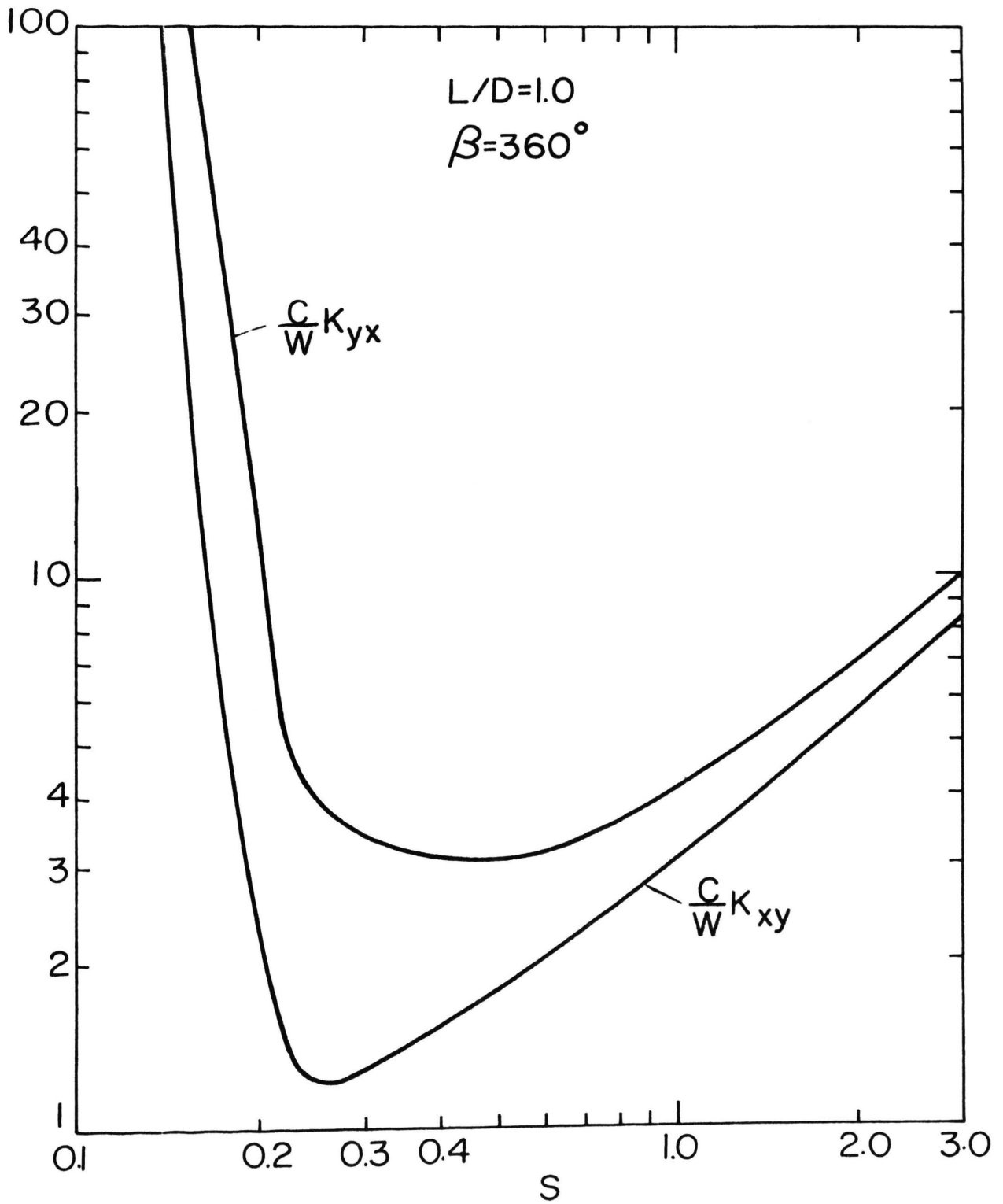


Fig. 24. Non-dimensional Cross Elastic Coefficients.

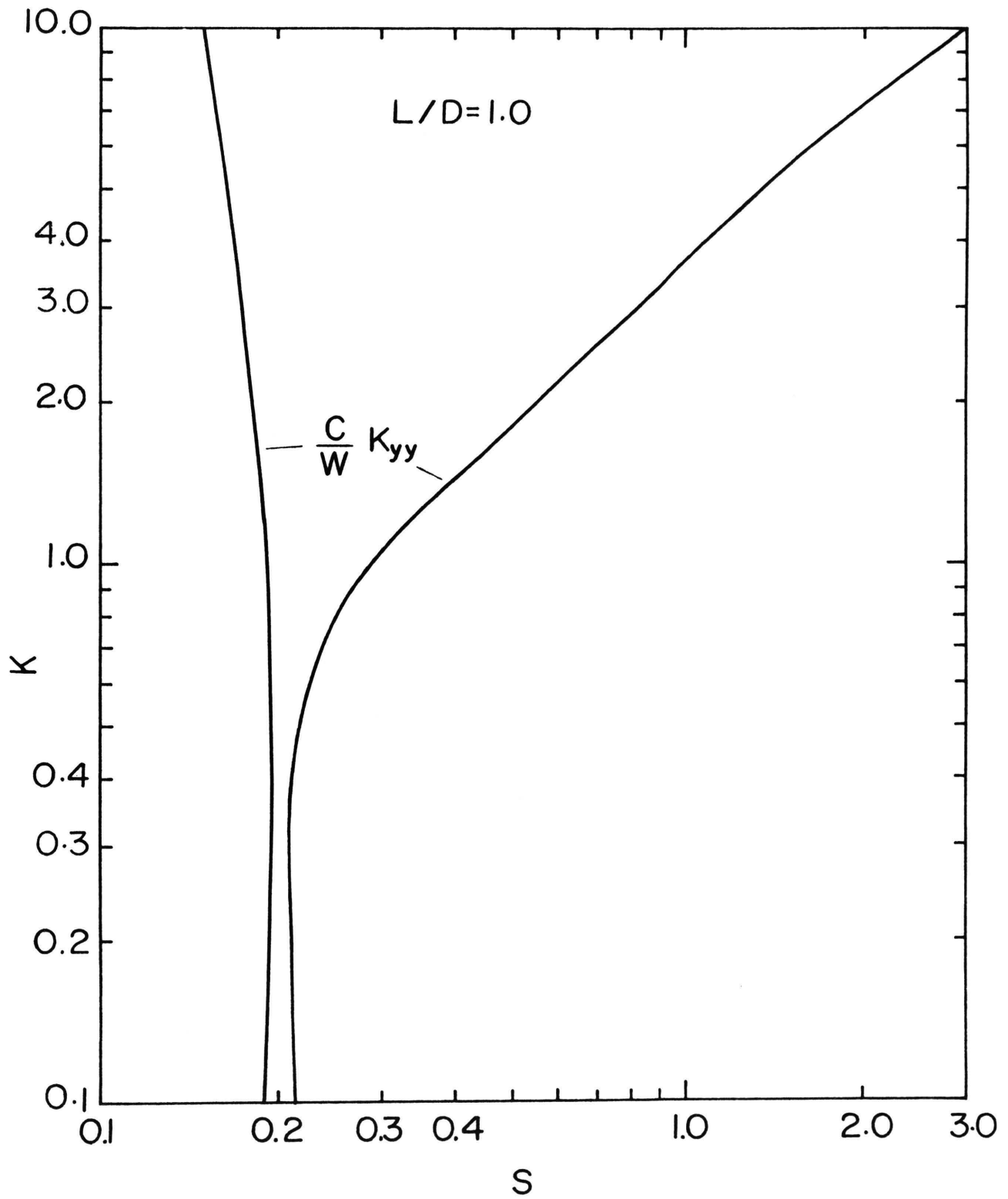


Fig. 25. Non-dimensional Elastic Coefficient K_{yy} .

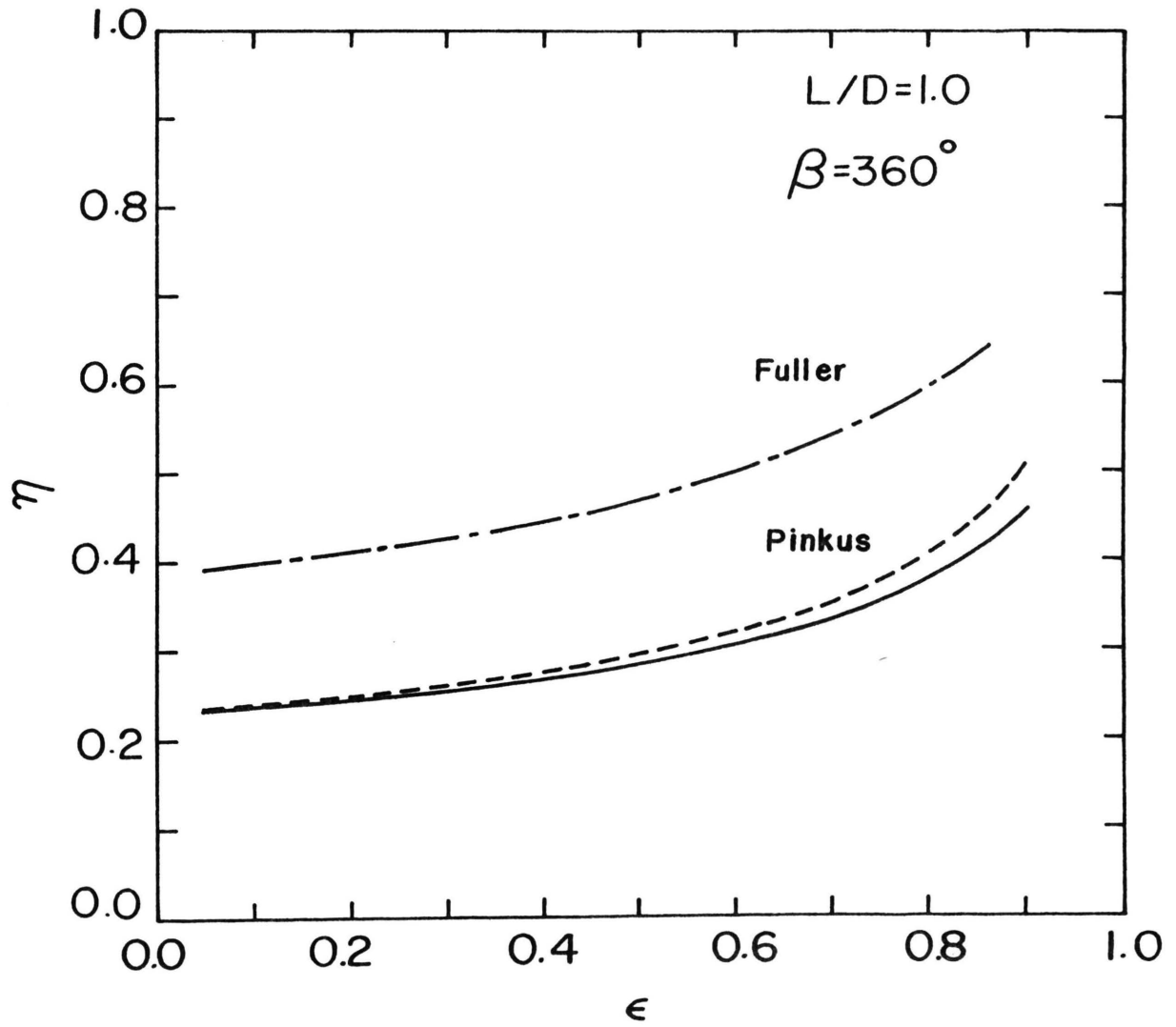


Fig. 26. Side Leakage Factor - η .

REFERENCES

1. "The Hydrodynamical Theory of the Lubrication of a Cylindrical Bearing Under Variable Load, and of a Pivot Bearing", W.J. Harrison, Cambridge Philosophical Society, vol. 22, 1920, pp. 373.
2. "Fluctuating Loads in Sleeve Bearings", H.W. Swift, Journal of the Institutions of Civil Engineers (London), vol. 5, 1937, pp. 161-195.
3. "Alternating Loads on Sleeve Bearings", J. Dick, Philosophical Magazine (London), vol. 35, 1944, pp. 841-850.
4. "Analytical Study of Journal-Bearing Performance Under Variable Loads", G.S.A. Shawki, Paper No. 55-Lub.-16, Trans. ASME, 1956, pp. 457-464.
5. "The Calculated Performance of Dynamically Loaded Sleeve Bearings", J.T. Burwell, Journal of Applied Mechanics, Trans. ASME, vol. 69, 1947, pp. A231-A245.
6. "Characteristics of Centrally Supported Journal Bearings", E.O. Waters, Trans. ASME, vol. 64, 1942, pp. 711-719.
7. "Dynamically Loaded Journal Bearings: Mobility Method of Solution", J.F. Booker, Journal of Basic Engineering, Trans. ASME, vol. 87, No. 3, September 1965, pp. 537-546.
8. "Dynamically Loaded Journal Bearing of Finite Length", Heinz W. Hahn, Institution of Mechanical Engineering, (London), 1957, pp. 100-110.
9. "A Variational Approach to Lubrication Problems and the Solution of the Finite Journal Bearings", D.F. Hays,

Journal of Basic Engineering, Trans. ASME, vol. 81, 1959, pp. 13-23.

10. "Squeeze Film: A Finite Journal Bearing with a Fluctuating Load", D.F. Hays, Journal of Basic Engineering, Trans. ASME, vol. 87, 1961, pp. 579-588.

11. "Static and Dynamic Properties of Partial Journal Bearings", Paul C. Warner; Journal of Basic Engineering, Trans. ASME, vol. 85, June 1963, pp. 247-257.

12. "Journal Bearing Dynamic Characteristics Effect of Inertia of Lubricant", D.M. Smith, Proc. Institution of Mechanical Engineers, (London), vol. 179, 1964, pp. 37-44.

13. "Tests on a 24-in Diameter Journal Bearing: Transition from Laminar to Turbulent Flow", N.J. Huggins, Proc. Institution of Mechanical Engineers (London), vol. 181, 1966, pp. 81-88.

14. "Measurement of Oil-Film Pressures in Journal Bearings Under Constant and Variable Loads", A. Buske and W. Rolli, NACA Technical Memorandum No. 1200, 1937.

15. "Hydrodynamic Lubrication of Cyclically Loaded Bearings", R.W. Dayton and E.M. Simmons, NACA, Technical Notes No. 2544, 1948, pp. 1-22.

16. "Foundation of Fluid Mechanics", S.W. Tuan, Prentice Hall, New Jersey, 1967.

17. "An Experimental Investigation of a Cylindrical Journal Bearing Under Constant and Sinusoidal Loading", T.E. Carl, Proc. Institution of Mechanical Engineers (London), vol. 178, 1963, pp. 100-119.

18. "Lubrication of Bearings", E.I. Radzimonsky, Ronald Press, New York, 1959.
19. "Theory of Hydrodynamic Lubrication", O. Pinkus and B. Sternlicht, McGraw-Hill, New York, 1961.
20. "Theory and Practice of Lubrication for Engineers", D.D. Fuller, John Wiley and Sons, New York, 1956, pp. 200-204.
21. "Effects of Side Leakage in 120 Degree Centrally Supported Journal Bearings", S.J. Needs, Trans. ASME, vol. 56, 1934, pp. 721-732, vol. 57, pp. 123-137.

APPENDIX A

Literature Review

Journal bearings were developed for centuries by empirical methods before engineers came to understand the physical action of a hydrodynamic lubricating film. Empirical methods still retain an important place in journal-bearing development.

In 1883 Beauchamp Tower [1] carried out an investigation to determine suitable methods of lubricating railway axle bearings. His tests were performed on partial bearings in which the rotating shaft picked up lubricant from an oil bath. He soon made the unexpected discovery that under loaded conditions, the peak pressure was several times the mean pressure on the projected area. Three years later, Osborne Reynolds [2] demonstrated that the build-up of pressure was due to viscous action in a convergent film. The physical understanding thus obtained assisted designers in choosing the position of oil-supply and drain grooves in journal bearings. The first analytical investigation of power loss in a hydrodynamic journal bearing was published in Russia, by Petroff, in 1883 [3].

Much analytical work on bearing lubrication was subsequently published, but for many years, engineers found this analysis of little relevance to journal-bearing design. Application of Reynolds's theory led to a revolutionary advance in thrust-bearing design with the invention of the tilting-pad thrust bearing by Kingsbury [4].

By 1950, the theory was giving results in reasonable accord with the observed steady-running of many bearings. There were, however, some anomalous results, particularly on large high-speed bearings [5]. Most of these anomalies have been explained by considering the occurrence of non-laminar flow in the bearings.

In the operation of turbomachinery, it has long been known that journal bearings greatly influence machine vibration, both in response to disturbance (such as out-of-balance) and in stability of running. The problem was attacked analytically and experimentally, but engineers were perplexed by discordant theories of the dynamic phenomena in the bearings, and by difficulty in distinguishing the dynamic effects of the bearings from the dynamic effects of the bearing supports [6]. Acceptance of a conventional theory relating to dynamic characteristics of journal bearings became widespread about 1960, although an understanding of dynamic characteristics of journal bearings is still far from complete.

The solution of Reynold's equation as applied to dynamically loaded journal bearings was developed by W. J. Harrison [7] who, in part, examined the case of constant load, with the shaft slightly displaced from the equilibrium position. H.W. Swift [8] examined the paths followed by journal centers assuming no transverse flow of oil in the bearing while the load rotates with constant angular velocity. As such, it is accurate only for bearings which have a large width compared

to their diameter, and in this respect, is analogous to the familiar Sommerfeld solution for constant-load bearings [9].

Michell [10] and Muskat, Morgan and Meres [11] eliminated the need for side flow factors from the case of plain slider bearings by solving the fundamental equation for slider pads of finite length-to-width ratios. But, unfortunately, the case of the finite journal bearing can not be dealt with in the same manner because of the more complicated film shape.

In 1949, Cameron and Wood [12] published data for 360 degree finite bearings for eccentricity ratios up to 0.8 which they obtained by relaxation methods. Raimondi and Boyd [13] have published extensive design data and various information in the form of charts and graphs for bearings of length-to-width of 0.25, 0.5, 1 and ∞ with bearing arcs of 360, 180 and 60 degrees. Data on finite partial bearings with 100 and 75 degree arcs has been presented by Pinkus [14].

The complete case including side leakage in journal bearings subjected to dynamic loading has not been solved exactly, and it appears to be quite complicated. However, some approximate methods have been found by Burwell [15], who resolved Swift's equations into more simple forms, and applied a side-leakage factor obtained by Water's [16]. To actual bearings, however, this implies that the side leakage factor will be the same at the same eccentricity ratio for both statically and dynamically loaded bearings.

Also, Heinz W. Hahn [17] used a finite difference method to calculate the pressure distribution of finite 360

degree journal bearings, and its relation to time, for dynamic loading. Donald F. Hays [18,19] solved the Reynold's equation by variational methods and applied this general solution to finite 360 degree journal bearings under dynamic loading, but without journal rotation, i.e., "squeeze film" lubrication. Another important paper is by Paul C. Warner [20] who solved Reynold's equation by using the technique of separation of variables reducing the Reynold's equation to two ordinary differential equations. He, then, approximated the pressure series to the first term of the series as a side leakage factor. J.F. Booker [21] has introduced the Mobility method which predicts the motion of a journal bearing center under arbitrary loading, and states that since the equations of motion are in explicit form, iteration calculations are avoided. The method is much faster than usual numerical solutions, but is limited to full journal bearings with circumferential symmetry.

Furthermore, C.S.A. Shawki [22] presented a basic theoretical investigation into the performance of a complete journal bearing of infinite width under variable load, excluding the existance of negative pressures. J.Dick [23] presented the case where the locus of the journal center is an ellipse. The journal center is assumed to move round the ellipse in such a way that the dydrodynamic load along one axis of the ellipse in zero. He compared the hydrodynamic load along the other axis to a sinusoidal load. D.M. Smith [24] introduced a technique for calculating the inertia

effect of a hydrodynamic film in journal bearings.

On the experimental side Buske and Rolli [25] in 1937 carried out pressure measurements in the oil film of a full journal bearing under alternating loads applied at the same frequency as that of the rotation of the journal. Recorded diagrams give evidence that film pressures at any cross-section vanish along a portion of the journal periphery, thus, confirming that negative pressures (below vapor pressure of lubricant) do not exist in a bearing. Theodor E. Carl [26] made simultaneous measurements of film pressure and journal displacement of a full journal bearing both under constant load and rotating load. He notices the modification of the oil film profile due to bending of the journal which resulted in shifting the maximum film pressure closer to the position of the minimum film thickness. N.J. Huggins [27] by experimenting with a 24 inch diameter journal indicated that even at low speeds there is a dependence on the Reynold's number. He suggests that the inertia of the oil film has a pronounced influence on the journal bearing variables.

R.W. Dayton and E.M. Simons [28] by an experimental investigation of shaft center location and displacement for various ratios of rotating load to journal speed showed that the shaft reaches an equilibrium point despite Swift's theoretical work which indicates that the shaft will not be static under no load or a constant load.

APPENDIX B

Derivation of General Reynolds' Equation

In Figure (B-1a,b) coordinate systems and an element are shown in the hydrodynamic film of journal bearing under load W , which could be constant or variable.

The following assumptions are made:

- (i) the height of film y is very small compared to the other dimensions of the bearing (in x and z direction),
- (ii) no variation of pressure across the fluid film i.e., pressure is function of x, z only, $P = P(x, z)$,
- (iii) the flow is laminar in the film,
- (iv) compared to velocity gradients $\frac{\partial u}{\partial y}$ and $\frac{\partial w}{\partial y}$ all other velocity gradients are considered negligible,
- (v) the lubricant is a Newtonian fluid.

By summing the forces in the x direction, from the stresses shown in Figure (B-1c):

$$\Sigma F_x = 0$$

$$\begin{aligned} & [\tau_{yx} + \frac{\partial \tau_{yx}}{\partial y}] dx dz - \tau_{yx} dx dy + [\tau_{zx} + \frac{\partial \tau_{zx}}{\partial z} \frac{dz}{2}] dx dy - \\ & [\tau_{zx} - \frac{\partial \tau_{zx}}{\partial z} \frac{dz}{2}] dx dy + [P - \frac{\partial P}{\partial x} \frac{dx}{2}] dy dz - [P + \frac{\partial P}{\partial x} \frac{dx}{2}] dz dy = 0 \end{aligned}$$

Canceling like terms and simplifying,

$$\frac{\partial \tau_{yx}}{\partial y} + \frac{\partial \tau_{zx}}{\partial z} = \frac{\partial P}{\partial x} \quad (B-1)$$

Since it is assumed that the lubricant is a Newtonian fluid, the shear stress is proportional to the rate of shear, i.e.,

$$\tau_{yx} = \mu \frac{\partial u}{\partial y} \quad (\text{B-2})$$

and

$$\tau_{zx} = \mu \frac{\partial u}{\partial z} \quad (\text{B-3})$$

Substituting Equation (B-2) and (B-3) in Equation (B-1):

$$\frac{\partial}{\partial y} \left(\mu \frac{\partial u}{\partial y} \right) + \frac{\partial}{\partial z} \left(\mu \frac{\partial u}{\partial z} \right) = \frac{\partial P}{\partial x} \quad (\text{B-4})$$

But now by using assumption (iv) Equation (B-4) becomes,

$$\frac{\partial^2 u}{\partial y^2} = \frac{1}{\mu} \frac{\partial P}{\partial x} \quad (\text{B-5})$$

By integrating Equation (B-5) twice and using Boundary conditions,

$$u = U \quad \text{at} \quad y = 0$$

$$u = U \quad \text{at} \quad y = h$$

$$u = \frac{1}{2\mu} \frac{\partial P}{\partial x} y(y-h) + \frac{U_1 - U_0}{h} y + U_0 \quad (\text{B-6})$$

Summation of forces in z direction:

$$\Sigma F_z = 0$$

$$\begin{aligned} & [\tau_{yz} + \frac{\partial \tau_{yz}}{\partial y} dy] dx dz - \tau_{yz} dx dz + [\tau_{xz} + \frac{\partial \tau_{xz}}{\partial x} \frac{dx}{2}] dy dz - \\ & [\tau_{xz} - \frac{\partial \tau_{xz}}{\partial x} \frac{dx}{2}] dy dz + [P - \frac{\partial P}{\partial z} \frac{dz}{2}] dx dy - [P + \frac{\partial P}{\partial z} \frac{dz}{2}] dx dy = 0 \end{aligned}$$

again, canceling like terms and simplifying:

$$\frac{\partial \tau_{yz}}{\partial y} + \frac{\partial \tau_{xz}}{\partial x} = \frac{\partial P}{\partial z} \quad (\text{B-7})$$

Referring to assumption (v):

$$\tau_{yz} = \mu \frac{\partial \omega}{\partial y} \quad \tau_{xz} = \mu \frac{\partial \omega}{\partial x} \quad (\text{B-8})$$

Therefore by placing Equation (B-8) in Equation (B-7):

$$\frac{\partial^2 \omega}{\partial y^2} + \frac{\partial^2 \omega}{\partial x^2} = \frac{1}{\mu} \frac{\partial P}{\partial z} \quad (\text{B-9})$$

By integrating Equation (B-9) twice with respect to y and using boundary conditions,

$$w = 0 \quad \text{at} \quad y = 0$$

$$w = 0 \quad \text{at} \quad y = h$$

(B-10)

$$w = \frac{1}{2\mu} \frac{\partial P}{\partial X} y(y-h)$$

(B-11)

Since the lubricant is considered incompressible, the continuity equation becomes:

$$\frac{\partial(\rho u)}{\partial x} + \frac{\partial(\rho v)}{\partial y} + \frac{\partial(\rho w)}{\partial z} = 0$$

or

$$\frac{\partial v}{\partial y} = - \frac{\partial u}{\partial x} - \frac{\partial w}{\partial z} \quad \text{(B-12)}$$

where ρ , mass density is considered to be constant. Now by integrating Equation (B-12) between $y = 0$ and $y = h$:

$$\int_0^h dv = - \int_0^h \frac{\partial}{\partial x} (u) dy - \int_0^h \frac{\partial}{\partial z} (w) dy \quad \text{(B-13)}$$

Consider the Leibnitz integral (24), i.e.,

$$\int_a^{\Psi(x)} \frac{\partial}{\partial x} f(x, y) dy = \frac{\partial}{\partial x} \int_a^{\Psi(x)} f(x, y) dy - f[x, \Psi(x)] \Psi'(x) - f[x, a] a' \quad \text{(B-14)}$$

In the upper limit of Equation (B-13), h is a function of coordinates (x, z) , i.e., $h = h(x, z)$. Applying Equation (B-14) to each term on the right hand side of Equation (B-13):

$$\int_0^h \frac{\partial}{\partial x} (u) dy = \frac{\partial}{\partial x} \int_0^h u dy + U_1 \frac{\partial h}{\partial x} \quad \text{(B-15)}$$

and

$$\int_0^h \frac{\partial}{\partial z} (w) dy = \frac{\partial}{\partial z} \int_0^h w dy \quad \text{(B-16)}$$

Therefore, by using Equation (B-15) and (B-16), and performing the integration before differentiation, Equation (B-13)

becomes,

$$2(V_1 - V_0) = \frac{\partial}{\partial X} \left[\frac{h^3}{6\mu} \frac{\partial P}{\partial X} \right] + \frac{\partial}{\partial Z} \left[\frac{h^3}{6\mu} \frac{\partial P}{\partial Z} \right] - \frac{\partial h}{\partial X} [(U_1 - U_0) - h \frac{\partial}{\partial X} (U_1 + U_0)]$$

and therefore

$$\frac{\partial}{\partial X} \left[\frac{h^3}{6\mu} \frac{\partial P}{\partial X} \right] + \frac{\partial}{\partial Z} \left[\frac{h^3}{6\mu} \frac{\partial P}{\partial Z} \right] = (U_1 - U_0) \frac{\partial h}{\partial X} + h \frac{\partial}{\partial X} (U_1 + U_0) + 2V_1 - 2V_0, \quad (B-17)$$

which is the general Reynolds' equation. If the bearing is stationary, i.e., $U_0 = V_0 = 0$

$$\frac{\partial}{\partial X} \left[\frac{h^3}{\mu} \frac{\partial P}{\partial X} \right] + \frac{\partial}{\partial Z} \left[\frac{h^3}{\mu} \frac{\partial P}{\partial Z} \right] = 6 U_1 \frac{\partial h}{\partial X} + 6 h \frac{\partial U_1}{\partial X} + 12V_1,$$

where:

$6 U_1 \frac{\partial h}{\partial X}$ represents the action of the journal rotating with a velocity U , over a wedge-shaped fluid film given by $h(x)$.

In order for this term to generate positive pressures, it must be negative since a wedge-shaped film implies that $\frac{\partial h}{\partial X} < 0$. $6h \frac{\partial U_1}{\partial X}$ represents a variation of tangential velocity along the bearing surface, and in order that this term contributes to positive pressures $\frac{\partial U_1}{\partial X}$ must be negative, i.e., the velocity must decrease along the fluid film. $12 V_1$ is the expression for the velocity of the shaft center and is responsible for squeeze film action.

Since $V_1 = \frac{dh}{dt}$, it can be seen that, when V acts in the same direction as the applied load, the film decreases and the velocity will contribute to the load capacity. By writing Reynolds' equation (B-17) in terms of cylindrical coordinates (r, ϕ, Z) :

$$\frac{1}{r^2} \frac{\partial}{\partial \phi} \left(\frac{h^3}{\mu} \frac{\partial P}{\partial \phi} \right) + \frac{\partial}{\partial z} \left(\frac{h^3}{\mu} \frac{\partial P}{\partial z} \right) = \frac{6}{r} \frac{\partial}{\partial \phi} (U_1 h) - 12V_1 \quad (\text{B-18})$$

The right hand side of Equation (B-18) is in terms of the bearing variables, i.e., r, c, ϵ, ψ , etc. By referring to Figure (B-1a), it can be seen that,

$$U_1 = r\omega + C \frac{d\epsilon}{dt} \cos(\phi - \frac{\pi}{2}) + C \frac{d\psi}{dt} \cos(\pi - \phi) \quad (\text{B-19})$$

and

$$V_1 = C \frac{d\epsilon}{dt} \sin(\phi - \frac{\pi}{2}) - C\epsilon \frac{d\psi}{dt} \sin(\pi - \phi) \quad (\text{B-20})$$

Or:

$$U_1 = r\omega + C \frac{d\epsilon}{dt} \sin \phi - C\epsilon \frac{d\psi}{dt} \cos \phi \quad (\text{B-21})$$

$$V_1 = -C \frac{d\epsilon}{dt} \cos \phi - C\epsilon \frac{d\psi}{dt} \sin \phi \quad (\text{B-22})$$

Placing Equation (B-21) and Equation (B-22) in the right side of Equation (B-18):

$$\begin{aligned} 12 \left[\frac{1}{r} \frac{\partial}{\partial \phi} \left(\frac{U_1 h}{2} \right) - V_1 \right] &= 12C \frac{d\psi}{dt} \left[\frac{C\epsilon}{2r} \sin \phi + \frac{C\epsilon^2}{r} \cos \phi \sin \phi + \epsilon \sin \phi \right] + \\ 12C \frac{d\epsilon}{dt} \left[\frac{C}{2r} \cos \phi - \frac{C}{2r} \sin^2 \phi + \cos \phi \right] &- 6C \epsilon \sin \phi \end{aligned} \quad (\text{B-23})$$

By examining the value of $\frac{C}{2r}$ for most journal bearings, we find that $\frac{C}{2r} \ll 1$, therefore, it could be neglected as compared to 1, so Equation (B-23) becomes,

$$12 \left[\frac{1}{r} \frac{\partial}{\partial \phi} \left(\frac{U_1 h}{2} \right) - V_1 \right] = 12 \left[-(\omega - 2 \frac{d\psi}{dt}) \frac{C\epsilon}{2} \sin \phi + C \frac{d\psi}{dt} \cos \phi \right] \quad (\text{B-24})$$

Therefore, it can be easily seen that Equation (B-24) i.e., the right-hand side of Reynolds' equation [Equation (B-18)] is not a function of z , and as shown is a function of ϕ only.

Thus, Equation (B-18) becomes:

$$\frac{1}{r^2} \frac{\partial}{\partial \phi} \left(\frac{h^3}{\mu} \frac{\partial P}{\partial \phi} \right) + \frac{\partial}{\partial Z} \left(\frac{h^3}{\mu} \frac{\partial P}{\partial Z} \right) = 12C \frac{d\varepsilon}{dt} \cos \phi - 6(\omega - 2 \frac{d\Psi}{dt}) C \varepsilon \sin \phi \quad (\text{B-25})$$

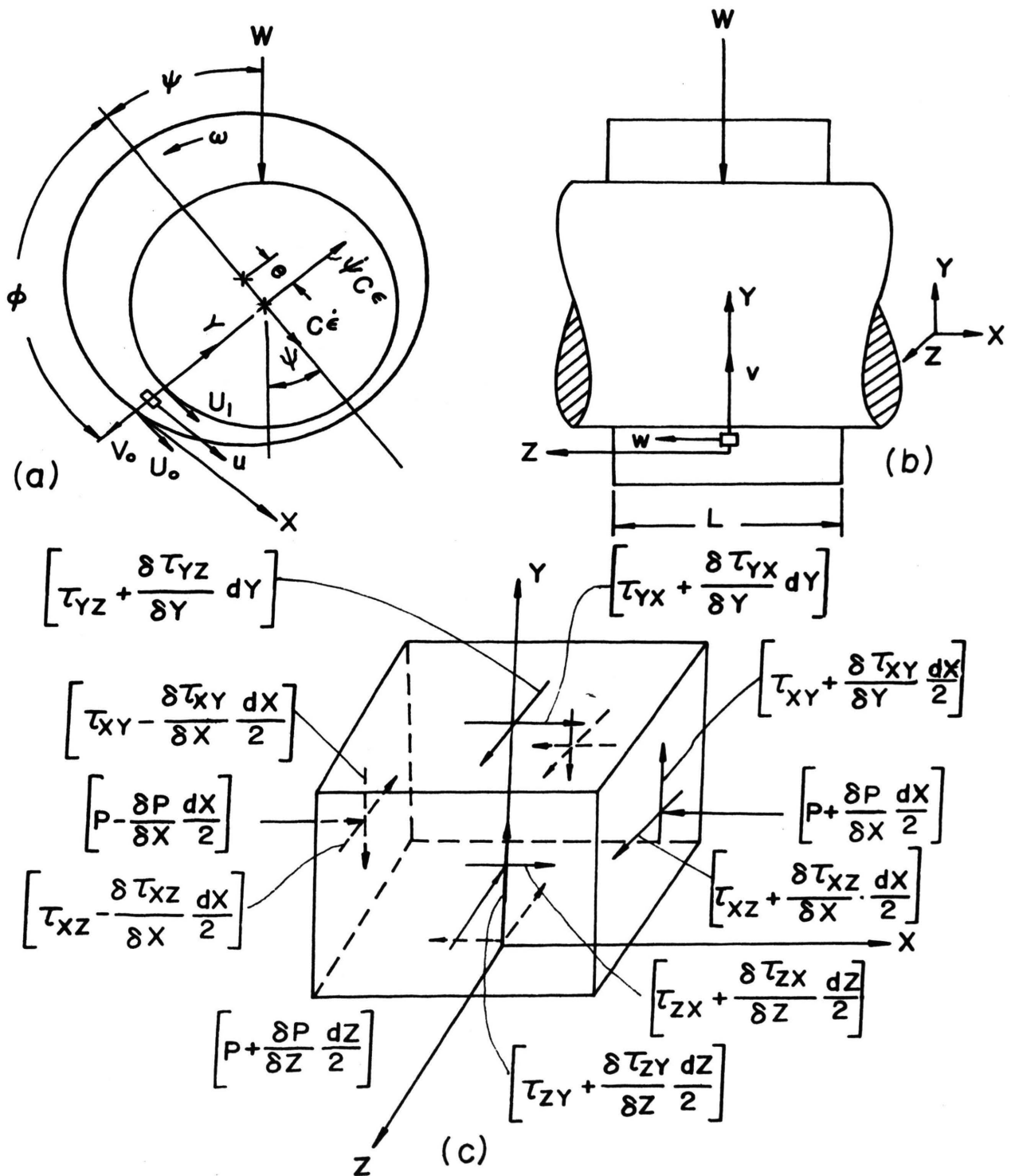


Fig. B-1. Components of Normal and Shear Stresses on Element.

APPENDIX C

An Approximate Solution to Reynold's Equation

In Appendix B Reynold's equation for stationary bearings was found Equation (B-25) as:

$$\frac{1}{r^2} \frac{\partial}{\partial \phi} \left(\frac{h^3}{\mu} \frac{\partial P}{\partial \phi} \right) + \frac{\partial}{\partial Z} \left(\frac{h^3}{\mu} \frac{\partial P}{\partial Z} \right) = 12C\dot{\epsilon} \cos \phi - 6(\omega - 2\dot{\psi})C\epsilon \sin \phi$$

But considering dynamic loading, it can be seen that pressure is a function of ϕ , Z and time. Therefore, at any instant of time, $P = P(\phi, Z)$.

Warner [9] assumed a solution for Reynold's equation (B-25) in the following form:

$$P = F(\phi) + g(\phi)q(Z) \quad (C-1)$$

where $F(\phi)$, $g(\phi)$, $q(Z)$ are functions that are to be determined. By substitution Equation (C-1) in Reynold's equation, and using the principle of superposition:

$$\frac{d}{d\phi} \left(\frac{h^3}{\mu} \frac{dF}{d\phi} \right) = r^2 [12C\dot{\epsilon} \cos \phi - 6(\omega - 2\dot{\psi})C\epsilon \sin \phi] \quad (C-2)$$

and

$$\frac{\mu}{h^3 r^2} \frac{d}{d\phi} \left(\frac{h^3}{\mu} \frac{dg}{d\phi} \right) + \frac{d^2 q}{dZ^2} = 0 \quad (C-3)$$

where Equation (C-3) could be written as:

$$\frac{d^2 q}{dZ^2} - \lambda^2 q = 0 \quad (C-4) \quad \text{and} \quad \frac{d}{d\phi} \left(\frac{h^3}{\mu} \frac{dg}{d\phi} \right) + (\lambda r)^2 \frac{h^3}{\mu} g \quad (C-5)$$

where λ is an eigenvalue from Equation (C-4), and also (λr) is the characteristic value for Equation (C-5).

By examining Equation (C-2) it can be determined that $F(\phi)$ is the solution of Reynold's equation for a bearing with infinite width (side flow neglected).

Considering the boundary conditions for a finite journal bearing:

$$(i) \quad P(\phi, Z) = P(\phi + \beta, Z) = P_0$$

$$(ii) \quad P(\phi, \pm L/2) = 0$$

It is obvious that (i) can be satisfied by $F(\phi)$ and that (ii) cannot be satisfied by $F(\phi)$ in Equation (C-2).

In order to satisfy boundary condition (ii), it is necessary to expand $F(\phi)$ in a series of functions $g_N(\phi)$. Where $g_N(\phi)$ corresponds to the N^{th} characteristic value of λ_N . This still satisfies condition (i).

By applying boundary condition (ii) to pressure P in Equation (C-1):

$$P(\phi, L/2) = F(\phi) + g(\phi)q(L/2) = 0$$

$$\text{and} \tag{C-6}$$

$$P(\phi, -L/2) = F(\phi) + g(\phi)q(-L/2) = 0$$

But by considering the geometry of the journal bearing, it can be assumed that

$$q(Z) = q(-Z)$$

Therefore, from Equation (C-6):

$$F(\phi) = q(L/2)g(\phi) \tag{C-7}$$

Expanding Equation (C-1) in series,

$$P(\phi, Z) = \sum_{n=1}^{\infty} a_n g_n(\phi) + \sum_{n=1}^{\infty} b_n g_n(\phi) q_n(Z),$$

but from Equation (C-7):

$$P(\phi, Z) = \sum_{n=1}^{\infty} a_n g_n(\phi) + \sum_{n=1}^{\infty} b_n g_n(\phi) q_n(Z). \tag{C-8}$$

By using the boundary condition (ii) in the series:

$$\sum_{n=1}^{\infty} a_n g_n(\phi) + \sum_{n=1}^{\infty} b_n g_n(\phi) q_n(L/2) = 0,$$

or

$$\sum_{n=1}^{\infty} g_n(\phi) [a_n + b_n q_n(L/2)] = 0,$$

therefore

$$b_n = - \frac{a_n}{q_n(L/2)}$$

So finally,

$$P(\phi, Z) = \sum_{n=1}^{\infty} a_n g_n(\phi) \left[1 - \frac{q_n(Z)}{q_n(L/2)} \right] \quad (C-9)$$

It is obvious now, that Equation (C-9) can satisfy both boundary conditions. Therefore, it is a solution of Reynold's equation. However, the exact solution of the series seems quite complicated.

Since this series converges rapidly (9), and due to the physical conditions, much of the solution is included within the leading series term. The series could be approximated as:

$$P(\phi, Z) = \sum_{n=1}^{\infty} a_n g_n(\phi) \left[1 - \frac{q_1(Z)}{q_1(L/2)} \right] \quad (C-10)$$

or

$$P(\phi, Z) = \left[1 - \frac{q_1(Z)}{q_1(L/2)} \right] \sum_{n=1}^{\infty} a_n g_n(\phi)$$

Therefore

$$P(\phi, Z) = \left[1 - \frac{q_1(Z)}{q_1(L/2)} \right] F(\phi) \quad (C-11)$$

The first and the most important term in Equation (C-11)

is computed exactly. The second and higher terms are approximate, but because of rapid convergence of the series, higher order terms rapidly decrease in importance.

The term $[1 - \frac{q_1(Z)}{q_1(L/2)}]$ in Equation (C-11) could be called a correction factor for side leakage. This factor can be determined by solution of Equation (C-4), i.e.:

$$\frac{d^2q}{dZ^2}(Z) - \lambda^2q(Z) = 0$$

But as was assumed above, the side leakage from both sides of the bearing are the same, i.e. $q(Z)$ is an even function. Therefore,

$$q(Z) = \text{Cosh}(\lambda Z). \tag{C-12}$$

APPENDIX D

Determination of Eigenvalues

Solution of Equation (7) is necessary so that side-leakage factors may be found.

Since it was assumed that viscosity is not a function of ϕ , Equation (7) can be written as:

$$\frac{d}{d\phi} (h^3 \frac{dg}{d\phi}) + (\lambda r)^2 h^3 g = 0 \quad (D-1)$$

The functional for equation (D-1) in the general form is:

$$J[g] = \int F(\phi, g, g_\phi) d\phi, \quad (D-2)$$

where the Euler-Lagrange differential equation for the above functional is: (25)

$$F - \frac{d}{d\phi} [Fg_\phi] = 0 \quad (D-3)$$

where

$$F_g = \frac{\partial F}{\partial g}, \quad g_\phi = \frac{\partial g}{\partial \phi} \quad \text{and} \quad Fg_\phi = \frac{\partial F}{\partial \phi} g$$

In order for Functional (D-2) to satisfy Equation (D-1):

$$Fg - \frac{d}{d\phi} Fg_\phi = \frac{d}{d\phi} (h^3 \frac{dg}{d\phi}) + (\lambda r)^2 h^3 g$$

Comparing terms,

$$Fg = (\lambda r)^2 h^3 g$$

Integrating with respect to g :

$$F = \frac{1}{2} (\lambda r)^2 h^3 g + \Theta(\phi, g_\phi) \quad (a)$$

and also

$$Fg_\phi = -h^3 \frac{dg}{d\phi}$$

$$\text{By integrating: } F = -\frac{1}{2} h^3 \left(\frac{dg}{d\phi}\right)^2 + \Omega(\phi, g) \quad (b)$$

Therefore, from (a) and (b):

$$F = \frac{1}{2} [(\lambda r)^2 h^3 g - h^3 \left(\frac{dg}{d\phi}\right)^2] \quad (D-4)$$

therefore,

$$J[g] = \frac{1}{2} \int_0^{2\pi} [(\lambda r)^2 h^3 g^2 - h^3 \left(\frac{dg}{d\phi}\right)^2] d\phi \quad (D-5)$$

By setting the variation $\delta J = 0$:

$$(\lambda r)^2 = \frac{\int_0^{2\pi} h^3 \left(\frac{dg}{d\phi}\right)^2 d\phi}{\int_0^{2\pi} h^3 g^2 d\phi} \quad (D-6)$$

In order to determine λ ,

$$g(\phi) = F(\phi) = F_a(\phi) + F_b(\phi)$$

By referring to Equations (11) and (12) for F_a and F_b , the numerator of Equation (D-6) becomes:

$$\int_0^{2\pi} h^3 \left(\frac{dg}{d\phi}\right)^2 d\phi = [6\left(\frac{r}{c}\right)^2 \mu]^2 \{4\dot{\epsilon}^2 (F_{11} + C_1^2 F_2 + 2C_1 F_1) + (\omega - 2\dot{\Psi}) [F_{10} + C_3 F_2 + 2C_3 F_3] + 4\dot{\epsilon}(\omega - 2\dot{\Psi}) [F_{12} + C_3 F_1 + C_1 F_3 + C_1 C_3 F_2]\} \int_0^{2\pi} d\phi \quad (D-7)$$

The denominator of Equation (D-6) is quite difficult to integrate, and thus, numerical integration, namely Simpson's Rule was employed. Therefore, λ and in turn η [see Equation (18)] can be calculated.

η_s is determined as above but for $\dot{\epsilon} = \dot{\Psi} = 0$.

Determining λ_a :

Equation (G-3) as given in Appendix-G is:

$$\frac{d}{d\phi} [h \frac{dg}{d\phi}] + (\lambda_a r)^2 h g = 0$$

Thus, due to similarity to Equation (D-1) it is apparent

that by the same procedure;

$$(\lambda_a r)^2 = \frac{\int_0^{2\pi} h \left(\frac{dg}{d\phi} \right)^2 d\phi}{\int_0^{2\pi} h g^2 d\phi} \quad (D-8)$$

where numerical integration techniques were used for both numerator and denominator.

Finally by determining λ_a , the leakage factor η_a can be determined by Equation (51).

APPENDIX E

Integration Constants for Pressure
and Load Equations

Considering the boundary conditions due to film continuity assuming no film rupture;

$$P(\phi_1, Z) = P(\phi_1 + 2\pi, Z) = 0, \quad (\text{E-1})$$

or in case of full journal bearing:

$$P(0, Z) = P(2\pi, Z) = 0.$$

From Eq.(8) pressure was given as:

$$P(\phi, Z) = \left[1 - \frac{\text{Cosh}(\lambda Z)}{\text{Cosh}(\lambda L/2)}\right] F(\phi).$$

Therefore, the boundary conditions (E-1) can be written as:

$$F(\phi_1) = F(\phi_1 + \beta) = 0 \quad (\text{E-2})$$

But,

$$F(\phi) = F_a(\phi) + F_b(\phi), \quad (\text{E-3})$$

where,

$$F_a(\phi) = 12 \left(\frac{r}{c}\right)^2 \mu \dot{\epsilon} [F_1(\phi) + C_1 F_2(\phi) + C_2]$$

and

$$F_b(\phi) = 6 \left(\frac{r}{c}\right)^2 \mu (\omega - 2\psi) [F_3(\phi) + C_3 F_2(\phi) + C_4].$$

By applying the boundary conditions (E-2) to Eq.(E-3):

$$C_1 = - \frac{[F_1(\phi)]_{\phi_1}^{\phi_1+\beta}}{[F_2(\phi)]_{\phi_1}^{\phi_1}}, \quad C_2 = -F_2(\phi_1) - C_1 F_2(\phi_1) \quad (\text{E-4})$$

$$C_3 = - \frac{[F_3(\phi)]_{\phi_1}^{\phi_1+\beta}}{[F_2(\phi)]_{\phi_1}^{\phi_1+\beta}}, \quad C_4 = -F_3(\phi_1) - C_3 F_2(\phi_1) \quad (\text{E-4})$$

For the full journal bearing i.e. $\phi_1=0$, $\beta=2\pi$,

$$C_1 = 0, \quad C_2 = - \frac{1}{2\varepsilon(1+\varepsilon)^2} \quad (\text{E-5})$$

$$C_3 = - \frac{2(1-\varepsilon^2)}{(2+\varepsilon)^2}, \quad C_4 = 0$$

APPENDIX F

Elastic Coefficients

Equations (19) and (20) give

$$F_x = W_{px} \cos (\Psi_0 - \Psi) + W_{py} \sin (\Psi_0 - \Psi),$$

$$F_y = -W_{px} \sin (\Psi_0 - \Psi) + W_{py} \cos (\Psi_0 - \Psi).$$

Consider Taylor's series of the form:

$$F(x+h, y+k) = F(x, y) + \{h \frac{\partial F(x, y)}{\partial x} + k \frac{\partial F(x, y)}{\partial y} + \dots \quad (F-1)$$

From Equation (21),

$$\Psi = \Psi_0 + \frac{y}{e} \quad \text{and} \quad \epsilon = \epsilon_0 + \frac{x}{c} \quad (F-2)$$

Now expanding F_x and F_y by (F-1):

$$F_x(\epsilon, \Psi) = F_x(\epsilon_0, \Psi_0) + \left[\frac{\partial F_x}{\partial \Psi} \frac{\partial \Psi}{\partial x} + \frac{\partial F_x}{\partial \epsilon} \frac{\partial \epsilon}{\partial x} \right] x + \left[\frac{\partial F_x}{\partial \Psi} \frac{\partial \Psi}{\partial y} + \frac{\partial F_x}{\partial \epsilon} \frac{\partial \epsilon}{\partial y} \right] y \quad (F-3)$$

$$F_y(\epsilon, \Psi) = F_y(\epsilon_0, \Psi_0) + \left[\frac{\partial F_y}{\partial \Psi} \frac{\partial \Psi}{\partial x} + \frac{\partial F_y}{\partial \epsilon} \frac{\partial \epsilon}{\partial x} \right] x + \left[\frac{\partial F_y}{\partial \Psi} \frac{\partial \Psi}{\partial y} + \frac{\partial F_y}{\partial \epsilon} \frac{\partial \epsilon}{\partial y} \right] y \quad (F-4)$$

Now by taking derivatives,

$$\frac{\partial F_x}{\partial \epsilon} = \frac{\partial W_{px}}{\partial \epsilon} \cos (\Psi_0 - \Psi) + \frac{\partial W_{py}}{\partial \epsilon} \sin (\Psi_0 - \Psi)$$

$$\frac{\partial F_y}{\partial \Psi} = \frac{\partial W_{px}}{\partial \Psi} \cos (\Psi_0 - \Psi) + W_{px} \sin (\Psi_0 - \Psi) + \frac{\partial W_{py}}{\partial \Psi} \sin (\Psi_0 - \Psi)$$

$$\frac{\partial F_y}{\partial \epsilon} = -\frac{\partial W_{px}}{\partial \epsilon} \sin (\Psi_0 - \Psi) + \frac{\partial W_{py}}{\partial \epsilon} \cos (\Psi_0 - \Psi)$$

$$\frac{\partial F_x}{\partial \Psi} = -\frac{\partial W_{px}}{\partial \Psi} \sin (\Psi_0 - \Psi) + W_{px} \cos (\Psi_0 - \Psi) + \frac{\partial W_{py}}{\partial \Psi} \cos (\Psi_0 - \Psi)$$

Assuming the approximation of Equation (22), i.e.,

$$\sin (\Psi_0 - \Psi) = 0, \quad \cos (\Psi_0 - \Psi) = 1,$$

therefore,

$$\frac{\partial F_x}{\partial \epsilon} = \frac{\partial W_{px}}{\partial \epsilon} \quad (F-5)$$

$$\frac{\partial F_x}{\partial \Psi} = \frac{\partial W_{px}}{\partial \Psi} - W_{py} \quad (F-6)$$

$$\frac{\partial F_y}{\partial \epsilon} = \frac{\partial W_{py}}{\partial \epsilon} \quad (F-7)$$

$$\frac{\partial F_y}{\partial \Psi} = W_{px} + \frac{\partial W_{py}}{\partial \Psi} \quad (F-8)$$

By noting from Equation (F-2) that:

$$\frac{\partial \epsilon}{\partial x} = \frac{1}{c} \quad \frac{\partial \epsilon}{\partial y} = 0$$

and (F-9)

$$\frac{\partial \Psi}{\partial x} = -\frac{y}{c^2 \epsilon^2}, \quad \frac{\partial \Psi}{\partial y} = \frac{1}{c \epsilon}$$

Thus, by using Equations (F-5) thru (F-8) and Equation (F-9) the elastic coefficients as given by Equations (25), (26), (27) and (28) are determined.

APPENDIX G

Inertia Coefficients

Equation (43) is the differential equation found for the acceleration effect. By assuming the solution of the form:

$$P_a(\phi, z) = F'(\phi) + g'(\phi) q'(z) \quad (G-1)$$

and using the same procedure as was applied for the solution of Reynolds' equation to Equation (43):

$$\frac{d}{d\phi} \left(h \frac{dF'}{d\phi} \right) = \frac{\rho r}{c} [a_x \cos\phi + a_y \sin\phi] \quad (G-2)$$

and

$$\frac{d}{d\phi} \left(h \frac{dg'}{d\phi} \right) + (\lambda_a r)^2 h g' = 0, \quad (G-3)$$

also

$$\frac{d^2 q'}{dz^2} - \lambda_a^2 q' = 0 \quad (G-4)$$

Due to symmetry of the bearing along its length, the solution of (G-4) is:

$$q'(z) = \text{Cosh}(\lambda_a z) \quad (G-5)$$

Therefore, the approximate solution for Equation (43) is:

$$P_a(\phi, z) = \left[1 - \frac{\text{Cosh}(\lambda_a z)}{\text{Cosh}(\lambda_a L/2)} \right] F'(\phi)$$

Integrating Equation (G-2) twice with respect to ϕ :

$$F'(\phi) = \frac{\rho r^2}{c} [a_x F_2'(\phi) - a_y F_3'(\phi) + C_1' F_1'(\phi) + C_2'] \quad (G-7)$$

By using the boundary conditions: $P_a(\phi, z) = P_a(\phi_1 + \beta, z) = 0$

C_1' and C_2' will be:

$$C_1' = \frac{-a_x [F_2'(\phi)]_{\phi_1}^{\phi_1+\beta} + a_y [F_3'(\phi)]_{\phi_1}^{\phi_1+\beta}}{F_1'(\phi)]_{\phi_1}^{\phi_1+\beta}} \quad (G-8)$$

$$C_2' = -a_x F_2'(\phi_1+\beta) + a_y F_3'(\phi_1+\beta) - C_1' F_1'(\phi_1+\beta)$$

where for a full journal bearing,

$$C_1' = \frac{a_y}{\varepsilon} [(1-\varepsilon^2)^{1/2} - 1] \quad (G-9)$$

$$C_2' = \frac{a_x}{\varepsilon} \log_e (1+\varepsilon) \frac{2\pi}{\varepsilon} a_y$$

Equation (44) was obtained from the above.

Forces due to pressure in (x,y) coordinate system can be obtained from Equation (44).

$$W_{ax} = - \int_{-L/2}^{L/2} \int_{\phi_1}^{\phi_1+\beta} P_a(\phi, Z) \cos\phi \cdot r d\phi dZ \quad (G-10)$$

$$W_{ay} = \int_{-L/2}^{L/2} \int_{\phi_1}^{\phi_1+\beta} P_a(\phi, Z) \sin\phi \cdot r d\phi dZ \quad (G-11)$$

where after integration becomes:

$$W_{ax} = - \frac{r^3 L \rho \eta a}{C} [a_x F_7'(\phi) - a_y F_9'(\phi) + C_1' F_5'(\phi) + C_2' \sin\phi]_{\phi_1}^{\phi_1+\beta} \quad (G-12)$$

$$W_{ay} = \frac{r^3 L \rho \eta a}{C} [a_x F_6'(\phi) + a_y F_8'(\phi) + C_1' F_4'(\phi) - C_2' \cos\phi]_{\phi_1}^{\phi_1+\beta} \quad (G-13)$$

APPENDIX H

Numerical Solutions of the General and Eigenvalue Equations
i-Runge-Kutta Methods,

A Runge-Kutta method is one which employs a recurrence formula of the form,

$$Y_{i+1} = Y_i + a_1K_1 + a_2K_2 + a_3K_3 + \dots + a_nK_n \quad (H-1)$$

to calculate successive values of the dependent variable y of the differential equation

$$\frac{d^2y}{dt} = y' = f(t,y) \quad (H-2)$$

where:

$$K_n = (\Delta t) f(t_i + p_{n-1} \Delta t, y_i + q_{n-1,1} K_1 + q_{n-1,2} K_2 + \dots + q_{n-1,n-1} K_{n-1}) \quad (H-3)$$

The a 's, p 's and q 's must assume values such that Equation (H-1) accurately yields successive values of y . These values are determined by making Equation (H-1) equivalent to a certain specified number of terms of a Taylor-series expansion of y about t_i .

Runge-Kutta methods are self-starting and it is theoretically possible to develop one having any desired degree of accuracy. As with any method, they possess certain advantages and disadvantages which must be considered. The principal advantage of the Runge-Kutta methods is their self-starting feature and resulting ease of programming. One disadvantage is the requirement that the function $f(t,y)$ usually results in a less efficient method, with respect to

computing time, than do other methods of comparable accuracy.
Fourth-order Runge-Kutta Method:

A well-known fourth order Runge-Kutta method results with $n=4$ in Equation (H-1). The a 's are determined equating terms of expanded Taylor series including those of $(\Delta t)^4$. Selecting a particular set of two ordinary parameter value yields (24):

$$y_{i+1} = y_i + \frac{1}{6}(K_1 + 2K_2 + 2K_3 + K_4) \quad (H-4)$$

where

$$\begin{aligned} K_1 &= \Delta t \cdot f(t_i, y_i) \\ K_2 &= \Delta t \cdot f\left(t_i + \frac{\Delta t}{2}, y_i + \frac{K_1}{2}\right) \\ K_3 &= \Delta t \cdot f\left(t_i + \frac{\Delta t}{2}, y_i + \frac{K_2}{2}\right) \\ K_4 &= \Delta t \cdot f(t_i + \Delta t, y_i + K_3) \end{aligned} \quad (H-5)$$

In this method the pre-step error is of order $(\Delta t)^5$.

The above method could be applied to Equation (52):

$$M_{xx} \ddot{X} + M_{xy} \ddot{Y} + B_{xx} \dot{X} + B_{xy} \dot{Y} + K_{xx} X + K_{xy} Y = W_x \quad (a)$$

$$M_{yx} \ddot{X} + M_{yy} \ddot{Y} + B_{yx} \dot{X} + B_{yy} \dot{Y} - K_{yx} X + K_{yy} Y = -W_y \quad (b)$$

Multiplying Equation (a) by M_{yx} , and Equation (b) by M_{xx} , and eliminating the \ddot{X} terms in the process, results in:

$$\ddot{Y} + A_2 \dot{X} + A_1 \dot{Y} + A_4 X + A_3 Y = A_5 \quad (H-6)$$

where

$$A_1 = \frac{\begin{vmatrix} M_{yx} & M_{xx} \\ B_{yy} & B_{xy} \end{vmatrix}}{|d|} \quad |d| = \begin{vmatrix} M_{xy} & M_{xx} \\ M_{yy} & M_{yx} \end{vmatrix} \quad A_2 = \frac{\begin{vmatrix} M_{yx} & M_{xx} \\ B_{yx} & B_{xx} \end{vmatrix}}{|d|}$$

$$A_3 = \frac{\begin{vmatrix} K_{xy} & K_{yy} \\ M_{xx} & M_{yx} \end{vmatrix}}{|d|}, \quad A_4 = \frac{\begin{vmatrix} K_{xx} & -K_{yx} \\ M_{xx} & M_{yx} \end{vmatrix}}{|d|}, \quad A_5 = \frac{\begin{vmatrix} W_x & -W_y \\ M_{yx} & M_{xx} \end{vmatrix}}{|d|}$$

Introducing a new variable u for simplicity such that:

$$\dot{y} = u_1 \quad \dot{x} = u_2 \quad y = u_3 \quad x = u_4 \quad \ddot{y} = u_1 \quad \ddot{x} = u_2,$$

Equation (H-6) becomes:

$$\dot{u}_1 + A_1 u_1 + A_2 u_2 + A_3 u_3 + A_4 u_4 = A_5 \quad (\text{H-7})$$

Using the same procedure only this time eliminating the \ddot{y} terms, yields:

$$\dot{u}_2 + B_2 \dot{x} + B_1 \dot{y} + B_4 x + B_3 y = B_5 \quad (\text{H-8})$$

Where B's are to be determined in the same manner as A's.

Therefore, in this manner Equations (a) and (b) are reduced to four first order differential equations which are:

$$\begin{aligned} \dot{u}_1 + A_1 u_1 + A_2 u_2 + A_3 u_3 + A_4 u_4 &= A_5 \\ \dot{u}_2 + B_1 u_1 + B_2 u_2 + B_3 u_3 + B_4 u_4 &= B_5 \end{aligned} \quad (\text{H-9})$$

$$\dot{u}_3 - u_1 = 0$$

$$\dot{u}_4 - u_2 = 0$$

Equation (H-8) in form of:

$$\begin{aligned} \dot{u}_1 &= A_5 - A_1 u_1 - A_2 u_2 - A_3 u_3 - A_4 u_4 = F_1(t, u_1, u_2, u_3, u_4) \\ \dot{u}_2 &= B_5 - B_1 u_1 - B_2 u_2 - B_3 u_3 - B_4 u_4 = F_2(t, u_1, u_2, u_3, u_4) \\ \dot{u}_3 &= u_1 = F_3(t, u_1, u_2, u_3, u_4) \\ \dot{u}_4 &= u_2 = F_4(t, u_1, u_2, u_3, u_4) \end{aligned} \quad (\text{H-10})$$

where F's are functions.

Now by applying Equations (H-5) and remembering that K's are double subscripted as K_{ij} where:

$$K_{j1} = \Delta t \cdot F_j(t, u_1, u_2, u_3, u_4),$$

$$\begin{aligned}
 K_{j_2} &= \Delta t \cdot F_j \left(t + \frac{\Delta t}{2}, u_1 + \frac{K_{11}}{2}, u_2 + \frac{K_{21}}{2}, u_3 + \frac{K_{31}}{2}, u_4 + \frac{K_{41}}{2} \right) \\
 K_{j_3} &= \Delta t \cdot F_j \left(t + \frac{\Delta t}{2}, u_1 + \frac{K_{12}}{2}, u_2 + \frac{K_{22}}{2}, u_3 + \frac{K_{33}}{2}, u_4 + \frac{K_{42}}{2} \right) \quad (H-11) \\
 K_{j_4} &= \Delta t \cdot F_j \left(t + \Delta t, u_1 + K_{13}, u_2 + K_{23}, u_3 + K_{33}, u_4 + K_{43} \right)
 \end{aligned}$$

In each equation $j = 1, 2, 3, 4$.

Equation (H-4) becomes:

$$\begin{aligned}
 u_j &= u_j + \frac{1}{6} [K_{j_1} + 2K_{j_2} + 2K_{j_3} + K_{j_4}] \quad (H-12) \\
 (\text{new}) & \quad (\text{old})
 \end{aligned}$$

Equation (H-11) and Equation (H-12) have been programmed as subroutine "SOLVE".

ii-Integration by Simpson's Rule:

Simpson's rule gives a more accurate approximation than the trapezoidal rule, since it consists of connecting groups of three points on the curve by second-degree parabolas and summing the areas under the parabolas to obtain the approximate area under the curve.

If it is desired to integrate the function $y = F(x)$ by Simpson's rule:

$$\int_{x_i=0}^{x_{n+1}} F(x) dx = \frac{\Delta x}{3} (y_1 + 4 \sum_{i=2,4,6}^{i=n} y_i + 2 \sum_{i=3,5,7}^{i=n-1} y_i + y_{n+1}) \quad (H-13)$$

where n is even.

Equation (H-13) is called Simpson's one-third rule for obtaining the approximate area under a curve. This rule was used in integrating the functions for determining eigenvalues λ and λ_a in Equations (D-6) and (D-8) respectively.

'MAIN'

```

read: r,L,C,e, $\mu$ ,N,
      W0,W1,Wd
      call steady
      call solve

```

'SOLVE'

'FUNCT'

```

call DYLEAK
call ACREAK
call INERTIA
call SPRING
call DAMP
solving Equation
(H-11)

```

```

1-at t=0, $\epsilon=\epsilon_0$  and  $\Psi=\Psi_0$ 
2-calculating W1x,W1y
   call FUNCT
3-solving Equation (52)
  by Runge-Kutta method
  (Appendix H)
4-print: t,ui,vj,x,y, $\dot{x}$ ,
 $\dot{y}$ , $\epsilon$ , $\Psi$ , $\dot{\epsilon}$ , $\dot{\Psi}$ ,S,W, $\eta$ , $\eta_a$ .

```

'STEADY'

```

call SLEAK
finding: $\epsilon_0$ , $\Psi_0$ ,
 $e_0$ , for the
static load.

```

'INERTIA'

```

call ACLEAK
calculating M,s
Equations (47) to (50)

```

'DAMP'

```

call ACLEAK
call SPRING
calculating B,s
Equations (36) to (39)

```

'SPRING'

```

calculating F,s
call DYLEAK
calculating K's
Equations (29) to
(32)

```

'ACLEAK'

```

by Simpson's Rule
(Appendix H)
calculating  $\eta_a$  for
every  $\epsilon$  (Equation
(D-8))

```

'DYLEAK'

```

by Simpson's Rule
(Appendix H)
calculating  $\eta$  for
every  $\epsilon$  (Equation
(51))

```

'SLEAK'

```

by Simpson's Rule
(Appendix H)
calculating  $\eta$  for
every  $\epsilon$  (Equation
(51))

```

'ACPRES'

```

1-call SOLVE
2-calculating
Pa( $\phi$ ,z),
Equation (44)

```

'PRESS'

```

1-call SOLVE
2-calculating
P( $\phi$ ,z)
Equation (13)
3-Pt=P( $\phi$ ,z)+Pa

```


APPENDIX I

A Method for Identifying Journal Center Loci

In Figure (I-1) the placement of proximity sensors with respect to the journal and the bearing is shown. Due to the geometry involved the sensor readings are not true values, so a procedure will be given here to determine the true values of the journal center loci.

From triangle Aco_{j_1} of Figure (I-1), and noting that $Ac = r - u + \Delta q$:

$$V_j^2 + u_i^2 + (\Delta q)^2 - 2ru_i + 2r\Delta q - 2u_i\Delta q = 0 \quad (I-1)$$

Similarly from triangle HDo_{j_1} :

$$V_j^2 + u_i^2 + (\Delta e)^2 - 2rV_j\Delta e + 2r\Delta e = 0 \quad (I-2)$$

where Δe and Δq are sensor readings. u_i and V_j are true coordinates of the journal center position. Thus, by solving two Equation (I-1) and (I-2) the journal center for every set of sensor's reading could be determined. However, Equations (I-1) and (I-2) are non-linear, and, therefore, a numerical technique was employed.

Newton's Method: (27)

In the general case, the system to be solved is of the form:

$$f(x) = 0 \quad (I-3)$$

where $f(x) = [f_1(x), f_2(x), \dots, f_n(x)]^T$ is an n-component column vector. Such a system can be written in a variety of ways. We examine here the choice

$$g(x) = x - A(x)f(x) \quad (I-4)$$

where $A(x)$ is an n^{th} order non-singular square matrix with components $a_{ij}(x)$. The simplest choice for $A(x)$ is:

$$A(x) = A, \quad (\text{I-5})$$

a constant non-singular matrix. The matrix

$$J(\bar{x}) = \left(\frac{\partial f_n(x)}{\partial x_j} \right) \quad (\text{I-6})$$

is introduced whose determinant is the Jacobian of the function $f_n(x)$.

The iteration is accomplished by using

$$\bar{x}^{(i+1)} = \bar{x}^{(i)} - A^{-1} F(\bar{x}^{(i)}) \quad (\text{I-7})$$

In this method Equation (I-5) is replaced by the choice:

$$A(x) \equiv J^{-1}(x) \quad (\text{I-8})$$

with the assumption that $\det|J(x)| \neq 0$ for x in $||x - x^*|| < \epsilon_x$

Note that by using Equation (I-8) in Equation (I-7):

$$x^{(i+1)} = x^{(i)} - J^{-1}[x^{(i)} F(x^{(i)})] \quad (\text{I-9})$$

In order to apply this to solve Equation (I-1) and (I-2), they could be written as:

$$F_1(u_i, V_j) = u_i^2 + a_1^2 + a_2 u_i + V_j^2 = 0 \quad (\text{I-10})$$

$$F_2(u_i, V_j) = V_j^2 + u_i^2 + b_1^2 + b_2 V_j = 0$$

where

$$a_1 = \sqrt{(\Delta q)^2 + 2r\Delta q} \quad a_2 = -2(r + \Delta q)$$

$$b_1 = \sqrt{(\Delta e)^2 + 2r\Delta e} \quad b_2 = -2(r + \Delta e)$$

therefore, for a system of two equations,

$$J(u_i, V_j) = \begin{pmatrix} F_{1u} & F_{1V} \\ F_{2u} & F_{2V} \end{pmatrix}, \quad (\text{I-12})$$

where as e.g. $F_{1u} = \frac{\partial F_1}{\partial u}$, and so on.

From Equation (I-12) we could determine:

$$J^{-1}(u_i, v_j) = \frac{1}{|J|} \begin{pmatrix} 2v_j + b_2 & -2v_j \\ -2u_i & 2u_i + a_2 \end{pmatrix} \quad (\text{I-13})$$

where $|J| = 2 u_i b_2 + 2 v_j a_2 + a_2 b_2$.

Therefore, from Equation (I-9):

$$u_{i+1} = u_i - \left\{ \frac{F_1 \cdot (2v_j + b_2) - F_2 \cdot (2v_j)}{|J|} \right\}^i \quad (\text{I-14})$$

$$v_{i+1} = v_j - \left\{ \frac{F_2 \cdot (2u_i + a_2) - F_1 \cdot (2u_i)}{|J|} \right\}^i \quad (\text{I-15})$$

Equations (I-14) and (I-15) were programmed in double precision. Starting values were $u_i = \Delta q$ and $v_j = \Delta e$. Convergence was usually better than four iterations.

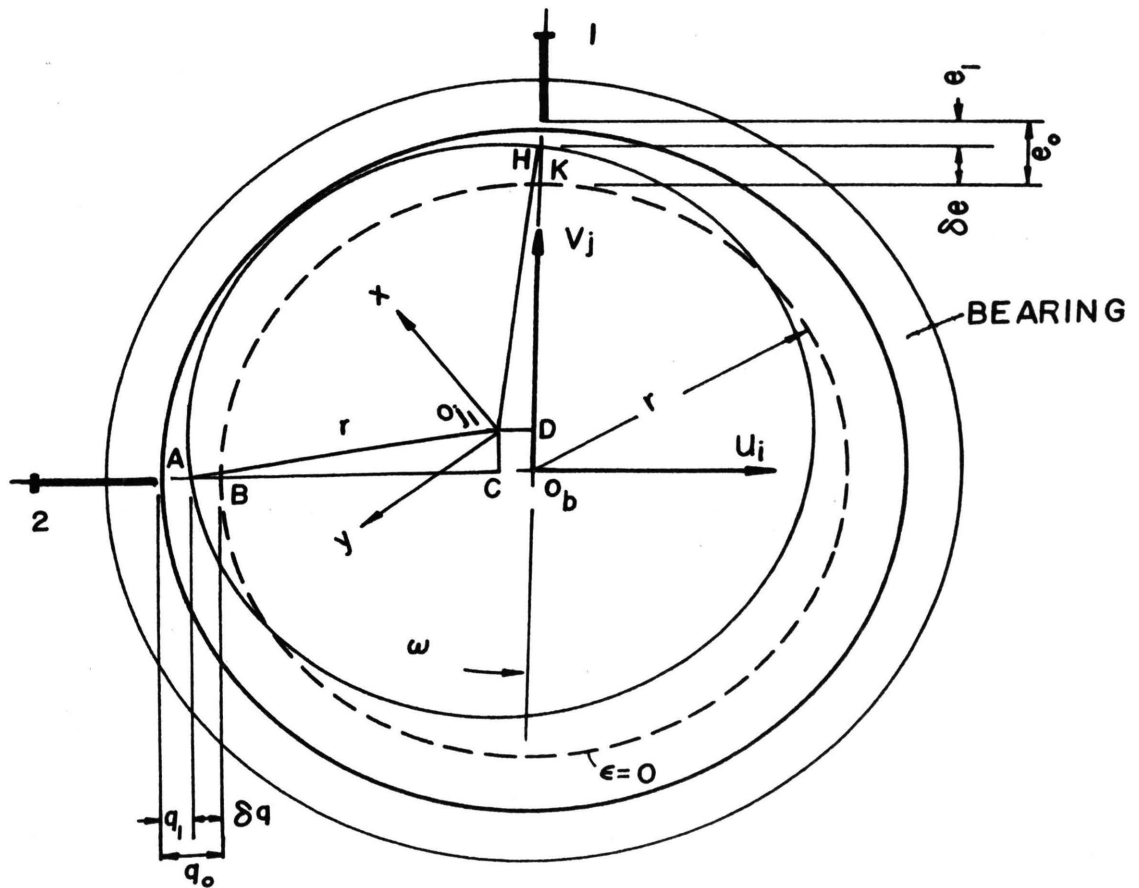


Fig. I-1. Displacement of Journal Center.

APPENDIX J

Effect of Journal Mass

In determining the effect of the acceleration terms, the mass of the journal was not accounted for. Here, an attempt is made to find the significance of this simplification.

The forces due to acceleration in direction x and y are defined by Equations (45) and (46). If now from Equation (45) the first term be considered only, i.e.,

$$W_{ax} = M_{xx} \cdot a_x \quad (J-1)$$

where M_{xx} is given by Equation (47), and may be written as:

$$M_{xx} = \left(\frac{r^3 L \rho}{c} \eta_a \right) \Omega_{xx} \quad (J-2)$$

where

Ω_{xx} could be determined from Equation (47).

$$W_{ax} = \left(\frac{-r^3 L \rho}{c} \eta_a \right) \Omega_{xx} \quad (J-3)$$

Therefore, lubricant has an effective mass in x-direction as:

$$\frac{W_{ax}}{a_x} = \Omega_{xx} \frac{\rho L r^3}{c} \eta_a \quad (J-4)$$

But the mass of journal within the bearing is $m_j = \pi \rho_j r^3 L$, where ρ_j is the density of journal material. Therefore:

$$\frac{\text{effective mass of lubricant film in x direction}}{\text{mass of journal within the bearing}} = \frac{\rho L r^3 \eta_a \Omega_{xx}}{\pi \rho_j r^3 L} \quad (J-5)$$

"

$$= \frac{\rho \eta_a L}{\rho_j \pi} \left(\frac{r}{c} \right) \Omega_{xx} \quad (J-6)$$

Where same form of relation could be found for y direction.

Now for typical Sommerfeld No., i.e.,

$$S = -275 \quad \eta_a = 0.30 \quad \Omega_{xx} = 3.5 \text{ (from Figure 21)}$$

$$\rho_{oil} = 0.0310 \frac{\text{lb}}{\text{in}^3} \quad \rho_{steel} = 0.289 \frac{\text{lb}}{\text{in}^3} \quad \frac{r}{c} = 980$$

Therefore:

$$\frac{\text{Effective mass of lubricant film in x-direction}}{\text{mass of the journal within the bearing}} = 35.0$$

Thus, it can be seen that the effective mass of the lubricant is much larger than mass of the journal within the bearing.

APPENDIX K.

Integrals and Differentiation

(i) Integrals:

$$I_1 = \int \frac{d\phi}{(1+\epsilon \cos \phi)} = \frac{\delta}{(1-\epsilon^2)} \cos^{-1} \left(\frac{\epsilon + \cos \phi}{1+\epsilon \cos \phi} \right) \begin{matrix} \delta = 1 & \sin \phi > 0 \\ \delta = -1 & \sin \phi < 0 \end{matrix}$$

$$[I_1]_0^{2\pi} = \frac{2\pi}{(1-\epsilon^2)} 1/2$$

$$I_2 = \int \log_e (1+\epsilon \cos \phi) \sin \phi \, d\phi = -\cos \phi \log_e (1+\epsilon \cos \phi) - \frac{1}{\epsilon} \log_e (1+\epsilon \cos \phi) + \cos \phi$$

$$I_3 = \int \log_e (1+\epsilon \cos \phi) \cos \phi \, d\phi = \sin \phi \log_e (1+\epsilon \cos \phi) - \frac{\delta(1-\epsilon^2)1/2}{\epsilon}$$

$$\cos^{-1} \left(\frac{\epsilon + \cos \phi}{1+\epsilon \cos \phi} \right) + \frac{\phi}{\epsilon} - \sin \phi$$

$$I_4 = \int \cos^{-1} \left(\frac{\epsilon + \cos \phi}{1+\epsilon \cos \phi} \right) \cos \phi \, d\phi = \sin \phi \cos^{-1} \left(\frac{\epsilon + \cos \phi}{1+\epsilon \cos \phi} \right) + \frac{\delta(1-\epsilon^2)1/2}{\epsilon}$$

$$\log_e (1+\epsilon \cos \phi)$$

$$I_5 = \int \cos^{-1} \left(\frac{\epsilon + \cos \phi}{1+\epsilon \cos \phi} \right) \sin \phi \, d\phi = -\cos \phi \cos^{-1} \left(\frac{\epsilon + \cos \phi}{1+\epsilon \cos \phi} \right) - \frac{1}{\epsilon} \cos$$

$$^{-1} \left(\frac{\epsilon + \cos \phi}{1+\epsilon \cos \phi} \right) + \frac{\delta(1-\epsilon^2)1/2}{\epsilon} \phi$$

(ii) Differentiation:

$$\frac{\partial C_3}{\partial \Psi} = \frac{\partial C_3}{\partial \phi_1} = \frac{-[2\epsilon F_1(\phi)]_0^{2\pi}}{[F_2(\phi)]_0^{2\pi}} + \frac{[F_3(\phi)]_0^{2\pi} \cdot \left[\frac{1}{(1+\epsilon \cos \phi)^3} \right]_0^{2\pi}}{\{ [F_2(\phi)]_0^{2\pi} \}^2}$$

$$\frac{\partial C_4}{\partial \Psi} = \frac{\partial C_4}{\partial \phi_1} = -2 F_1(0) + \frac{[F_3(\phi)]_0^{2\pi}}{(1+\epsilon \cos \phi)^3 [F_2(\phi)]_0^{2\pi}} +$$

$$\frac{F_2(0) [2\epsilon F_1(\phi)]_0^{2\pi}}{[F_2(\phi)]_0^{2\pi}} - \frac{F_2(0) \cdot [F_3(\phi)]_0^{2\pi} \left[\frac{1}{(1+\cos)} \right]_0^{2\pi}}{\{ [F_2(\phi)]_0^{2\pi} \}^2}$$

APPENDIX L

Dynamic Response of Bearing

i-Experimental:

In order to examine the response of the bearing a square-wave load was placed on the bearing. The maximum pressure and journal center displacement were observed. By plotting the ratio of amplitudes of, e.g., pressure over the load versus time, it was noticed that the system has a decaying response. A frequency response was also performed. The result is shown in Figure (L-1), which indicates the system has two break points in the range of this test. The break slope is not exactly that of a first order system (1 unit/db).

ii-Analytical:

From Appendix H Equation (52) could be written in form of:

$$\begin{Bmatrix} \ddot{x} \\ \ddot{y} \end{Bmatrix} + \begin{bmatrix} B_2 & B_1 \\ A_2 & A_1 \end{bmatrix} \begin{Bmatrix} \dot{x} \\ \dot{y} \end{Bmatrix} + \begin{bmatrix} B_4 & B_3 \\ A_4 & A_3 \end{bmatrix} \begin{Bmatrix} x \\ y \end{Bmatrix} = \begin{Bmatrix} B_5 \\ B_5 \end{Bmatrix} \quad (L-1)$$

where, A's and B's can be determined from Appendix H.

Now if for a typical eccentricity ratio e.g. $\epsilon = .2064$ the A's and B's calculated, i.e.,

$$\begin{array}{llll} B_1 = 0.0 & B_2 = 151 & B_3 = 329 & B_4 = 26,720 \\ A_1 = 7.8 & A_2 = 0.0 & A_3 = 238 & A_4 = 230 \end{array}$$

and for, $\epsilon = 0.53$

$$\begin{array}{llll} B_1 = 0.0 & B_2 = 214 & B_3 = 2600 & B_4 = 15,000 \\ A_1 = 22.6 & A_2 = 0.0 & A_3 = 372 & A_4 = 945 \end{array}$$

for $\varepsilon = 0.750$

$$\begin{array}{llll} B_1 = 0.0 & B_2 = 411 & B_3 = 3120 & B_4 = 26,220 \\ A_1 = 41.0 & A_2 = 0.0 & A_3 = 131 & A_4 = 4906 \end{array}$$

Equation (L-1) could be written as:

$$\begin{aligned} \ddot{x} + B_2 \dot{x} + B_4 x &= B_5 - B_3 y \\ \ddot{y} + A_1 \dot{y} + A_3 y &= A_5 - A_4 x, \end{aligned} \tag{L-2}$$

or:

$$\begin{aligned} (D^2 + B_2 D + B_4)x &= B_5 - B_3 y \\ (D^2 + A_1 D + A_3)y &= A_5 - A_4 x \end{aligned} \tag{L-2}$$

Note that B_5 and A_5 are load terms. Solving the Equations (L-2) for x and y :

$$x = \frac{B_5(D^2 + A_1 D + A_3) - B_3 A_5}{D^4 + (A_1 + B_2)D^3 + (A_1 B_2 + B_4 + A_3)D^2 + (A_1 B_4 + A_3 B_2)D + A_3 B_4 - B_3 A_4} \tag{L-3}$$

and

$$y = \frac{A_5(D^2 + B_2 D + B_4) - A_4 B_5}{D^4 + (A_1 + B_2)D^3 + (A_1 B_2 + B_4 + A_3)D^2 + (A_1 B_4 + A_3 B_2) + (A_3 B_4 - B_3 A_4)} \tag{L-4}$$

As can be seen from Equation (L-3) and (L-4), x and y have four negative roots, either real or imaginary. But in order to find these roots exactly additional work is required. In order to estimate the effect of the system, the coupling terms of Equation (L-2) are neglected. Thus, approximate values for the natural frequencies, ω_n , and damping ratios ξ , can be found as:

$$\begin{aligned} B_2 &= 2\xi_1 \omega_{n1} & B_4 &= \omega_{n1}^2 \\ A_1 &= 2\xi_2 \omega_{n2} & A_3 &= \omega_{n2}^2 \end{aligned} \tag{L-5}$$

Thus, calculating ω_n and ξ :

(i) For $\epsilon = .206$

$$\omega_{n1} = 163.46 \text{ rad/sec.} \quad \xi_1 = 0.4663$$

$$\omega_{n2} = 15.43 \text{ rad/sec.} \quad \xi_2 = 0.253$$

(ii) For $\epsilon = .53$

$$\omega_{n1} = 122.47 \text{ rad/sec.} \quad \xi_1 = 0.874$$

$$\omega_{n2} = 19.28 \text{ rad/sec.} \quad \xi_2 = .59$$

(iii) For $\epsilon = .750$

$$\omega_{n1} = 161.92 \text{ rad/sec.} \quad \xi_1 = 1.26$$

$$\omega_{n2} = 11.44 \text{ rad/sec} \quad \xi_2 = 1.79$$

By comparing the natural frequencies and damping ratios, it can be concluded that the bearing at low eccentricity ratios acts as a second order lightly-damped system, and at high eccentricity ratios, it acts as a second order heavily damped system.

The results of Figure (L-1) would seem to indicate that the bearing at that eccentricity ($\epsilon = .4$), is acting as an over-damped second order system, in other words, two coupled first order systems. The breaks in frequency response occurring at $\omega_1 = 3.2 \text{ rad/sec.}$ and $\omega_2 = 7.8 \text{ rad/sec.}$

The analytical results seem to indicate that there are higher natural frequencies beyond the range of the experimentation.

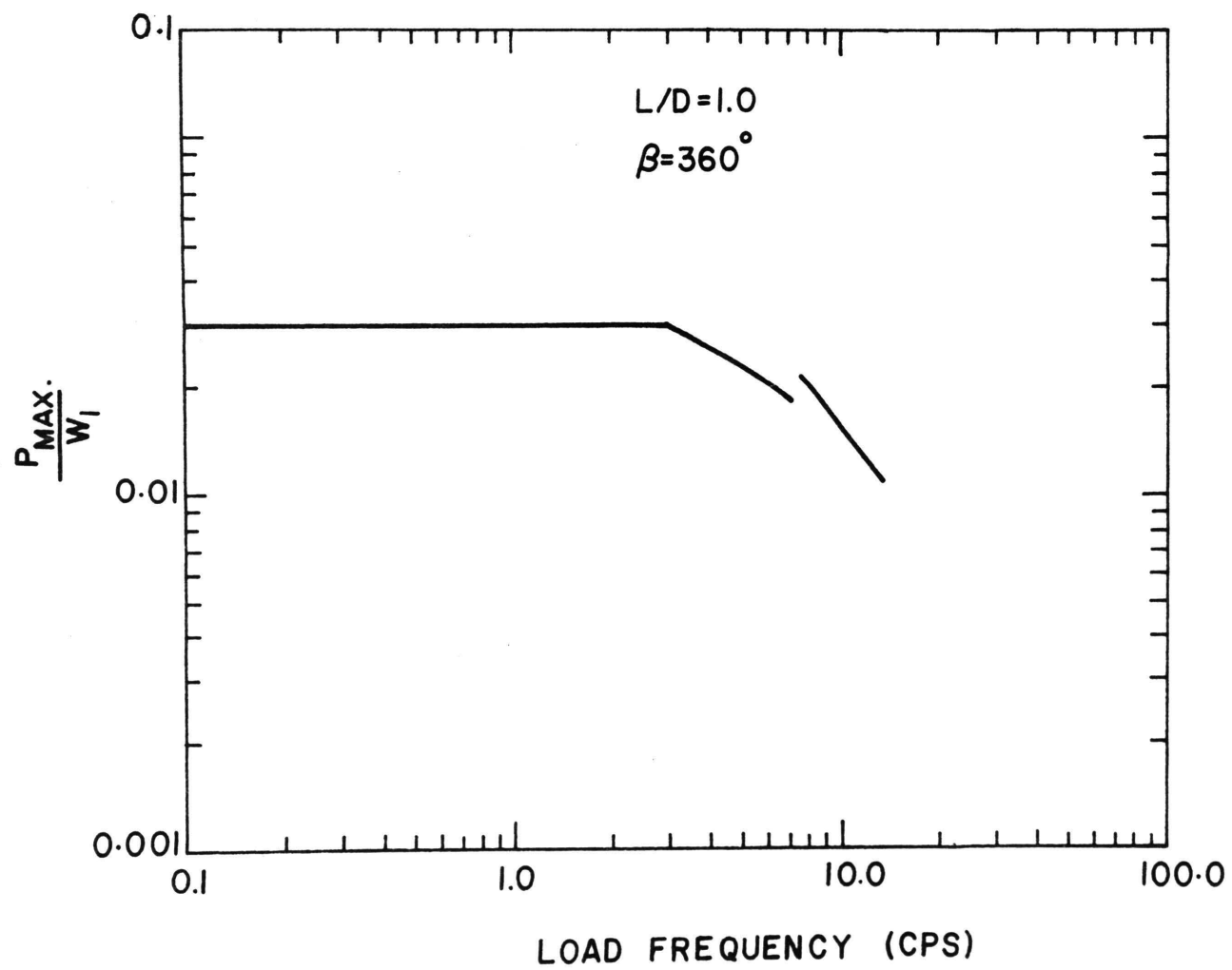


Fig. L-1. Frequency Response of the Bearing.

REFERENCES

1. "First Report on Function Experiments" B. Tower, Proc. Institutions of Mechanical Engineers (London), 1883, pp. 632.
2. "On the Theory of Lubrication" O. Reynolds, Philosophical Transaction Royal Society (London), vol. 177, pp. 157.
3. "Friction in Machines and the Effect of the Lubrication" N. Petroff, Engineering Journal, St. Petersburg (Russia), 1883, Nos. 1,2,3 and 4.
4. "On Problems in the Theory of Fluid Film Lubrication with an Experimental Method of Solution", A. Kingsbury, ASME paper APM-53-5, 1930.
5. "Journal Bearings in Turbomachinery", D.M. Smith, Chapman and Hall Ltd., (London), 1969.
6. "Rig for Testing and Developing Large Turbine-generator Bearings", S. Duffin and W.H. Gibson, The Engineer (London), vol. 222, 1966, pp. 785.
7. "The Hydrodynamical Theory of the Lubrication of a Cylindrical Bearing Under Variable Load, and of a Direct Bearing", W.J. Harrison, Cambridge Philosophical Society, vol. 22, 1920, pp. 373.
8. "Fluctuating Loads in Sleeve Bearings", H.W. Swift, Journal of the Institutions of Civil Engineers (London), vol. 5, 1937, pp. 161-195.
9. "The Calculated Performance of Dynamically Loaded Sleeve Bearings-III", J.T. Burwell, Journal of Applied

Mechanics, vol. 18, Trans. ASME. vol. 73, 1951, pp. 393-404

10. "Die Schmierung ebener Flächen ", A.G.M. Michell, Zeitschrift für Mathematik und Physik, vol. 52, 1905, pp. 123-138.

11. "The Lubrication of Plane Sliders", M.F. Muskat, M.F. Morgan and M.W. Meres, Journal of Applied Physics, vol. 11, March 1940.

12. "The Full Journal Bearing", A. Cameron and W.L. Wood, Proceedings of the Institution of Mechanical Engineers, vol. 161, 1949, pp. 59-64.

13. "A Solution for the Finite Journal Bearings and its Application to Analysis and Design, part III", A. A. Ramondi and J. Boyd, Trans. ASLE, vol. 1, No.1, April 1958, pp. 175-193.

14. "Solution of Reynolds' Equation for Finite Journal Bearings", O.Pinkus, ASME Trans., vol. 80, No. 4, May 1958, pp. 858-864.

15. "The Calculated Performance of Dynamically Loaded Sleeve Bearings", J.T. Burwell, Journal of Applied Mechanics, Trans. ASME, vol. 69, 1947, pp. A231-A245.

16. "Characteristics of Centrally Supported Journal Bearings", E.O. Waters, Trans. ASME, vol. 64, 1942, pp. 711-719.

17. "Dynamically Loaded Journal Bearing of Finite Length", Heinz W. Hahn, Institution of Mechanical Engineering (London), 1957, pp. 100-110.

18. "A Variational Approach to Lubrication Problems

and the Solution of the Finite Journal Bearings" D.F. Hays, Journal of Basic Engineering, Trans. ASME, vol. 81, 1959, pp. 13-23.

19. "Squeeze Film: A Finite Journal Bearing with a Fluctuating Load", D.F. Hays, Journal of Basic Engineering, Trans. ASME, vol. 87, 1961, pp. 579-588.

20. "Static and Dynamic Properties of Partial Journal Bearings", Paul C. Warner, Journal of Basic Engineering, Trans. ASME, vol. 85, 1963, pp. 247-257.

21. "Dynamically-Loaded Journal Bearings", J.F. Booker, ASME, Spring Lubrication Symposium, Boston, June 1963.

22. "Analytical Study of Journal-Bearing Performance Under Variable Loads", G.S.A. Shawki, Paper No. 55-Lub.-16., Trans. ASME, 1956, pp. 457-464.

23. "Alternating Loads on Sleeve Bearings", J. Dick, Philosophical Magazine (London), vol. 35, 1944, pp. 841-850.

24. "Journal Bearing Dynamic Characteristics-Effect of Inertia of Lubricant", D.M. Smith, Proc. Institution of Mechanical Engineers (London), vol. 179, 1964, pp. 37-44.

25. "Measurement of Oil-Film Pressures in Journal Bearings Under Constant and Variable Loads", A. Buske and W. Rolli, NACA Technical Memorandum No. 1200, 1937.

26. "An Experimental Investigation of a Cylindrical Journal Bearing Under Constant and Sinusoidal Loading", T.E. Carl, Proc., Institution of Mechanical Engineers (London), vol. 178, 1963, pp. 100-119.

27. "Tests on a 24-in Diameter Journal Bearing: ~~...~~

Transition from Laminar to Turbulent Flow", N.J. Huggins, Proc., Institution of Mechanical Engineers (London), vol. 181, 1966, pp. 81-88.

28. "Hydrodynamic Lubrication of Cyclically Loaded Bearings", R.W. Dayton and E.M. Simmons, NACA, Technical Notes No. 2544, 1948, pp. 1-22.

29. "Operational Mathematics", R.W. Churchill, McGraw-Hill Co., New York, 1958, pp.31.

30. "Calculus of Variations", I.M. Gelfand and S.V. Famin, Prentice-Hall Inc., New Jersey, 1963, pp. 60.

31. "Applied Numerical Methods", J.L. Merlin, G.M. Smith and J.C. Wolford, International Textbook Co., Scranton, Pennsylvania, 1967, pp. 345-361 and 272-284.

32. "Analysis of Numerical Methods", H. Keller and E. Isaacson, Prentice-Hall Inc., New Jersey, 1966, pp. 113-119.

VITA

Nader Khorzad was born on June 14, 1939 in Tehran, Iran. He received his primary and secondary education in Ghemiran, Tehran. He first enrolled at University of Missouri-Rolla in September of 1960 and was graduated with Bachelor of Science in Mechanical Engineering in August, 1964, and was employed as a design engineer at Linberg Steel Treating Company, Melrose Park, Illinois. He, then, returned to U.M.R. in September, 1965 and graduated with Master of Science in Mechanical Engineering in August, 1966, and was employed as lecturer and later as acting head of Mechanical Engineering of Tehran Polytechnic, Tehran, Iran.

He began a program leading to a Doctor of Philosophy in Mechanical Engineering at U.M.R. in June, 1971.

He was married to former Miss Kataline Egresits in November, 1967 and they have one son, Davoud.

243108